Title

How to compartmentalize signaling: lipids, Hedgehog, and ciliary PKA

ISBN

9798293851447

Author

Nguyen, Thi Dan

Publication Date

2025-09-19

Peer reviewed|Thesis/dissertation

How to compartmentalize signaling: lipids, Hedgehog, and ciliary PKA

by
Thi Dan Nguyen

DISSERTATION
Submitted in partial satisfaction of the requirements for degree of
DOCTOR OF PHILOSOPHY

in

Developmental and Stem Cell Biology

in the

GRADUATE DIVISION
of the
UNIVERSITY OF CALIFORNIA, SAN FRANCISCO

Approved:

DocuSigned by:
Licia Selleri
C310C42C7D294CB...

Licia Selleri
Chair

DocuSigned by:
Jeremy Reiter
DocuSigned by:
Tien Peng
256E38508AB94C9...

Jeremy Reiter

Tien Peng

Committee Members

Dedications

To my father, thank you for everything. I wish that you could have been here to see me finish this journey. I am only able to be here because of you, your sacrifices, and your support. You've instilled in me a lifelong love of learning, and that has brought me to where I am today.

To Frances, thank you for being a loving and supporting partner throughout my PhD. I could not have done this without you. Thank you for being with me as I defend myself from the great unknowable universe. I love you.

To my friends and family, thank you for sticking with me through and giving me a place to belong outside of lab.

To the Reiter lab, thank you for creating a welcoming and intellectually stimulating environment for me to grow into the scientist that I am today. I could not have asked for a better scientific home to complete my PhD.

To my thesis committee members, Licia and Tien, thank you for your patience with me as I changed projects countless times over the course of my PhD. Your insights have always been incredibly helpful and I could always count on you to point me in the right direction.

To Jeremy, thank you so much for taking me on as your advisee. You have been and will continue to be my role model for decades to come. Your insight, enthusiasm, and ability to ask the most incisive questions has been incredibly inspiring to me. I can only hope that one day I'll be able to be even half as good a mentor to a young scientist as you have been to me.

Contributions and Acknowledgements

This dissertation is adapted from work originally published in *Frontiers in Cell and Developmental Biology* entitled "The Intimate Connection Between Lipids and 'Hedgehog Signaling," by Thi D. Nguyen, Melissa E. Truong, and Jeremy F. Reiter, and on BioRxiv entitled "Smoothened inhibition of PKA at cilia transduces Hedgehog signals," by Thi D. Nguyen, Mia J. Konjikusic, Lorenzo M. Del Castillo, and Jeremy F. Reiter. This work was funded by NIH R01GM095941, R01AR054396, and R01HD089918 to JR. Data for this study were acquired at the Center for Advanced Light Microscopy at UCSF on an OMX-SR obtained using grants from the NIH (5R35GM118119), the UCSF Program for Breakthrough Biomedical Research funded in part by the Sandler Foundation, the UCSF Research Resource Fund Award, and HHMI. Flow cytometry was performed at the UCSF Helen Diller Family Comprehensive Cancer Center LCA and LCA-Genomic Core Facility using grants from the NIH (P30CA082103).

We thank Roshanak Irannejad for the VASP plasmid; Aaron Marley for the SSTR3 plasmid; members of the Reiter laboratory for discussion and advice; Licia Selleri, Tien Peng, and Frances Ding for comments on the manuscript; DeLaine Larsen, Kari Herrington, SoYeon Kim, Micaela Lasser, and Nico Stuurman from the UCSF Center for Advanced Light Microscopy for microscope use and imaging assistance; Sara Elmes from the UCSF Laboratory for Cell Analysis for cell sorting instrument use and flow cytometry; Gary Moulder, Louie Ramos, William Figueroa, Francesca Penny, and Stephanie Gilbert from the UCSF Cardiovascular Building fish facility for fish husbandry; and Frances Ding for assistance writing data processing scripts.

Abstract

Cells coordinate nearly countless numbers of signaling reactions within them at any given time. To distinguish between different signaling inputs and outputs, cells utilize spatially compartmentalized signaling hubs to regulate their biochemical processes. We review how the primary cilium, an organelle specialized in intracellular signaling, utilizes lipids to create a specialized microenvironment. Hedgehog (HH) signaling in vertebrates is dependent on the primary cilium, an organelle that scaffolds signal transduction. HH signals induce Smoothened (SMO) enrichment in the cilium and indirectly triggers the conversion of GLI proteins into transcriptional activators of HH target genes. Recently, SMO has been shown to inhibit protein kinase A (PKA). To test the hypothesis that SMO specifically inhibits PKA at cilia to activate the HH signal transduction pathway, we developed a ciliary PKA biosensor. Activation of the HH signal transduction pathway by either Sonic hedgehog (SHH) or SMO agonist (SAG) inhibited ciliary PKA activity. Blocking SMO phosphorylation by GRK2/3 prevented ciliary SMO from inhibiting ciliary PKA activity. $G\alpha_{i/o}$ was dispensable for SMO inhibition of ciliary PKA. In contrast, mutating the SMO C-terminal tail protein kinase inhibitor (PKI) pseudosubstrate site interfered with the ability of SMO to inhibit ciliary PKA. Therefore, HH signaling is transduced via SMO direct inhibition of PKA at cilia, in a manner dependent on GRK2/3.

Table of Contents

List of Figures

CHAPTER 1:

The intimate connection between lipids and Hedgehog signaling

1.1 Abstract

Hedgehog (HH) signaling is an intercellular communication pathway involved in directing the development and homeostasis of metazoans. HH signaling depends on lipids that covalently modify HH proteins and participate in signal transduction downstream. In many animals, the HH pathway requires the primary cilium, an organelle with a specialized protein and lipid composition. Here, we review the intimate connection between HH signaling and lipids. We highlight how lipids in the primary cilium create a specialized microenvironment to facilitate signaling, and how HH and components of the HH signal transduction pathway use lipids to communicate between cells.

1.2 Introduction

The HH pathway functions in metazoan development as one of the principal means of cell-cell communication (Ingham and McMahon, 2001; Ingham, 2018). HH was discovered in a *Drosophila* genetic screen for developmental regulators (Nüsslein-Volhard and Wieschaus, 1980). HH proteins are secreted ligands that are interpreted by receiving cells via the transmembrane proteins Patched (PTCH) and Smoothened (SMO) to control the activity of the downstream transcription factor effectors, called Cubitus interruptus in *Drosophila* and GLI in vertebrates (Nüsslein-Volhard and Wieschaus, 1980; Nüsslein-Volhard et al., 1984; Forbes et al., 1993; Quirk et al., 1997).

HH signaling is one fundamental mechanism by which cells communicate and is deployed both in development and adult physiology to control diverse tissue dynamics, including patterning and the regulation of cell growth. Consequently, defective HH signaling in development causes birth defects, and mis-activation of HH signaling postnatally can cause cancer.

As many HH pathway components are conserved between insects and vertebrates, it was unexpected when a genetic screen in mice identified proteins required for both vertebrate HH signaling and the formation of an organelle called the primary cilium (Huangfu et al., 2003). The primary cilium is a microtubule-based organelle found on most vertebrate cells (Wheatley, 1995; Wheatley et al., 1996). Unlike motile cilia, such as those found on cells in the airway, the brain ventricles, and the oviduct that beat to move overlying fluid, primary cilia are immotile and specialized for signal transduction (Ishikawa and Marshall, 2011).

The discovery that primary cilia are required to transduce mammalian HH signaling sparked investigation into the connection between HH signaling and the primary cilium (Bangs and Anderson, 2017). Research into primary cilia in diverse organisms has revealed that evolution has played with the role of cilia in transducing HH signals. Cilia are present in all clades of extant eukaryotes, indicating that they were probably present in the last eukaryotic common ancestor (LECA), whereas the HH pathway probably arose with multicellularity (**Figure 1.1**).

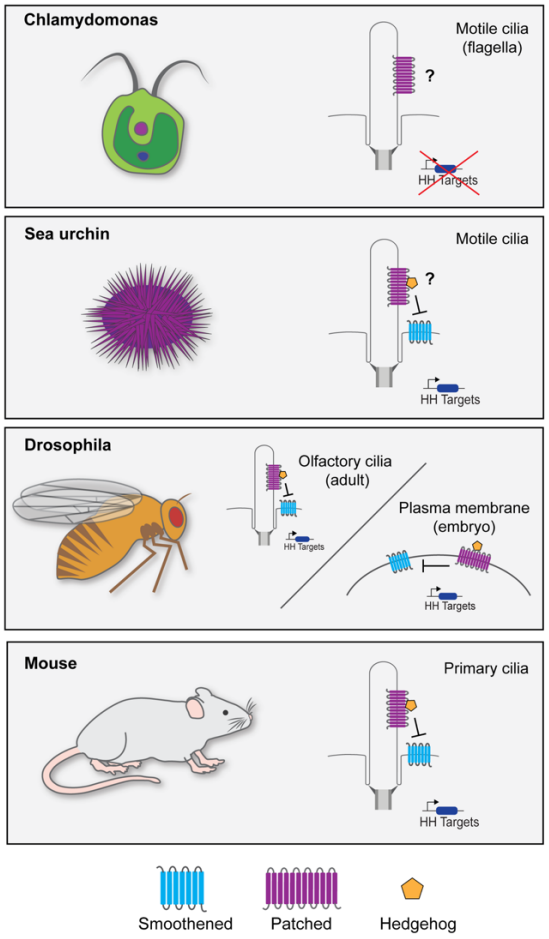

Figure 1.1 Cilia and Hedgehog signaling throughout evolution.

Though cilia are highly conserved, the reliance of HH signaling on the cilium varies through evolution. The green alga ***Chlamydomonas reinhardtii*** genome possesses two homologs of ***PTCH*** (Cre02.g093500 and Cre12.g496350), but not other components of the HH pathway. It will be interesting to determine whether either acts at the ***Chlamydomonas*** flagella. In sea urchin embryos, SMO localizes to cilia to activate HH signaling for mesoderm specification (Warner et al., 2014). Different tissues in ***Drosophila*** transduce HH signals with or without cilia. Most ***Drosophila*** cells lack cilia and transduce HH signals via Smo at the plasma membrane (Zhu et al., 2003; Jia et al., 2004). However, olfactory sensory neuron cilia in the adult fly brain signal through ciliary Smo (Kuzhandaivel et al., 2014). Vertebrates require primary cilia to transduce HH signals (Bangs and Anderson, 2017). Defects in ciliary transport or structure cause a wide range of HH-related phenotypes (Reiter and Leroux, 2017).

In vertebrates, coordinated protein trafficking of HH pathway components into and out of cilia is required for regulated signal transduction. In the absence of HH signals, Patched1 (PTCH1) and the G protein-coupled receptor GPR161 localize to the ciliary membrane (Rohatgi et al., 2007; Mukhopadhyay et al., 2013). Binding of a HH ligand, such as Sonic Hedgehog (SHH), to PTCH1 triggers exit of PTCH1 from the cilium which cues ciliary accumulation of SMO (Corbit et al., 2005). Once localized to the cilium, SMO converts GLI proteins, which localize to the ciliary tip, into transcriptional activators which leave the cilium, enter the nucleus, and induce HH target genes (Haycraft et al., 2005; Wen et al., 2010; Santos and Reiter, 2014).

One theoretical evolutionary advantage of scaffolding signal transduction within the primary cilium is that it may increase signaling fidelity by imposing an additional level of regulation through subcellular trafficking. Although the primary cilium shares a membrane that is contiguous with the plasma membrane, the cilium can signal distinctly from the rest of the cell (Delling et al., 2013; Marley et al., 2013; Truong et al., 2021). Key to its signaling functions is the maintenance of distinct ciliary protein and lipid compositions (Nachury, 2014; Mick et al., 2015).

Over the last decade, we have gained some understanding of how the protein composition of the cilium is controlled. For example, a region near the base of the cilium called the transition zone, recognized electron micrographically by prominent structures called Y-fibers connecting the axoneme to the ciliary membrane, controls protein accumulation within the cilium (Garcia-Gonzalo and Reiter, 2017; Nachury and Mick, 2019).

The distinct protein composition of the ciliary membrane raises the interesting question of whether the lipid composition of the ciliary membrane similarly differs from that of other cellular

membranes. Less is understood about how different lipids are distributed throughout the cell, including at the cilium.

Broadly speaking, lipids play three biological functions: as energy storage, as the principal components of cellular membranes, and as participants in signal transduction. Lipid droplets store neutral lipids that can be catabolized to generate ATP. Cellular membranes are primarily composed of bilayers of amphipathic phospholipids. Other lipids, such as sterols and phosphoinositides, are non-uniformly distributed and define distinct cellular membranes. Subcellular differences in lipid composition affect membrane curvature, tension, and the function of signaling proteins (van Meer et al., 2008; Harayama and Riezman, 2018).

One intercellular communication pathway dependent on lipids is HH signaling. For example, lipidation of HH ligands is key to their activity and extracellular distribution as gradients to pattern developing tissues (Eaton, 2008). Downstream of HH, the HH receptor PTCH1 transports sterols to affect the composition of the membrane (Zhang et al., 2018; Kinnebrew et al., 2021; Qi et al., 2019). Sterols also regulate the activity of the central HH pathway component SMO (Cooper et al., 2003; Myers et al., 2013, 2017; Nachtergaele et al., 2013; Nedelcu et al., 2013; Byrne et al., 2016; Huang et al., 2016; Luchetti et al., 2016; Xiao et al., 2017; Huang et al., 2018; Raleigh et al., 2018). Still other lipids, phosphoinositides, are read out by TUBBY family proteins to control the trafficking of HH signal transduction component GPR161 to cilia (Chávez et al., 2015; Garcia-Gonzalo et al., 2015). In this review, we focus on the role of lipids in HH signaling, especially at the ciliary membrane. We examine how the lipid composition of the primary cilium creates a specialized microenvironment essential for vertebrate HH signaling. Additionally, we dissect how these lipids function in embryonic development and how their dysregulation causes birth defects. Further research into how lipids function in HH signaling, particularly within the primary cilium,

may illuminate general principles by which the subcellular distribution of lipids is controlled to contribute to protein function and the propagation of information.

1.3 Ciliary Membranes Have a Distinct Lipid Composition

In protists, biochemical assessments have indicated that the lipid composition of cilia is distinct. For example, the ciliary membranes of ***Paramecia*** and ***Tetrahymena*** are enriched in phosphonolipids (consisting of the well-named ciliatine attached to a lipid backbone) and sphingolipids (Kennedy and Thompson, 1970; Smith et al., 1970; Andrews and Nelson, 1979; Kaneshiro et al., 1984). In ***Paramecia***, a mutation that alters ciliary sphingolipid levels compromises the function of voltage-sensitive channels, suggesting that its distinct lipid composition is critical for ciliary protein function and that sphingolipids may be particularly important for ciliary biology (Forte et al., 1981).

One sphingolipid, sphingomyelin, can sequester sterols in complexes (Leathes, 1925; McConnell and Radhakrishnan, 2003; Das et al., 2014). Filipin, a mixture of polyene macrolides, binds 3-β-hydroxysterols and can be observed in freeze-fracture electron microscopy (Kinsky et al., 1966). In the distantly related protists Euglena and Trypanosomes, filipin staining revealed that sterols are enriched in the flagellar membrane (Melkonian et al., 1982; Souto-Padrón and de Souza, 1986; Tetley, 1986). In quail, filipin staining also demonstrated robust enrichment of 3-β-hydroxysterols in the ciliary membrane (Chailley and Boisvieux-Ulrich, 1985). Similarly, Laurdan staining of ordered lipids suggested that ciliary membranes are enriched in sterols (Tyler et al., 2009). As described further below, sterols contribute to HH signaling, and thus ciliary sphingolipids, by controlling the accessibility of sterols, can limit the signaling functions of the

cilium. Indeed, sphingomyelin biosynthetic pathway enzymes restrain HH signaling (Kinnebrew et al., 2019).

How else might ciliary lipids contribute to ciliary protein function? One possibility is that they function as specific cofactors for ciliary proteins. Some lipids, such as phosphoinositides, may be at lower molar concentrations than their interacting proteins and thus may function as regulatory cofactors. Another possibility is that ciliary lipids impart a distinct biophysical or biochemical property to the ciliary membrane which is itself important for protein function. Lipids help determine membrane viscosity, surface charge and ion-binding capacity. By affecting any of these parameters, ciliary lipids may affect signal transduction by ciliary proteins, and perhaps especially ciliary membrane-associated proteins.

The ciliary membrane consists of a fraction of the cellular membrane, less than 0.01% of the total (Mukhopadhyay et al., 2017) and, to date, lipidomic characterizations of cilia have been restricted to those of organisms from which cilia can be collected in biochemical quantities (Lobasso et al., 2010; Raleigh et al., 2018). Previously, we fractionated membranes of sea urchin cilia from other cellular membranes and discovered that sea urchin cilia were enriched in several oxysterols, oxygenated derivatives of cholesterol (Raleigh et al., 2018).

Due to technical challenges in purifying mammalian primary ciliary membranes, we know less about which lipids compose vertebrate primary cilia than the cilia of protists and invertebrates. Techniques for determining the subcellular localization of lipids lag behind equivalent approaches for proteins. For example, proximity labeling approaches have greatly accelerated elucidation of the mammalian ciliary proteome (Mick et al., 2015). The ability to label lipids in specific subcellular domains does not currently exist, but its development would be a boon to comparing

the lipid composition of many subcellular membranes, not just that of the ciliary membrane. Similarly, fluorescence imaging of lipids is hampered by the lack of molecular probes for most lipids (Balla and Várnai, 2002; Wills et al., 2018).

Because of the limitations to identifying ciliary lipids in vertebrate cells, we do not know whether the enrichment of sphingolipids and sterols extends to the many types of animal cilia. Indeed, staining of mammalian cilia for sterols has shown conflicting results about whether sterols are enriched (Nelson et al., 2008; Breslow et al., 2013; Kinnebrew et al., 2019; Miyamoto et al., 2020). Thus, sterol enrichment in cilia may be cell type-specific or be limited to a class of sterols detected by specific visualization methods.

However, like sea urchin, sea anemone, and protists, mammalian sperm can be fractionated into their heads, analogous to cell bodies, and tails, analogous to cilia (Toshimori et al., 1985; Connor et al., 1998; Mourvaki et al., 2010). Sterol levels in the sperm heads and tails differ, suggesting that, as in protists, lipids may be differentially distributed between the cilium and other subcellular compartments in animal cells.

1.4 Ciliary Phosphoinositides Regulate GPCR Delivery and HH Signaling

Recent reviews have described how lipids contribute to ciliary structure (Garcia et al., 2018; Nechipurenko, 2020). In this section, we focus specifically on how ciliary lipids participate in the transduction of HH signals, the best understood of the intercellular cues communicated via cilia. The best understood of the lipids participating in ciliary signaling are the phosphoinositides.

Phosphoinositides are phosphorylated lipids that confer molecular identity to cellular membranes (di Paolo and de Camilli, 2006; Shewan et al., 2011). Reversible phosphorylation of

phosphatidylinositol can give rise to seven distinct phosphoinositides which exhibit distinct subcellular distributions (Schink et al., 2016). For instance, the Golgi membrane is enriched in PI(4)P, whereas the nuclear envelope is enriched in PI(5)P (Shewan et al., 2011). Physical separation of these membranes helps partition these distinct phosphoinositides.

Thus, it is surprising that the phosphoinositide compositions of the ciliary and plasma membranes are distinct despite being contiguous, with the ciliary membrane being relatively enriched in PI(4)P and the plasma membrane relatively enriched in $PI(4,5)P_2$ (Conduit and Vanhaesebroeck, 2020; Conduit et al., 2021). An additional domain of $PI(3,4,5)P_3$ localizes near the ciliary base (**Figure 1.2**) (Dyson et al., 2017).

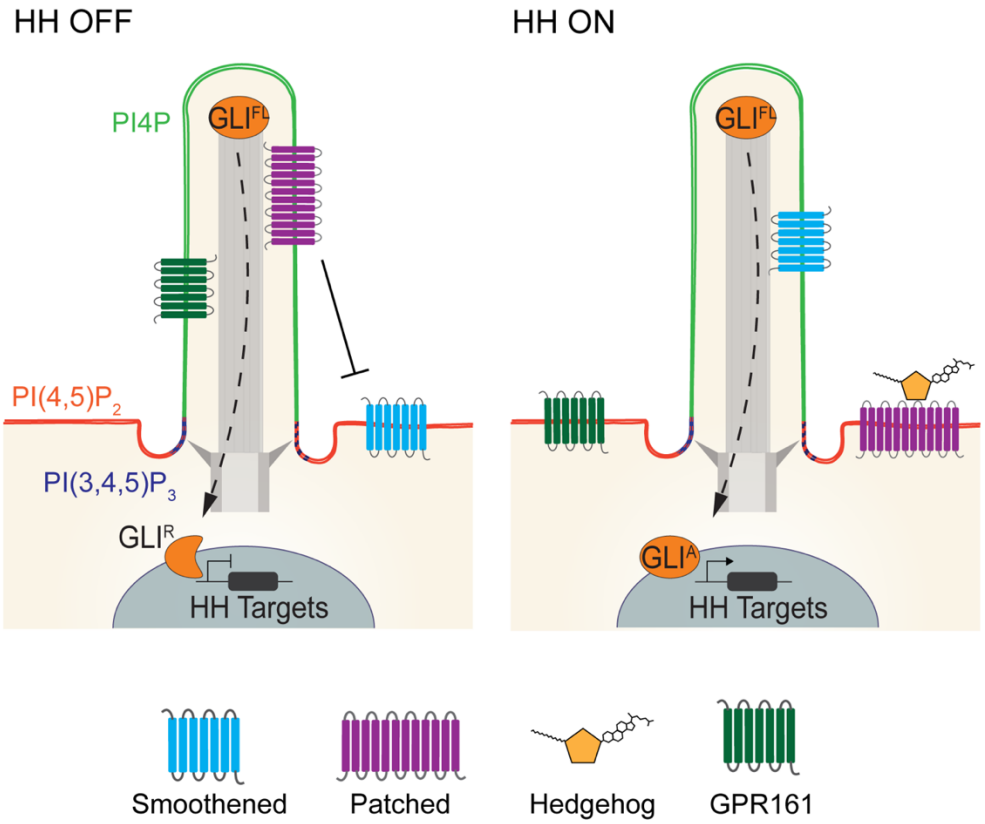

Figure 1.2. Lipid domains within vertebrate cilia.

Vertebrate HH signaling depends on the tightly coordinated trafficking of pathway components into and out of cilia. In the absence of HH signals, PTCH1 localizes to cilia and represses SMO. Consequently, GLI transcription factors are proteolytically processed to their repressor state to inhibit HH target genes. HH binding to PTCH1 leads to SMO accumulation in cilia, GPR161 exit, and GLI activator formation to induce HH target gene expression (Bangs and Anderson, 2017; Kong et al., 2019). Specialized membrane domains within mouse and human cilia allow for HH signal transduction. Mouse and human cilia are enriched in the phosphoinositide PI(4)P, whereas PI(4,5)P_2 is enriched outside of the cilium. Defects in the distribution of these two lipids causes mislocalization of HH pathway components such as GPR161 to cause birth defects (Chávez et al., 2015; Garcia-Gonzalo et al., 2015). In contrast to PI(4)P, PI(4,5)P_2 and PI(3,4,5)P_3 are enriched at the transition zone at the ciliary base (Dyson et al., 2017; Conduit and Vanhaesebroeck, 2020).

How might this phosphoinositide boundary be maintained? One strategy for maintaining distinct lipid compositions within a contiguous membrane is through control of the localization of lipid biosynthetic enzymes. In mammals, three phosphoinositide 5-phosphatases (INPP5E, INPP5B and OCRL) convert PI(4,5)P_2 into PI(4)P and localize to primary cilium (Bielas et al., 2009; Jacoby et al., 2009; Luo et al., 2012, 2013). Though these proteins may share overlapping functions, INPP5E is required to generate PI(4)P in the primary cilia of many cells (Chávez et al., 2015; Garcia-Gonzalo et al., 2015).

Maintenance of elevated PI(4)P and depleted PI(4,5)P_2 within the ciliary membrane is critical for HH signal transduction (Chávez et al., 2015; Garcia-Gonzalo et al., 2015; Dyson et al., 2017). Loss of INPP5E reduces ciliary PI(4)P and increases ciliary PI(4,5)P_2. The Tubby-family protein TULP3 binds PI(4,5)P_2 to control the delivery of a negative regulator of HH signaling, GPR161, to cilia. In the absence of INPP5E and ciliary PI(4)P, TULP3 and GPR161 mis-accumulate in cilia (Chávez et al., 2015; Garcia-Gonzalo et al., 2015). GPR161 activates protein kinase A (PKA), a negative regulator of GLI activity via direct binding to the regulatory subunit of PKA (PKA-R), and constitutive coupling to the G-protein Gαs, to generate cAMP, the principal PKA activator (Mukhopadhyay et al., 2010, 2013; Bachmann et al., 2016). We recently identified a pool of ciliary PKA (Truong et al., 2021). Thus, mis-activation of ciliary PKA to tonically inhibit GLI activity is likely to be how loss of INPP5E or ciliary PI(4)P suppresses HH signaling. Future work may elucidate how TULP3, and its paralogs including the obesity-associated protein TUBBY, read ciliary phosphoinositide composition to limit the ciliary localization of GPR161 and perhaps other GPCRs.

Aside from affecting GPCR localization, ciliary phosphoinositides may also directly affect GPCR function. Phosphoinositides can stabilize GPCR active states or enhance specific G-protein

coupling (Yen et al., 2018). Differences in phosphoinositide composition between the ciliary and plasma membranes may allow cells to control GPCR output with spatial precision. For example, perhaps ciliary GPCRs, such as GPR161, may be tuned to be active specifically in domains rich in PI(4)P. And perhaps other GPCRs, such as FFAR4, which may operate at the ciliary membrane in preadipocytes and at the plasma membrane in adipocytes, may couple differently to G-proteins in these two different domains to allow for different outputs at different stages of differentiation (Hilgendorf et al., 2019).

1.5 Ciliary Sterols Activate Smoothened

Sterol lipids are a diverse class of lipids synthesized by the mevalonate pathway. Both cholesterol, the predominant sterol in vertebrate cells, and select oxysterols can bind to SMO to activate the HH pathway (Cooper et al., 2003; Dwyer et al., 2007; Myers et al., 2017). As SMO localization to primary cilia is required for activation of the HH pathway, the sterol composition of the ciliary membrane may contribute to SMO function. A recent study used a loss-of-function CRISPR-based approach to identify sterol biosynthetic genes that influence the strength of HH signaling (Kinnebrew et al., 2019). Liquid chromatography-tandem mass spectrometry of biochemically isolated sea urchin and porcine renal cells (LLC-PK1) helped to identify SMO-activating oxysterols enriched in cilia (Raleigh et al., 2018).

Unlike the case with phosphoinositides, there is not clear evidence of enriched localization of sterol or oxysterol catabolic enzymes at the cilium itself. However, a recent study identified sterol biosynthetic enzymes that localize at the ciliary base, including DHCR7 (Findakly et al., 2021). DHCR7 is mutated in Smith-Lemli-Opitz syndrome, an inherited disease characterized by holoprosencephaly. The holoprosencephaly is thought to be secondary to reduced HH signaling

caused by the accumulation of SMO-inhibiting sterols (Fitzky et al., 1998; Wassif et al., 1998; Matsumoto et al., 2005; Nowaczyk and Irons, 2012; Sever et al., 2016). DHCR7 catalyzes the terminal step in cholesterol and 24,25-epoxycholesterol synthesis. As an integral membrane protein, DHCR7 near the ciliary base may be in the ciliary pocket membrane, a membrane invagination that surrounds the cilium (Findakly et al., 2021). DHCR7 relocalizes away from the ciliary base upon HH pathway activation, suggesting that control of the subcellular localization of sterol biosynthetic machinery may modulate ciliary lipid composition to tune HH signaling. However, understanding how sterol content in cilia is controlled remains a major challenge, particularly as existing sterol biosensors are less specific than biosensors for other lipids such as phosphoinositides (Maekawa and Fairn, 2014; Wills et al., 2018).

1.6 Hedgehog Ligands Are Both Cholesterylated and Palmitoylated

Not only are lipids critical for creating specialized sub-cellular compartments that facilitate signaling, but lipids participate with certain core components of the HH pathway in ways critical for signaling. For example, HH proteins are covalently linked to palmitoyl and cholesterol (Porter et al., 1996a; Porter et al., 1996b; Pepinsky et al., 1998). Initially, HH is synthesized as a 45 kDa precursor comprised of a signal peptide, an N-terminal signaling domain (HhN) and a C-terminal intein (HhC) (Lee et al., 1994). Concurrent with synthesis, the signal peptide is cleaved, revealing a highly conserved N-terminal cysteine residue that is palmitoylated by Hedgehog acetyltransferase (called HHAT or SKI) (Pepinsky et al., 1998; Amanai and Jiang, 2001; Chamoun et al., 2001; Micchelli et al., 2002; Buglino and Resh, 2008). Additionally, the intein catalyzes HH cleavage and links cholesterol with the newly exposed C-terminus of HhN, thereby creating a fully processed, ~19 kDa protein that is dually lipidated (Porter et al., 1996a; Porter et al.,

1996b; Pepinsky et al., 1998). Perturbing HH lipidation has different effects in vertebrates and in ***Drosophila***, which we discuss in two broad categories: signaling activity and signal distribution.

1.7 Palmitoylation Is Important for HH Signaling Strength

The signaling potency of *Drosophila* HH and vertebrate SHH are differentially dependent on palmitoylation. In mouse fibroblast cells, non-palmitoylated SHH can still signal, albeit at reduced strength (Pepinsky et al., 1998). Similarly, non-palmitoylated SHH exhibits attenuated signaling ***in vivo***, but, when overexpressed in the mouse embryonic limb bud, can, like overexpressed wild-type SHH, induce HH target genes and polydactyly (Lee et al., 2001; Chen et al., 2004).

In contrast to the mouse, un-palmitoylated Hh in *Drosophila* interferes with the signaling activity of wild-type Hh when globally overexpressed (Lee et al., 2001). Interestingly, this lack of activity seems to be specific to the ligand, and not to the system, since un-palmitoylated mouse SHH retains some signaling ability when ectopically expressed in the ***Drosophila*** wing disc (Chamoun et al., 2001). Un-palmitoylated HH can still partially rescue HH loss-of-function in the embryo (Gallet et al., 2003) and can induce HH signaling in the ***Drosophila*** wing disc (Callejo et al., 2006). Despite some species-specific dependence on palmitoylation, the palmitoyl moiety on Hedgehog proteins is critical for full signaling activity.

Cryo-EM structures of PTCH1 binding SHH reveal that SHH can bind in multiple conformations. In one conformation, the palmitoyl group makes extensive interactions in an extracellular cleft of PTCH1 composed of its two major extracellular loops, providing structural

insight into one way that SHH blocks PTCH1 to activate the pathway (Qi et al., 2018a; Qi et al., 2018b; Qian et al., 2019).

1.8 HH Cholesterylation Promotes Long-Distance Signaling

In addition to binding PTCH1 to activate the downstream pathway, the developmental functions of HH ligands in tissue patterning depend on its distribution. In the neural tube, SHH forms a gradient, highest ventrally at its sites of production, the notochord and floor plate, and decreases dorsally. In the limb bud, SHH produced posteriorly in the zone of polarizing activity decreases in concentration anteriorly. Palmitoylation of vertebrate SHH is required for long-distance signaling as un-palmitolyated SHH is largely restricted to its sites of production (Lee et al., 2001; Chen et al., 2004). Importantly, both HH and SHH proteins that lack cholesterol are still competent to induce downstream transcriptional changes in receiving cells (Porter et al., 1996a; Lewis et al., 2001; Zeng et al., 2001; Li et al., 2006). Still, un-cholesterylated SHH cannot signal over long distances (Lewis et al., 2001). Thus, both lipid modifications are critical for vertebrate HH distribution, but cholesterylation may be more relevant to the range of signaling, rather than its signaling potency.

Drosophila demonstrate a cell-type specific requirement for lipidation, as un-cholesterylated Hh exhibits either restricted (Porter et al., 1996b; Burke et al., 1999; Dawber et al., 2005; Callejo et al., 2006; Gallet et al., 2006; Su et al., 2007) or expanded (Gallet et al., 2003, 2006; Panáková et al., 2005) spatial distribution in different tissues.

These differences in HH distribution in different organisms or tissues represents just one way in which HH signaling can be adapted. Another difference is the requirement for primary cilia

in HH signal transduction. HH signal transduction in the *Drosophila* wing disc is independent of primary cilia. Indeed, wing disc cells lack cilia. In stark contrast, vertebrate HH signal transduction requires primary cilia (Huangfu and Anderson, 2005).

Additional vertebrate-specific requirements in HH signal transduction include the involvement of Scube-family proteins, vertebrate-specific extracellular proteins that facilitate HH release from producing cells. Scube proteins, though dispensable individually, are collectively required for HH signaling (Kawakami et al., 2005; Woods and Talbot, 2005; Hollway et al., 2006; Johnson et al., 2012). ***In vitro***, SCUBE2 specifically binds to and promotes the release of cholesteroylated SHH (Creanga et al., 2012; Tukachinsky et al., 2012; Wierbowski et al., 2020). Perhaps these species-specific differences in how HH signals are released from producing cells account for the different dependencies on lipidation for signaling by ***Drosophila*** HH and vertebrate SHH.

1.9 HH May Communicate Over Long Distances via Multiple Mechanisms

How can HH act over multiple cell diameters as a morphogen once it is dually lipidated? As both lipid adducts on HH, cholesterol and palmitoyl, are poorly soluble in aqueous environments, HH would be expected to remain associated with membranes and not diffuse in the extracellular space. Conflicting results from studies done in *Drosophila***,** zebrafish, and mouse are difficult to reconcile, raising the possibility that different organisms or different tissues distribute HH proteins in different ways. For example, there is evidence supporting the presence of HH in higher order assemblies that are less hydrophobic than monomeric lipidated HH, including as multimers, as constituents of liposomes, and as components of extracellular vesicles called exosomes.

One possibility is that HH multimerizes and internalizes its lipid moieties, exposing its hydrophilic proteinaceous face to the extracellular environment**.** ***In vitro*****,** overexpressed HH will contribute to signaling-competent, high-molecular weight species in a way that depends on lipidation (Zeng et al., 2001; Chen et al., 2004; Gallet et al., 2006; Goetz et al., 2006). It remains unclear whether these high-molecular weight species exist *in vivo***.**

It also is unclear whether proteins beyond HH contribute to these high-molecular weight complexes. Lipoprotein particles are extracellular macromolecular assemblies comprised of a core of esterified cholesterol moieties and triglycerides in association with apolipoproteins (Babin et al., 1999). HH can be released from *Drosophila* wing disc cells and human cultured cells as part of lipoprotein particles (Panáková et al., 2005; Palm et al., 2013). HH associated with liproprotein particles has low signaling activity (Palm et al., 2013), raising a question of whether this form of HH is critical to its function in developing tissues.

Additionally, HH may traffic on extracellular vesicles *in vitro*, in the *Drosophila* wing disc, and in developing mouse embryos (Tanaka et al., 2005; Matusek et al., 2014; Vyas et al., 2014). These extracellular vesicles may be formed via multivesicular body assembly or plasma membrane budding, mechanisms that are dependent on the endosomal sorting complex required for transport (ESCRT) (Matusek et al., 2014; Coulter et al., 2018). Whether these HH-containing extracellular vesicles have signaling capabilities and whether they can generate a morphogen gradient ***in vivo*** remain to be determined.

Some HH is not secreted but, rather, remains attached to the membrane and trafficked on long and thin cytonemes, specialized, actin-based cytoplasmic extensions as long as 200 µm (Kornberg, 2014). Cytonemes observed in the *Drosophila* wing disc correspond in length to the

distribution of HH signaling and can also contain PTCH, raising the possibility that cytonemes can both send and receive signals (Bischoff et al., 2013; Gradilla et al., 2014). In the developing chick limb, cytonemes also contain HH, indicating that cytonemes may represent an evolutionarily conserved mechanism for distributing HH signals (Sanders et al., 2013). It will be of interest to specifically disrupt vertebrate cytonemes to assess how they shape HH signaling.

1.10 The HH Receptor, PTCH, Transports Sterols

Beyond HH itself, constituents of the HH signal transduction pathway are intimately associated with lipids. The HH receptor is a twelve-pass transmembrane protein called Patched (PTCH), of which most vertebrates have two homologs, PTCH1 and PTCH2 (Ingham and McMahon, 2001). PTCH proteins form a clade of the larger resistance-nodulation-division (RND) transporter-like family (Taipale et al., 2002). Bacterial RND proteins are exporters of diverse molecules that include hopanoids, sterol-like molecules (Tseng et al., 1999). In addition to PTCH, the RND family includes NPC1, a transporter which in animals conducts cholesterol across the lysosomal membrane (Kwon et al., 2009). Like NPC1, PTCH includes a sterol-sensing domain (SSD), implicated in the subcellular trafficking of sterols. Another similarity to NPC1 is that PTCH1 contains a hydrophobic channel that may contain sterols (Gong et al., 2018).

These structural similarities suggest that PTCH1 functions similarly to NPC1, validated by several cryo-EM-elucidated structures of the core of PTCH1 (Qi et al., 2018a; Qi et al., 2018b; Gong et al., 2018; Qi et al., 2019; Qian et al., 2019; Rudolf et al., 2019). Indeed, PTCH1 can efflux a fluorescent form of cholesterol and SHH inhibition of PTCH1 increases intracellular cholesterol concentration (Bidet et al., 2011). Structural analysis reveals that PTCH1 interacts with sterols at ten or more sites and can partially lift sterols out of the membrane bilayer (Qi et al., 2019).

Although the functional importance of the partial removal of a sterol from the membrane is unclear, it may represent an intermediate step in sterol transport. Indeed, PTCH1 can transport lipid sterols away from the inner leaflet of the membrane (Zhang et al., 2018; Qi et al., 2019) and it is likely that the binding of PTCH1 to HH blocks PTCH1 to allow buildup of a SMO-activating sterol, perhaps specifically in the ciliary membrane, thereby activating the downstream signal transduction pathway.

Numerous PTCH1 mutations associated with the human birth defect holoprosencephaly increase its ability to inhibit SMO (Petrov et al., 2021). Loss-of-function mutations in PTCH1 cause misactivation of SMO and some forms of cancer (Gailani et al., 1996; Hahn et al., 1996; Johnson et al., 1996). Whether either set of missense mutations alter sterol transport will be interesting to assess.

Other hints about PTCH function can be gleaned from evolutionary perspectives. Some bilateria, notably *Caenorhabditis elegans*, have lost the HH pathway but retained PTCH homologs. One of these, PTR-18 clears a secreted protein, GRL-7, distantly related to HH (Chiyoda et al., 2021), suggesting that PTCH can be repurposed to function independently of HH pathway regulation. Another *C. elegans* PTCH homolog, PTC-3, prevents intracellular cholesterol accumulation (Cadena del Castillo et al., 2021), further supporting the idea that PTCH family members are sterol transporters.

Interestingly, a paralog of PTCH cleverly called Dispatched1 (DISP1) functions not in HH reception but in transmitting HH from the cells in which it is produced (Burke et al., 1999). DISP1 forms a sodium channel and depends on the sodium gradient to release SHH from producing cells, raising the possibility that flux of sodium down its chemiosmotic gradient may power the

extraction of cholesteroylated HH from the membrane (Petrov et al., 2020; Wang et al., 2021). Recent structures of DISP1 reveal that, like PTCH1, it partially displaces a sterol from the membrane bilayer (Wang et al., 2021). This lifted sterol may represent an ability of DISP1 to pry the cholesterol adduct of HH out of the plasma membrane, potentially a step in its transfer of HH to SCUBE2.

Many of the residues involved in coordinating sodium are also present in PTCH1, consistent with evidence that a sodium or potassium gradient is critical to the ability of PTCH1 to suppress the signaling activity of SMO (Myers et al., 2017; Petrov et al., 2020). It will be interesting to determine how PTCH1 uses a monovalent cation gradient. Perhaps cation flux through PTCH1 powers the removal of SMO-activating sterols from the ciliary membrane in a way that is analogous to RND-mediated export of hopanoids from the inner membrane of bacteria.

In addition to PTCH, HH is bound by additional proteins not essential for all HH communication, including HHIP, CDON, BOC, GAS1 and LDL receptor-related protein 2 (LRP2) (Chuang and McMahon, 1999; Stebel et al., 2000; Yao et al., 2006; Zhang et al., 2006; Christ et al., 2012). These auxiliary HH-binding proteins operate differently from each other: HHIP negatively regulates HH signaling while the others potentiate HH signaling (except for in the retina, where LRP2 inhibits HH signaling) (Christ et al., 2015).

As its name implies, LRP2 is a member of the family of low-density lipoprotein (LDL) receptors. LRP2 is required, like SHH, for forebrain development in mice (Willnow et al., 1996). Inherited mutations of ***LRP2*** in humans cause Donnai-Barrow syndrome, which includes craniofacial defects that may be related to altered HH signaling (Kantarci et al., 2007, 2008).

Some other LRP family members also function in developmental pathways. For example, LRP5 and LRP6 are part of the WNT receptor complex (Pinson et al., 2000). WNT ligands, like HH, are palmitoylated (Willert et al., 2003). The best studied member of the family, LDLR, binds and endocytoses LDL, bringing cholesterol into the cell. In addition to HH, LRP2 binds to a variety of ligands, including proteins that carry steroid-like molecules (Christensen et al., 1999; Nykjaer et al., 1999; Hammes et al., 2005).

Where do ciliary lipids come from? In animals, cholesterol is generated within the cytosol and endoplasmic reticulum (ER) or delivered via LDLs. Upon uptake, LDL is endocytosed and fused with lysosomes to release cholesterol for delivery to the plasma membrane (Brown and Goldstein, 1986). A key regulator of plasma membrane cholesterol content is NPC1, mutated in Neiman-Pick disease. Mice lacking NPC1 show decreased ciliogenesis and shortened cilia, with decreased HH signaling in the cerebellum, raising the possibility that NPC1 helps deliver cholesterol to the ciliary membrane (Canterini et al., 2017). However, NPC1 is not generally required for HH signaling, indicating that either there are NPC1-independent mechanisms of delivering cholesterol to the ciliary membrane or that NPC1-dependent ciliary cholesterol is not essential for HH pathway activation.

The endocytosis of a variety of lipid-associated proteins via LRP family members raises the possibility that internalization of extracellular lipids was the original role for these proteins. Although speculative, it is possible to imagine that extracytosolic lipid-binding proteins, functionally akin to the evolutionarily ancient tubular lipid-binding proteins (TULIPs) or the more recently evolved cholesterol carrier NPC2, might have facilitated lipid uptake (Wong and Levine, 2017). Perhaps upon acquisition of multicellularity and increased needs for cell-cell communication, these extracellular lipid-binding proteins became lipoprotein receptors and

acquired new roles in information transmission. The genomes of the simple animals, such as *Trichoplax*, sea anemones and sponges, encode members of the LRP family member (e.g., TRIADDRAFT_27379, TRIADDRAFT_19424, A0A1X7TVZ2), suggesting that LRP proteins arose before porifera and placozoa split from each other early in the evolution of multicellular animals. Thus, it is possible that evolution acted on a system for lipid nutrient uptake, converting it into systems for cell-cell communication such as WNT and HH signaling.

Like LRP proteins, a canonical HH pathway is present in many basal animals, including sponges and sea anemones, but is absent from choanoflagellates and other single-celled eukaryotes (Figure 2.1). Despite the absence of the complete HH pathway in protists, PTCH homologs are present in some protist genomes, raising the intriguing possibility that PTCH is the most evolutionarily ancient member of the pathway and was subsequently co-opted for HH signal transduction. For example, *Chlamydomonas* possesses two PTCH orthologs (Cre02.g093500 and Cre12.g496350) which, unfortunately, have not been studied.

The main sterol in *Chlamydomonas* membranes is not cholesterol, but ergosterol (Gealt et al., 1981). It will be interesting to discover whether protist PTCH family members share the interaction with sterols with their metazoan cousins. As yeast NPC1 transports ergosterol and animal NPC1 transports cholesterol, it is possible that PTCH has similarly evolved to transport different sterols in different organisms. Interestingly, one ***Chlamydomonas*** flagellar lipid, an ergosterol endoperoxide, can inhibit mammalian HH signaling (Sever et al., 2016), raising the possibility that protist PTCH homologs could act on sterols with sufficient similarity to animal sterols that they can interact with the mammalian HH signal transduction pathway. Perhaps elucidating the functions of protist PTCH homologs will provide insights into the types of sterols transported by these elusive channels.

1.11 Cholesterol and Oxysterols Can Activate Smoothened

PTCH suppresses the function of SMO, the central positive activator of the downstream HH signal transduction pathway. SMO is comprised of an N-terminal, extracellular cysteine-rich domain (CRD), an extracellular linker domain, a transmembrane heptahelical bundle (HHB), and a C-terminal cytosolic tail.

How might PTCH inhibit SMO activity? Previous hypotheses posited that PTCH directly binds to and sequesters SMO in a way that is relieved upon HH binding to PTCH (Stone et al., 1996; Murone et al., 1999). However, PTCH and SMO do not interact tightly and have distinct subcellular distributions, even in the primary cilium (Denef et al., 2000; Corbit et al., 2005; Rohatgi et al., 2007). Moreover, PTCH can inhibit SMO sub-stoichiometrically, with half-maximal pathway activity observed only when SMO was in 50-fold molar excess of PTCH (Taipale et al., 2002). These data, combined with the ability of PTCH to transport sterols (Zhang et al., 2018; Qi et al., 2019), suggests that PTCH may export a SMO-activating sterol.

Like PTCH, SMO binds sterols at several sites (**Figure 1.3A,C**) (Myers et al., 2013; Rana et al., 2013; Byrne et al., 2016; Huang et al., 2016, 2018; Luchetti et al., 2016; Raleigh et al., 2018; Deshpande et al., 2019). SMO mutations that alter individual sterol sites, either within the CRD or HHB, compromise HH signal transduction (Myers et al., 2013; Nachtergaele et al., 2013; Raleigh et al., 2018), suggesting that sterol binding is important for signal transduction.

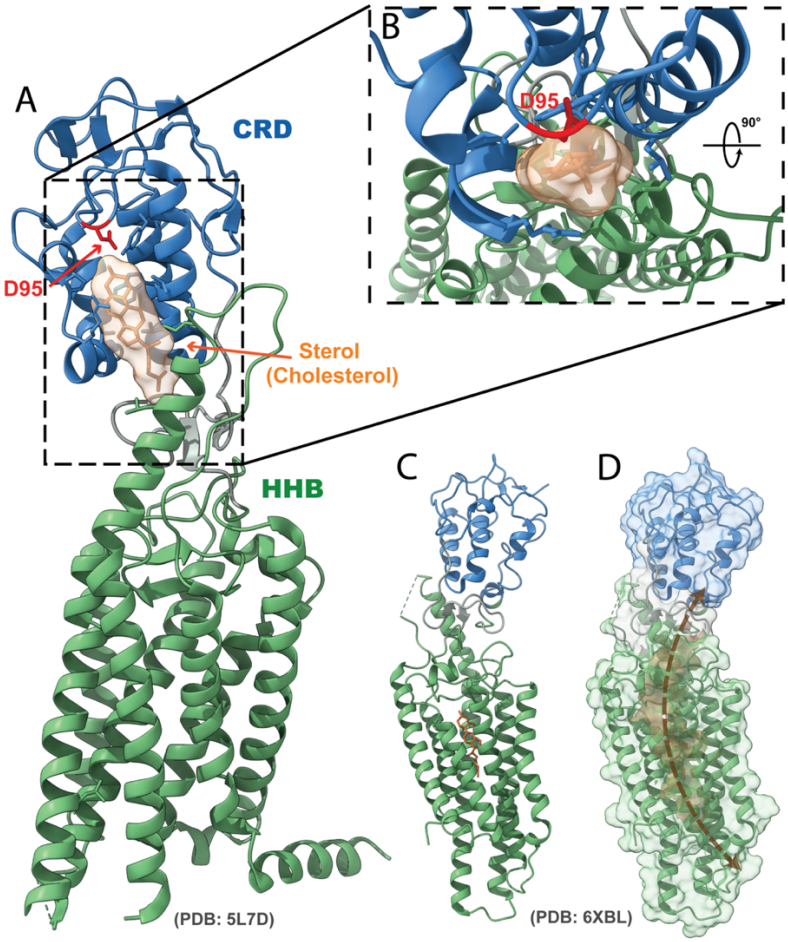

Figure 1.3. Structure of SMO bound to sterols.

(A) Ribbon representation of the crystal structure of human SMO bound to a sterol in the CRD, with cholesterol depicted (PDB: 5L7D). Blue, CRD; green, HHB; orange, sterol; red, residue D95. **(B)** Inset depicts a top-down view of the CRD binding pocket with a sterol bound. **(C)** Structure of human SMO with one of the putative sterol-binding sites in the HHB depicted (PDB: 6XLB). **(D)** Surface rendering of the potential sterol channel in SMO.

How sterols activate SMO binding remains unclear. Although unprecedented for a GPCR-like protein, one possibility is that these binding sites form a continuous intramolecular channel through SMO capable of sterol transport (Figure 2.3C,D) (Huang et al., 2018; Qi et al., 2020). Mutations in the HHB that are likely to prevent sterol movement within SMO constitutively activate signaling (Qi et al., 2020). Perhaps these mutations block sterol transit through SMO and increased sterol occupancy within SMO is sufficient to activate SMO.

In addition to interacting with sterols, SMO can be covalently modified by cholesterol at the CRD (Xiao et al., 2017). This cholesterylation occurs in human SMO at the D95 residue (mouse SMO D99) within the CRD sterol binding site (Byrne et al., 2016) (Figure 2.3A,B). Mutation of this aspartic acid to hinder cholesterol modification of SMO compromises ciliary localization and signaling (Xiao et al., 2017; Hu et al., 2022). Thus, it is likely that covalent binding of SMO to cholesterol stabilizes its active state. It will be interesting to establish whether both non-covalent and covalent interaction with cholesterol are sufficient to promote pathway activity ***in vivo***.

The cholesterylation of SMO is inhibited by PTCH1 and promoted by HH ligand (Xiao et al., 2017). Understanding where within the cell SMO is cholesterylated (e.g., before or after ciliary localization) will help reveal how sterols affect HH signaling. As SMO lacking the CRD domain is still able to weakly activate the downstream pathway (Raleigh et al., 2018), sterol interaction with the CRD is likely to be a modulatory effect on SMO activity.

Both oxysterols and cholesterol can bind SMO. However, it is still an open question which sterols activate SMO ***in vivo***. Indeed, the SMO-activating sterol may be cholesterol, oxysterol, or some combination thereof. Given that cholesterol is a highly abundant lipid in the plasma membranes of animal cells and quickly transits between the inner and outer leaflets, it is unclear

how PTCH1 could inhibit cholesterol accumulation specifically in the outer leaflet to prevent SMO misactivation. One possibility is that much of the membrane-associated cholesterol is sequestered as a form that cannot regulate SMO (Kinnebrew et al., 2019; Radhakrishnan et al., 2020). Thus, the pool of cholesterol relevant to SMO regulation ("accessible" cholesterol) may be smaller than the total cholesterol pool.

Certain oxysterols [e.g., 7β,27-DHC, 24k-C, and 24(S),25-EC] are enriched in the primary cilium, can bind to SMO, and can promote the accumulation of SMO in cilia, and thus are candidate regulators of SMO activation (Raleigh et al., 2018). As SMO possesses multiple sterol binding sites (Myers et al., 2013; Raleigh et al., 2018; Qi et al., 2020), multiple sterols may be relevant even to a single molecule of SMO. Indeed, it could even be possible that the same sterol could antagonize SMO function when binding at or near the orthosteric site within the heptahelical core and agonize SMO when binding the extracellular CRD.

1.12 Conclusion

In this review, we have summarized the intimate connection between HH signaling and lipids. Lipids participate in the HH-mediated orchestration of developmental and homeostatic processes at multiple levels, including as constituents of cellular membranes, as ligands or substrates for key pathway components, and as covalent modifiers of HH and SMO.

Cilia are evolutionarily ancient organelles which possess a distinct ciliary lipid composition in organisms as diverse as *Chlamydomonas***,** *Tetrahymena* and *Paramecia***.** In vertebrates, primary cilia also have a unique lipid composition, including enrichment in PI(4)P. Vertebrate HH signal

transduction depends on primary cilia, and on the lipids of the primary cilium, bringing a subcellular focus to many steps of HH signal transduction.

Despite remarkable advances, our understanding of the role and regulation of lipids trails our understanding of proteins. The development of new tools to detect and perturb specific lipids will diminish this gap. For example, specific and sensitive lipid biosensors will permit visualization of the spatial distribution of the ciliary lipid composition. To help unravel how lipids function in HH signaling, it will be particularly helpful to develop sterol biosensors, refine mass spectrometry-based lipidomic approaches, and create optogenetic or chemogenetic approaches to specifically deplete lipids in subcellular domains such as the primary cilium. Especially in the emerging era of superresolution microscopy, identification of lipid domains and how they are dynamically regulated may be in the offing. As we have some understanding of how HH signals remodel ciliary protein composition, it will be particularly interesting to assess whether HH signals also dynamically remodel the ciliary lipid composition to activate signaling.

1.13 References

Amanai, K., and Jiang, J. (2001). Distinct Roles of Central Missing and Dispatched in Sending the Hedgehog Signal. ***Development*** 128, 5119–5127. doi:10.1242/dev.128.24.5119

Andrews, D., and Nelson, D. L. (1979). Biochemical Studies of the Excitable Membrane of Paramecium Tetraurelia. II. Phospholipids of Ciliary and Other Membranes. ***Biochimica Biophysica Acta (BBA) - Biomembr.*** 550, 174–187. doi:10.1016/0005-2736(79)90205-0

Babin, P. J., Bogerd, J., Kooiman, F. P., van Marrewijk, W. J. A., and van der Horst, D. J. (1999). Apolipophorin II/I, Apolipoprotein B, Vitellogenin, and Microsomal Triglyceride Transfer Protein Genes Are Derived from a Common Ancestor. ***J. Mol. Evol.*** 49, 150–160. doi:10.1007/PL00006528

Bachmann, V. A., Mayrhofer, J. E., Ilouz, R., Tschaikner, P., Raffeiner, P., Röck, R., et al. (2016). Gpr161 Anchoring of PKA Consolidates GPCR and cAMP Signaling. ***Proc. Natl. Acad. Sci. U.S.A.*** 113, 7786–7791. doi:10.1073/pnas.1608061113

Balla, T., and Várnai, P. (2002). Visualizing Cellular Phosphoinositide Pools with GFP-Fused Protein-Modules. ***Sci. STKE*** 2002. pl3–pl3. doi:10.1126/STKE.2002.125.PL3

Bangs, F., and Anderson, K. V. (2017). Primary Cilia and Mammalian Hedgehog Signaling. ***Cold Spring Harb. Perspect. Biol.*** 9, a028175. doi:10.1101/cshperspect.a028175

Bidet, M., Joubert, O., Lacombe, B., Ciantar, M., Nehmé, R., Mollat, P., et al. (2011). The Hedgehog Receptor Patched Is Involved in Cholesterol Transport. ***PLoS ONE*** 6, e23834. doi:10.1371/journal.pone.0023834

Bielas, S. L., Silhavy, J. L., Brancati, F., Kisseleva, M. V., Al-Gazali, L., Sztriha, L., et al. (2009). Mutations in INPP5E, Encoding Inositol Polyphosphate-5-Phosphatase E, Link Phosphatidyl Inositol Signaling to the Ciliopathies. ***Nat. Genet.*** 419 41, 1032–1036. doi:10.1038/ng.423

Bischoff, M., Gradilla, A.-C., Seijo, I., Andrés, G., Rodríguez-Navas, C., González-Méndez, L., et al. (2013). Cytonemes Are Required for the Establishment of a Normal Hedgehog Morphogen Gradient in Drosophila Epithelia. ***Nat. Cell Biol.*** 15, 1269–1281. doi:10.1038/ncb2856

Breslow, D. K., Koslover, E. F., Seydel, F., Spakowitz, A. J., and Nachury, M. V. (2013). An ***In Vitro*** Assay for Entry into Cilia Reveals Unique Properties of the Soluble Diffusion Barrier. ***J. Cell Biol.*** 203, 129–147. doi:10.1083/jcb.201212024

Brown, M. S., and Goldstein, J. L. (19861979). A Receptor-Mediated Pathway for Cholesterol Homeostasis. ***Science*** 232, 34–47. doi:10.1126/science.3513311

Buglino, J. A., and Resh, M. D. (2008). Hhat Is a Palmitoylacyltransferase with Specificity for N-Palmitoylation of Sonic Hedgehog. ***J. Biol. Chem.*** 283, 22076–22088. doi:10.1074/jbc.M803901200

Burke, R., Nellen, D., Bellotto, M., Hafen, E., Senti, K.-A., Dickson, B. J., et al. (1999). Dispatched, a Novel Sterol-Sensing Domain Protein Dedicated to the Release of Cholesterol-Modified Hedgehog from Signaling Cells. ***Cell*** 99, 803–815. doi:10.1016/s0092-8674(00)81677-3

Byrne, E. F. X., Sircar, R., Miller, P. S., Hedger, G., Luchetti, G., Nachtergaele, S., et al. (2016). Structural Basis of Smoothened Regulation by its Extracellular Domains. ***Nature*** 535, 517–522. doi:10.1038/nature18934

Cadena del Castillo, C. E., Hannich, J. T., Kaech, A., Chiyoda, H., Brewer, J., Fukuyama, M., et al. (2021). Patched Regulates Lipid Homeostasis by Controlling Cellular Cholesterol Levels. ***Nat. Commun.*** 12, 4898. doi:10.1038/s41467-021-24995-9

Callejo, A., Torroja, C., Quijada, L., and Guerrero, I. (2006). Hedgehog Lipid Modifications Are Required for Hedgehog Stabilization in the Extracellular Matrix. ***Development*** 133, 471–483. doi:10.1242/dev.02217

Canterini, S., Dragotto, J., Dardis, A., Zampieri, S., de Stefano, M. E., Mangia, F., et al. (2017). Shortened Primary Cilium Length and Dysregulated Sonic Hedgehog Signaling in Niemann-Pick C1 Disease. ***Hum. Mol. Genet.*** 26, 2277–2289. doi:10.1093/hmg/ddx118

Chailley, B., and Boisvieux-Ulrich, E. (1985). Detection of Plasma Membrane Cholesterol by Filipin during Microvillogenesis and Ciliogenesis in Quail Oviduct. ***J. Histochem Cytochem.*** 33, 1–10. doi:10.1177/33.1.3965567

Chamoun, Z., Mann, R. K., Nellen, D., von Kessler, D. P., Bellotto, M., Beachy, P. A., et al. (20011979). Skinny Hedgehog, an Acyltransferase Required for Palmitoylation and Activity of the Hedgehog Signal. ***Science*** 293, 2080–2084. doi:10.1126/science.1064437

Chávez, M., Ena, S., Van Sande, J., de Kerchove d'Exaerde, A., Schurmans, S., and Schiffmann, S. N. (2015). Modulation of Ciliary Phosphoinositide Content Regulates Trafficking and

Sonic Hedgehog Signaling Output. ***Dev. Cell*** 34, 338–350. doi:10.1016/J.DEVCEL.2015.06.016

Chen, M.-H., Li, Y.-J., Kawakami, T., Xu, S.-M., and Chuang, P.-T. (2004). Palmitoylation Is Required for the Production of a Soluble Multimeric Hedgehog Protein Complex and Long-Range Signaling in Vertebrates. ***Genes Dev.*** 18, 641–659. doi:10.1101/gad.1185804

Chiyoda, H., Kume, M., del Castillo, C. C., Kontani, K., Spang, A., Katada, T., et al. (2021). ***Caenorhabditis elegans*** PTR/PTCHD PTR-18 Promotes the Clearance of Extracellular Hedgehog-Related Protein via Endocytosis. ***PLoS Genet.*** 17, e1009457. doi:10.1371/journal.pgen.1009457

Christ, A., Christa, A., Klippert, J., Eule, J. C., Bachmann, S., Wallace, V. A., et al. (2015). LRP2 Acts as SHH Clearance Receptor to Protect the Retinal Margin from Mitogenic Stimuli. ***Dev. Cell*** 35, 36–48. doi:10.1016/j.devcel.2015.09.001

Christ, A., Christa, A., Kur, E., Lioubinski, O., Bachmann, S., Willnow, T. E., et al. (2012). LRP2 Is an Auxiliary SHH Receptor Required to Condition the Forebrain Ventral Midline for Inductive Signals. ***Dev. Cell*** 22, 268–278. doi:10.1016/j.devcel.2011.11.023

Christensen, E. I., Moskaug, J. Ø., Vorum, H., Jacobsen, C., Gundersen, T. E., Nykjær, A., et al. (1999). Evidence for an Essential Role of Megalin in Transepithelial Transport of Retinol. ***J. Am. Soc. Nephrol.*** 10, 685–695. doi:10.1681/ASN.V104685

Chuang, P.-T., and McMahon, A. P. (1999). Vertebrate Hedgehog Signalling Modulated by Induction of a Hedgehog-Binding Protein. ***Nature*** 397, 617–621. doi:10.1038/17611

Conduit, S. E., Davies, E. M., Fulcher, A. J., Oorschot, V., and Mitchell, C. A. (2021). Superresolution Microscopy Reveals Distinct Phosphoinositide Subdomains within the Cilia Transition Zone. ***Front. Cell Dev. Biol.*** 9. doi:10.3389/fcell.2021.634649

Conduit, S. E., and Vanhaesebroeck, B. (2020). Phosphoinositide Lipids in Primary Cilia Biology. ***Biochem. J.*** 477, 3541–3565. doi:10.1042/BCJ20200277

Connor, W. E., Lin, D. S., Wolf, D. P., and Alexander, M. (1998). Uneven Distribution of Desmosterol and Docosahexaenoic Acid in the Heads and Tails of Monkey Sperm. ***J. Lipid Res.*** 39, 1404–1411. doi:10.1016/s0022-2275(20)32521-9

Cooper, M. K., Wassif, C. A., Krakowiak, P. A., Taipale, J., Gong, R., Kelley, R. I., et al. (2003). A Defective Response to Hedgehog Signaling in Disorders of Cholesterol Biosynthesis. ***Nat. Genet.*** 33 (4), 508–513. doi:10.1038/ng1134

Corbit, K. C., Aanstad, P., Singla, V., Norman, A. R., Stainier, D. Y. R., and Reiter, J. F. (2005). Vertebrate Smoothened Functions at the Primary Cilium. ***Nature*** 437, 1018–1021. doi:10.1038/nature04117

Coulter, M. E., Dorobantu, C. M., Lodewijk, G. A., Delalande, F., Cianferani, S., Ganesh, V. S., et al. (2018). The ESCRT-III Protein CHMP1A Mediates Secretion of Sonic Hedgehog on a Distinctive Subtype of Extracellular Vesicles. ***Cell Rep.*** 24, 973–986. e8. doi:10.1016/j.celrep.2018.06.100

Creanga, A., Glenn, T. D., Mann, R. K., Saunders, A. M., Talbot, W. S., and Beachy, P. A. (2012). Scube/You Activity Mediates Release of Dually Lipid-Modified Hedgehog Signal in Soluble Form. ***Genes Dev.*** 26, 1312–1325. doi:10.1101/gad.191866.112

Das, A., Brown, M. S., Anderson, D. D., Goldstein, J. L., and Radhakrishnan, A. (2014). Three Pools of Plasma Membrane Cholesterol and Their Relation to Cholesterol Homeostasis. ***Elife*** 3. doi:10.7554/eLife.02882

Dawber, R. J., Hebbes, S., Herpers, B., Docquier, F., and van den Heuvel, M. (2005). Differential Range and Activity of Various Forms of the Hedgehog Protein. ***BMC Dev. Biol.*** 5, 21. doi:10.1186/1471-213X-5-21

Delling, M., DeCaen, P. G., Doerner, J. F., Febvay, S., and Clapham, D. E. (2013). Primary Cilia Are Specialized Calcium Signalling Organelles. ***Nature*** 504, 311–314. doi:10.1038/nature12833

Denef, N., Neubüser, D., Perez, L., and Cohen, S. M. (2000). Hedgehog Induces Opposite Changes in Turnover and Subcellular Localization of Patched and Smoothened. ***Cell*** 102, 521–531. doi:10.1016/S0092-8674(00)00056-8

Deshpande, I., Liang, J., Hedeen, D., Roberts, K. J., Zhang, Y., Ha, B., et al. (2019). Smoothened Stimulation by Membrane Sterols Drives Hedgehog Pathway Activity. ***Nature*** 571, 284–288. doi:10.1038/s41586-019-1355-4

di Paolo, G., and de Camilli, P. (2006). Phosphoinositides in Cell Regulation and Membrane Dynamics. ***Nature*** 443, 651–657. doi:10.1038/nature05185

Dwyer, J. R., Sever, N., Carlson, M., Nelson, S. F., Beachy, P. A., and Parhami, F. (2007). Oxysterols Are Novel Activators of the Hedgehog Signaling Pathway in Pluripotent Mesenchymal Cells. ***J. Biol. Chem.*** 282, 8959–8968. doi:10.1074/JBC.M611741200

Dyson, J. M., Conduit, S. E., Feeney, S. J., Hakim, S., DiTommaso, T., Fulcher, A. J., et al. (2017). INPP5E Regulates Phosphoinositide-dependent Cilia Transition Zone Function. ***J. Cell Biol.*** 216, 247–263. doi:10.1083/jcb.201511055

Eaton, S. (2008). Multiple Roles for Lipids in the Hedgehog Signalling Pathway. ***Nat. Rev. Mol. Cell Biol.*** 9, 437–445. doi:10.1038/nrm2414

Findakly, S., Daggubati, V., Garcia, G., LaStella, S. A., Choudhury, A., Tran, C., et al. (2021). Sterol and Oxysterol Synthases Near the Ciliary Base Activate the Hedgehog Pathway. ***J. Cell Biol.*** 220. doi:10.1083/jcb.202002026

Fitzky, B. U., Witsch-Baumgartner, M., Erdel, M., Lee, J. N., Paik, Y.-K., Glossmann, H., et al. (1998). Mutations in the Δ7-sterol Reductase Gene in Patients with the Smith-Lemli-Opitz Syndrome. ***Proc. Natl. Acad. Sci. U.S.A.*** 95, 8181–8186. doi:10.1073/pnas.95.14.8181

Forbes, A. J., Nakano, Y., Taylor, A. M., and Ingham, P. W. (1993). Genetic Analysis of ***Hedgehog*** Signalling in the ***Drosophila*** Embryo. ***Development*** 119, 115–124. doi:10.1242/dev.119.Supplement.115

Forte, M., Satow, Y., Nelson, D., and Kung, C. (1981). Mutational Alteration of Membrane Phospholipid Composition and Voltage-Sensitive Ion Channel Function in Paramecium. ***Proc. Natl. Acad. Sci. U.S.A.*** 78, 7195–7199. doi:10.1073/pnas.78.11.7195

Gailani, M. R., Ståhle-Bäckdahl, M., Leffell, D. J., Glyn, M., Zaphiropoulos, P. G., Undén, A. B., et al. (1996). The Role of the Human Homologue of Drosophila Patched in Sporadic Basal Cell Carcinomas. ***Nat. Genet.*** 14, 78–81. doi:10.1038/ng0996-78

Gallet, A., Rodriguez, R., Ruel, L., and Therond, P. P. (2003). Cholesterol Modification of Hedgehog Is Required for Trafficking and Movement, Revealing an Asymmetric Cellular Response to Hedgehog. ***Dev. Cell*** 4, 191–204. doi:10.1016/S1534-5807(03)00031-5

Gallet, A., Ruel, L., Staccini-Lavenant, L., and Thérond, P. P. (2006). Cholesterol Modification Is Necessary for Controlled Planar Long-Range Activity of Hedgehog in Drosophila Epithelia. ***Development*** 133, 407–418. doi:10.1242/dev.02212

Garcia, G., Raleigh, D. R., and Reiter, J. F. (2018). How the Ciliary Membrane Is Organized Inside-Out to Communicate Outside-In. ***Curr. Biol.*** 28, R421–R434. doi:10.1016/j.cub.2018.03.010

Garcia-Gonzalo, F. R., Phua, S. C., Roberson, E. C., Garcia, G., Abedin, M., Schurmans, S., et al. (2015). Phosphoinositides Regulate Ciliary Protein Trafficking to Modulate Hedgehog Signaling. ***Dev. Cell*** 34, 400–409. doi:10.1016/j.devcel.2015.08.001

Garcia-Gonzalo, F. R., and Reiter, J. F. (2017). Open Sesame: How Transition Fibers and the Transition Zone Control Ciliary Composition. ***Cold Spring Harb. Perspect. Biol.*** 9, a028134. doi:10.1101/cshperspect.a028134

Gealt, M. A., Adler, J. H., and Nes, W. R. (1981). The Sterols and Fatty Acids from Purified Flagella of Chlamydomonas Reinhardi. ***Lipids*** 16, 133–136. doi:10.1007/BF02535687

Goetz, J. A., Singh, S., Suber, L. M., Kull, F. J., and Robbins, D. J. (2006). A Highly Conserved Amino-Terminal Region of Sonic Hedgehog Is Required for the Formation of its Freely Diffusible Multimeric Form. ***J. Biol. Chem.*** 281, 4087–4093. doi:10.1074/jbc.M511427200

Gong, X., Qian, H., Cao, P., Zhao, X., Zhou, Q., Lei, J., et al. (2018). Structural Basis for the Recognition of Sonic Hedgehog by Human Patched1. ***Science*** 361, 361. doi:10.1126/science.aas8935

Gradilla, A.-C., González, E., Seijo, I., Andrés, G., Bischoff, M., González-Mendez, L., et al. (2014). Exosomes as Hedgehog Carriers in Cytoneme-Mediated Transport and Secretion. ***Nat. Commun.*** 5. doi:10.1038/ncomms6649

Hahn, H., Wicking, C., Zaphiropoulos, P. G., Gailani, M. R., Shanley, S., Chidambaram, A., et al. (1996). Mutations of the Human Homolog of Drosophila Patched in the Nevoid Basal Cell Carcinoma Syndrome. ***Cell*** 85, 841–851. doi:10.1016/S0092-8674(00)81268-4

Hammes, A., Andreassen, T. K., Spoelgen, R., Raila, J., Hubner, N., Schulz, H., et al. (2005). Role of Endocytosis in Cellular Uptake of Sex Steroids. ***Cell*** 122, 751–762. doi:10.1016/j.cell.2005.06.032

Harayama, T., and Riezman, H. (2018). Understanding the Diversity of Membrane Lipid Composition. ***Nat. Rev. Mol. Cell Biol.*** 19, 281–296. doi:10.1038/nrm.2017.138

Haycraft, C. J., Banizs, B., Aydin-Son, Y., Zhang, Q., Michaud, E. J., and Yoder, B. K. (2005). Gli2 and Gli3 Localize to Cilia and Require the Intraflagellar Transport Protein Polaris for Processing and Function. ***PLoS Genet.*** preprint, e53. doi:10.1371/journal.pgen.001005310.1371/journal.pgen.0010053.eor

Hilgendorf, K. I., Johnson, C. T., Mezger, A., Rice, S. L., Norris, A. M., Demeter, J., et al. (2019). Omega-3 Fatty Acids Activate Ciliary FFAR4 to Control Adipogenesis. ***Cell*** 179, 1289–1305. e21. doi:10.1016/j.cell.2019.11.005

Hollway, G. E., Maule, J., Gautier, P., Evans, T. M., Keenan, D. G., Lohs, C., et al. (2006). Scube2 Mediates Hedgehog Signalling in the Zebrafish Embryo. ***Dev. Biol.*** 294, 104–118. doi:10.1016/j.ydbio.2006.02.032

Hu, A., Zhang, J.-Z., Wang, J., Li, C.-C., Yuan, M., Deng, G., et al. (2022). Cholesterylation of Smoothened Is a Calcium-Accelerated Autoreaction Involving an Intramolecular Ester Intermediate. ***Cell Res.*** 32, 288–301. doi:10.1038/s41422-022-00622-0

Huang, P., Nedelcu, D., Watanabe, M., Jao, C., Kim, Y., Liu, J., et al. (2016). Cellular Cholesterol Directly Activates Smoothened in Hedgehog Signaling. ***Cell*** 166, 1176–1187. e14. doi:10.1016/j.cell.2016.08.003

Huang, P., Zheng, S., Wierbowski, B. M., Kim, Y., Nedelcu, D., Aravena, L., et al. (2018). Structural Basis of Smoothened Activation in Hedgehog Signaling. ***Cell*** 174, 312–324. e16. doi:10.1016/j.cell.2018.04.029

Huangfu, D., and Anderson, K. V. (2005). Cilia and Hedgehog Responsiveness in the Mouse. ***Proc. Natl. Acad. Sci. U.S.A.*** 102, 11325–11330. doi:10.1073/pnas.0505328102

Huangfu, D., Liu, A., Rakeman, A. S., Murcia, N. S., Niswander, L., and Anderson, K. V. (2003). Hedgehog Signalling in the Mouse Requires Intraflagellar Transport Proteins. ***Nature*** 426, 83–87. doi:10.1038/nature02061

Ingham, P. W. (2018). From ***Drosophila*** Segmentation to Human Cancer Therapy. ***Development*** 145. doi:10.1242/dev.168898

Ingham, P. W., and McMahon, A. P. (2001). Hedgehog Signaling in Animal Development: Paradigms and Principles. ***Genes Dev.*** 15, 3059–3087. doi:10.1101/gad.938601

Ishikawa, H., and Marshall, W. F. (2011). Ciliogenesis: Building the Cell's Antenna. ***Nat. Rev. Mol. Cell Biol.*** 12, 222–234. doi:10.1038/nrm3085

Jacoby, M., Cox, J. J., Gayral, S., Hampshire, D. J., Ayub, M., Blockmans, M., et al. (20092009). INPP5E Mutations Cause Primary Cilium Signaling Defects, Ciliary Instability and Ciliopathies in Human and Mouse. ***Nat. Genet.*** 41 (9), 1027–1031. doi:10.1038/ng.427

Jia, J., Tong, C., Wang, B., Luo, L., and Jiang, J. (20042005). Hedgehog Signalling Activity of Smoothened Requires Phosphorylation by Protein Kinase A and Casein Kinase I. ***Nature*** 432, 1045–1050. doi:10.1038/nature03179

Johnson, J.-L. F. A., Hall, T. E., Dyson, J. M., Sonntag, C., Ayers, K., Berger, S., et al. (2012). Scube Activity Is Necessary for Hedgehog Signal Transduction ***In Vivo***. ***Dev. Biol.*** 368, 193–202. doi:10.1016/j.ydbio.2012.05.007

Johnson, R. L., Rothman, A. L., Xie, J., Goodrich, L. V., Bare, J. W., Bonifas, J. M., et al. (1996). Human Homolog of Patched, a Candidate Gene for the Basal Cell Nevus Syndrome. ***Science*** 272, 1668–1671. doi:10.1126/science.272.5268.1668

Kaneshiro, E. S., Matesic, D. F., and Jayasimhulu, K. (1984). Characterizations of Six Ethanolamine Sphingophospholipids from Paramecium Cells and Cilia. ***J. Lipid Res.*** 25, 369–377. doi:10.1016/S0022-2275(20)37810-X

Kantarci, S., Al-Gazali, L., Hill, R. S., Donnai, D., Black, G. C. M., Bieth, E., et al. (2007). Mutations in LRP2, Which Encodes the Multiligand Receptor Megalin, Cause Donnai-Barrow and Facio-Oculo-Acoustico-Renal Syndromes. ***Nat. Genet.*** 39, 957–959. doi:10.1038/ng2063

Kantarci, S., Ragge, N. K., Thomas, N. S., Robinson, D. O., Noonan, K. M., Russell, M. K., et al. (2008). Donnai-Barrow Syndrome (DBS/FOAR) in a Child with a homozygousLRP2mutation Due to Complete Chromosome 2 Paternal Isodisomy. ***Am. J. Med. Genet.*** 146A, 1842–1847. doi:10.1002/ajmg.a.32381

Kawakami, A., Nojima, Y., Toyoda, A., Takahoko, M., Satoh, M., Tanaka, H., et al. (2005). The Zebrafish-Secreted Matrix Protein You/Scube2 Is Implicated in Long-Range Regulation of Hedgehog Signaling. ***Curr. Biol.*** 15, 480–488. doi:10.1016/j.cub.2005.02.018

Kennedy, K. E., and Thompson, G. A. (1970). Phosphonolipids: Localization in Surface Membranes of ***Tetrahymena***. ***Science*** 168, 989–991. doi:10.1126/science.168.3934.989

Kinnebrew, M., Iverson, E. J., Patel, B. B., Pusapati, G. V., Kong, J. H., Johnson, K. A., et al. (2019). Cholesterol Accessibility at the Ciliary Membrane Controls Hedgehog Signaling. ***Elife*** 8. doi:10.7554/eLife.50051

Kinnebrew, M., Luchetti, G., Sircar, R., Frigui, S., Viti, L. V., Naito, T., et al. (2021). Patched 1 Reduces the Accessibility of Cholesterol in the Outer Leaflet of Membranes. ***Elife*** 10. doi:10.7554/eLife.70504

Kinsky, S. C., Luse, S. A., and van Deenen, L. L. (1966). Interaction of Polyene Antibiotics with Natural and Artificial Membrane Systems. ***Fed. Proc.*** 25, 1503–1510. Available at: http://www.ncbi.nlm.nih.gov/pubmed/5332190.

Kong, J. H., Siebold, C., and Rohatgi, R. (2019). Biochemical Mechanisms of Vertebrate Hedgehog Signaling. ***Development*** 146 (10), dev166892. doi:10.1242/dev.166892

Kornberg, T. B. (2014). The Contrasting Roles of Primary Cilia and Cytonemes in Hh Signaling. ***Dev. Biol.*** 394, 1–5. doi:10.1016/j.ydbio.2014.07.015

Kuzhandaivel, A., Schultz, S. W., Alkhori, L., and Alenius, M. (2014). Cilia-Mediated Hedgehog Signaling in Drosophila. ***Cell Rep.*** 7, 672–680. doi:10.1016/j.celrep.2014.03.052

Kwon, H. J., Abi-Mosleh, L., Wang, M. L., Deisenhofer, J., Goldstein, J. L., Brown, M. S., et al. (2009). Structure of N-Terminal Domain of NPC1 Reveals Distinct Subdomains for Binding and Transfer of Cholesterol. ***Cell*** 137, 1213–1224. doi:10.1016/j.cell.2009.03.049

Leathes, J. B. (1925). Croonian Lectures on the Rôle of Fats in Vital Phenomena. ***Lancet*** 205, 853–856. doi:10.1016/s0140-6736(01)22310-1

Lee, J. D., Kraus, P., Gaiano, N., Nery, S., Kohtz, J., Fishell, G., et al. (2001). An Acylatable Residue of Hedgehog Is Differentially Required in Drosophila and Mouse Limb Development. ***Dev. Biol.*** 233, 122–136. doi:10.1006/dbio.2001.0218

Lee, J., Ekker, S., von Kessler, D., Porter, J., Sun, B., and Beachy, P. (1994). Autoproteolysis in Hedgehog Protein Biogenesis. ***Science*** 266, 1528–1537. doi:10.1126/science.7985023

Lewis, P. M., Dunn, M. P., McMahon, J. A., Logan, M., Martin, J. F., St-Jacques, B., et al. (2001). Cholesterol Modification of Sonic Hedgehog Is Required for Long-Range Signaling Activity and Effective Modulation of Signaling by Ptc1. ***Cell*** 105, 599–612. doi:10.1016/S0092-8674(01)00369-5

Li, Y., Zhang, H., Litingtung, Y., and Chiang, C. (2006). Cholesterol Modification Restricts the Spread of Shh Gradient in the Limb Bud. ***Proc. Natl. Acad. Sci. U.S.A.*** 103, 6548–6553. doi:10.1073/pnas.0600124103

Lobasso, S., Lopalco, P., Angelini, R., Baronio, M., Fanizzi, F. P., Babudri, F., et al. (2010). Lipidomic Analysis of Porcine Olfactory Epithelial Membranes and Cilia. ***Lipids*** 45, 593–602. doi:10.1007/S11745-010-3432-1/FIGURES/6

Luchetti, G., Sircar, R., Kong, J. H., Nachtergaele, S., Sagner, A., Byrne, E. F., et al. (2016). Cholesterol Activates the G-Protein Coupled Receptor Smoothened to Promote Hedgehog Signaling. ***Elife*** 5. doi:10.7554/ELIFE.20304

Luo, N., Kumar, A., Conwell, M., Weinreb, R. N., Anderson, R., and Sun, Y. (2013). Compensatory Role of Inositol 5-Phosphatase INPP5B to OCRL in Primary Cilia Formation in Oculocerebrorenal Syndrome of Lowe. ***PLOS ONE*** 8, e66727. doi:10.1371/JOURNAL.PONE.0066727

Luo, N., West, C. C., Murga-Zamalloa, C. A., Sun, L., Anderson, R. M., Wells, C. D., et al. (2012). OCRL Localizes to the Primary Cilium: a New Role for Cilia in Lowe Syndrome. ***Hum. Mol. Genet.*** 21, 3333–3344. doi:10.1093/HMG/DDS163

Maekawa, M., and Fairn, G. D. (2014). Molecular Probes to Visualize the Location, Organization and Dynamics of Lipids. ***J. Cell Sci.*** 127, 4801–4812. doi:10.1242/jcs.150524

Marley, A., Choy, R. W.-Y., and von Zastrow, M. (2013). GPR88 Reveals a Discrete Function of Primary Cilia as Selective Insulators of GPCR Cross-Talk. ***PLoS ONE*** 8, e70857. doi:10.1371/journal.pone.0070857

Matsumoto, Y., Morishima, K.-I., Honda, A., Watabe, S., Yamamoto, M., Hara, M., et al. (2005). R352Q Mutation of the DHCR7 Gene Is Common Among Japanese Smith-Lemli-Opitz Syndrome Patients. ***J. Hum. Genet.*** 50, 353–356. doi:10.1007/s10038-005-0267-3

Matusek, T., Wendler, F., Polès, S., Pizette, S., D'Angelo, G., Fürthauer, M., et al. (2014). The ESCRT Machinery Regulates the Secretion and Long-Range Activity of Hedgehog. ***Nature*** 516, 99–103. doi:10.1038/nature13847

McConnell, H. M., and Radhakrishnan, A. (2003). Condensed Complexes of Cholesterol and Phospholipids. ***Biochimica Biophysica Acta (BBA) - Biomembr.*** 1610, 159–173. doi:10.1016/S0005-2736(03)00015-4

Melkonian, M., Robenek, H., and Rassat, J. (1982). Flagellar Membrane Specializations and Their Relationship to Mastigonemes and Microtubules in Euglena Gracilis. ***J. Cell Sci.*** 55, 115–135. doi:10.1242/jcs.55.1.115

Micchelli, C. A., The, I., Selva, E., Mogila, V., and Perrimon, N. (2002). Rasp, a Putative Transmembrane Acyltransferase, Is Required for Hedgehog Signaling. ***Development*** 129, 843–851. doi:10.1242/dev.129.4.843

Mick, D. U., Rodrigues, R. B., Leib, R. D., Adams, C. M., Chien, A. S., Gygi, S. P., et al. (2015). Proteomics of Primary Cilia by Proximity Labeling. ***Dev. Cell*** 35, 497–512. doi:10.1016/j.devcel.2015.10.015

Miyamoto, T., Hosoba, K., Itabashi, T., Iwane, A. H., Akutsu, S. N., Ochiai, H., et al. (2020). Insufficiency of Ciliary Cholesterol in Hereditary Zellweger Syndrome. ***Embo J.*** 39. doi:10.15252/embj.2019103499

Mourvaki, E., Cardinali, R., Roberti, R., Dal Bosco, A., and Castellini, C. (2010). Desmosterol, the Main Sterol in Rabbit Semen: Distribution Among Semen Subfractions and its Role in the ***In Vitro*** Spermatozoa Acrosome Reaction and Motility. ***Asian J. Androl.*** 12, 862–870. doi:10.1038/aja.2010.25

Mukhopadhyay, S., Badgandi, H. B., Hwang, S.-H., Somatilaka, B., Shimada, I. S., and Pal, K. (2017). Trafficking to the Primary Cilium Membrane. ***MBoC*** 28, 233–239. doi:10.1091/MBC.E16-07-0505/ASSET/IMAGES/LARGE/233FIG1

Mukhopadhyay, S., Wen, X., Chih, B., Nelson, C. D., Lane, W. S., Scales, S. J., et al. (2010). TULP3 Bridges the IFT-A Complex and Membrane Phosphoinositides to Promote Trafficking of G Protein-Coupled Receptors into Primary Cilia. ***Genes Dev.*** 24, 2180–2193. doi:10.1101/GAD.1966210

Mukhopadhyay, S., Wen, X., Ratti, N., Loktev, A., Rangell, L., Scales, S. J., et al. (2013). The Ciliary G-Protein-Coupled Receptor Gpr161 Negatively Regulates the Sonic Hedgehog Pathway via cAMP Signaling. ***Cell*** 152, 210–223. doi:10.1016/j.cell.2012.12.026

Murone, M., Rosenthal, A., and de Sauvage, F. J. (1999). Sonic Hedgehog Signaling by the Patched-Smoothened Receptor Complex. ***Curr. Biol.*** 9, 76–84. doi:10.1016/S0960-9822(99)80018-9

Myers, B. R., Neahring, L., Zhang, Y., Roberts, K. J., and Beachy, P. A. (2017). Rapid, Direct Activity Assays for Smoothened Reveal Hedgehog Pathway Regulation by Membrane Cholesterol and Extracellular Sodium. ***Proc. Natl. Acad. Sci. U.S.A.*** 114, E11141–E11150. doi:10.1073/PNAS.1717891115

Myers, B. R., Sever, N., Chong, Y. C., Kim, J., Belani, J. D., Rychnovsky, S., et al. (2013). Hedgehog Pathway Modulation by Multiple Lipid Binding Sites on the Smoothened Effector of Signal Response. ***Dev. Cell*** 26, 346–357. doi:10.1016/j.devcel.2013.07.015

Nachtergaele, S., Whalen, D. M., Mydock, L. K., Zhao, Z., Malinauskas, T., Krishnan, K., et al. (2013). Structure and Function of the Smoothened Extracellular Domain in Vertebrate Hedgehog Signaling. ***Elife*** 2. doi:10.7554/eLife.01340

Nachury, M. V. (2014). How Do Cilia Organize Signalling Cascades? ***Phil. Trans. R. Soc. B*** 369, 20130465. doi:10.1098/rstb.2013.0465

Nachury, M. V., and Mick, D. U. (2019). Establishing and Regulating the Composition of Cilia for Signal Transduction. ***Nat. Rev. Mol. Cell Biol.*** 20, 389–405. doi:10.1038/s41580-019-0116-4

Nechipurenko, I. V. (2020). The Enigmatic Role of Lipids in Cilia Signaling. ***Front. Cell Dev. Biol.*** 8, 777. doi:10.3389/FCELL.2020.00777

Nedelcu, D., Liu, J., Xu, Y., Jao, C., and Salic, A. (2013). Oxysterol Binding to the Extracellular Domain of Smoothened in Hedgehog Signaling. ***Nat. Chem. Biol.*** 9, 557–564. doi:10.1038/nchembio.1290

Nelson, L. D., Johnson, A. E., and London, E. (2008). How Interaction of Perfringolysin O with Membranes Is Controlled by Sterol Structure, Lipid Structure, and Physiological Low pH. ***J. Biol. Chem.*** 283, 4632–4642. doi:10.1074/jbc.M709483200

Nowaczyk, M. J. M., and Irons, M. B. (2012). Smith-Lemli-Opitz Syndrome: Phenotype, Natural History, and Epidemiology. ***Am. J. Med. Genet.*** 160C, 250–262. doi:10.1002/ajmg.c.31343

Nüsslein-Volhard, C., Wieschaus, E., and Kluding, H. (1984). Mutations Affecting the Pattern of the Larval Cuticle inDrosophila Melanogaster. ***Wilhelm Roux' Arch.*** 193, 267–282. doi:10.1007/BF00848156

Nüsslein-Volhard, C., and Wieschaus, E. (1980). Mutations Affecting Segment Number and Polarity in Drosophila. ***Nature*** 287, 795–801. doi:10.1038/287795a0

Nykjaer, A., Dragun, D., Walther, D., Vorum, H., Jacobsen, C., Herz, J., et al. (1999). An Endocytic Pathway Essential for Renal Uptake and Activation of the Steroid 25-(OH) Vitamin D3. ***Cell*** 96, 507–515. doi:10.1016/S0092-8674(00)80655-8

Palm, W., Swierczynska, M. M., Kumari, V., Ehrhart-Bornstein, M., Bornstein, S. R., and Eaton, S. (2013). Secretion and Signaling Activities of Lipoprotein-Associated Hedgehog and Non-sterol-modified Hedgehog in Flies and Mammals. ***PLoS Biol.*** 11, e1001505. doi:10.1371/journal.pbio.1001505

Panáková, D., Sprong, H., Marois, E., Thiele, C., and Eaton, S. (2005). Lipoprotein Particles Are Required for Hedgehog and Wingless Signalling. ***Nature*** 435, 58–65. doi:10.1038/nature03504

Pepinsky, R. B., Zeng, C., Wen, D., Rayhorn, P., Baker, D. P., Williams, K. P., et al. (1998). Identification of a Palmitic Acid-Modified Form of Human Sonic Hedgehog. ***J. Biol. Chem.*** 273, 14037–14045. doi:10.1074/jbc.273.22.14037

Petrov, K., de Almeida Magalhaes, T., and Salic, A. (2021). Mechanism and Ultrasensitivity in Hedgehog Signaling Revealed by Patched1 Disease Mutations. ***Proc. Natl. Acad. Sci. U.S.A.*** 118. doi:10.1073/pnas.2006800118

Petrov, K., Wierbowski, B. M., Liu, J., and Salic, A. (2020). Distinct Cation Gradients Power Cholesterol Transport at Different Key Points in the Hedgehog Signaling Pathway. ***Dev. Cell*** 55, 314–327. e7. doi:10.1016/j.devcel.2020.08.002

Pinson, K. I., Brennan, J., Monkley, S., Avery, B. J., and Skarnes, W. C. (2000). An LDL-Receptor-Related Protein Mediates Wnt Signalling in Mice. ***Nature*** 407, 535–538. doi:10.1038/35035124

Porter, J. A., Ekker, S. C., Park, W.-J., von Kessler, D. P., Young, K. E., Chen, C.-H., et al. (1996a). Hedgehog Patterning Activity: Role of a Lipophilic Modification Mediated by the Carboxy-Terminal Autoprocessing Domain. ***Cell*** 86, 21–34. doi:10.1016/s0092-8674(00)80074-4

Porter, J. A., Young, K. E., and Beachy, P. A. (1996b). Cholesterol Modification of Hedgehog Signaling Proteins in Animal Development. ***Science*** 274, 255–259. doi:10.1126/science.274.5285.255

Qi, C., di Minin, G., Vercellino, I., Wutz, A., and Korkhov, V. M. (2019). Structural Basis of Sterol Recognition by Human Hedgehog Receptor PTCH1. ***Sci. Adv.*** 5. doi:10.1126/sciadv.aaw6490

Qi, X., Friedberg, L., de Bose-Boyd, R., Long, T., and Li, X. (2020). Sterols in an Intramolecular Channel of Smoothened Mediate Hedgehog Signaling. ***Nat. Chem. Biol.*** 16, 1368–1375. doi:10.1038/s41589-020-0646-2

Qi, X., Schmiege, P., Coutavas, E., and Li, X. (2018a). Two Patched Molecules Engage Distinct Sites on Hedgehog Yielding a Signaling-Competent Complex. ***Science*** 362, 362. doi:10.1126/science.aas8843

Qi, X., Schmiege, P., Coutavas, E., Wang, J., and Li, X. (2018b). Structures of Human Patched and its Complex with Native Palmitoylated Sonic Hedgehog. ***Nature*** 560, 128–132. doi:10.1038/s41586-018-0308-7

Qian, H., Cao, P., Hu, M., Gao, S., Yan, N., and Gong, X. (2019). Inhibition of Tetrameric Patched1 by Sonic Hedgehog through an Asymmetric Paradigm. ***Nat. Commun.*** 10, 2320. doi:10.1038/s41467-019-10234-9

Quirk, J., van den Heuvel, M., Henrique, D., Marigo, V., Jones, T. A., Tabin, C., et al. (1997). The Smoothened Gene and Hedgehog Signal Transduction in Drosophila and Vertebrate Development. ***Cold Spring Harb. Symp. Quant. Biol.*** 62, 217–226. doi:10.1101/SQB.1997.062.01.027

Radhakrishnan, A., Rohatgi, R., and Siebold, C. (2020). Cholesterol Access in Cellular Membranes Controls Hedgehog Signaling. ***Nat. Chem. Biol.*** 16, 1303–1313. doi:10.1038/s41589-020-00678-2

Raleigh, D. R., Sever, N., Choksi, P. K., Sigg, M. A., Hines, K. M., Thompson, B. M., et al. (2018). Cilia-Associated Oxysterols Activate Smoothened. ***Mol. Cell*** 72, 316–327. e5. doi:10.1016/j.molcel.2018.08.034

Rana, R., Carroll, C. E., Lee, H.-J., Bao, J., Marada, S., Grace, C. R. R., et al. (2013). Structural Insights into the Role of the Smoothened Cysteine-Rich Domain in Hedgehog Signalling. ***Nat. Commun.*** 4, 2965. doi:10.1038/ncomms3965

Reiter, J. F., and Leroux, M. R. (2017). Genes and Molecular Pathways Underpinning Ciliopathies. ***Nat. Rev. Mol. Cell Biol.*** 18, 533–547. doi:10.1038/nrm.2017.60

Rohatgi, R., Milenkovic, L., and Scott, M. P. (2007). Patched1 Regulates Hedgehog Signaling at the Primary Cilium. ***Science*** 317, 372–376. doi:10.1126/science.1139740

Rudolf, A. F., Kinnebrew, M., Kowatsch, C., Ansell, T. B., el Omari, K., Bishop, B., et al. (2019). The Morphogen Sonic Hedgehog Inhibits its Receptor Patched by a Pincer Grasp Mechanism. ***Nat. Chem. Biol.*** 15, 975–982. doi:10.1038/s41589-019-0370-y

Sanders, T. A., Llagostera, E., and Barna, M. (2013). Specialized Filopodia Direct Long-Range Transport of SHH during Vertebrate Tissue Patterning. ***Nature*** 497, 628–632. doi:10.1038/nature12157

Santos, N., and Reiter, J. F. (2014). A Central Region of Gli2 Regulates its Localization to the Primary Cilium and Transcriptional Activity. ***J. Cell Sci.*** 127 (Pt 7), 1500–1510. doi:10.1242/jcs.139253

Schink, K. O., Tan, K.-W., and Stenmark, H. (2016). Phosphoinositides in Control of Membrane Dynamics. ***Annu. Rev. Cell Dev. Biol.*** 32, 143–171. doi:10.1146/ANNUREV-CELLBIO-111315-125349

Sever, N., Mann, R. K., Xu, L., Snell, W. J., Hernandez-Lara, C. I., Porter, N. A., et al. (2016). Endogenous B-Ring Oxysterols Inhibit the Hedgehog Component Smoothened in a Manner Distinct from Cyclopamine or Side-Chain Oxysterols. ***Proc. Natl. Acad. Sci. U.S.A.*** 113, 5904–5909. doi:10.1073/pnas.1604984113

Shewan, A., Eastburn, D. J., and Mostov, K. (2011). Phosphoinositides in Cell Architecture. ***Cold Spring Harb. Perspect. Biol.*** 3, a004796. doi:10.1101/cshperspect.a004796

Smith, J. D., Snyder, W. R., and Law, J. H. (1970). Phosphonolipids in Tetrahymena Cilia. ***Biochem. Biophysical Res. Commun.*** 39, 1163–1169. doi:10.1016/0006-291X(70)90682-0

Souto-Padrón, T., and de Souza, W. (1986). The Surface Charge of Trypanosoma Cruzi: Analysis Using Cell Electrophoresis, Lectins and Ultrastructural Cytochemistry. ***J. Submicrosc. Cytol.*** 18, 701–709.

Stebel, M., Vatta, P., Ruaro, M. E., del Sal, G., Parton, R. G., and Schneider, C. (2000). The growth suppressing gas 1 product is a GPI-Linked Protein. ***FEBS Lett.*** 481, 152–158. doi:10.1016/S0014-5793(00)02004-4

Stone, D. M., Hynes, M., Armanini, M., Swanson, T. A., Gu, Q., Johnson, R. L., et al. (1996). The Tumour-Suppressor Gene Patched Encodes a Candidate Receptor for Sonic Hedgehog. ***Nature*** 384, 129–134. doi:10.1038/384129a0

Su, V. F., Jones, K. A., Brodsky, M., and The, I. (2007). Quantitative Analysis of Hedgehog Gradient Formation Using an Inducible Expression System. ***BMC Dev. Biol.*** 7, 43. doi:10.1186/1471-213X-7-43

Taipale, J., Cooper, M. K., Maiti, T., and Beachy, P. A. (2002). Patched Acts Catalytically to Suppress the Activity of Smoothened. ***Nature*** 418, 892–896. doi:10.1038/nature00989

Tanaka, Y., Okada, Y., and Hirokawa, N. (2005). FGF-induced Vesicular Release of Sonic Hedgehog and Retinoic Acid in Leftward Nodal Flow Is Critical for Left-Right Determination. ***Nature*** 435, 172–177. doi:10.1038/nature03494

Tetley, L. (1986). Freeze-fracture Studies on the Surface Membranes of Pleomorphic Bloodstream and ***In Vitro*** Transformed Procyclic Trypanosoma Brucei. ***Acta Trop.*** 43, 307–317.

Toshimori, K., Higashi, R., and Ōura, C. (1985). Distribution of Intramembranous Particles and Filipin-Sterol Complexes in Mouse Sperm Membranes: Polyene Antibiotic Filipin Treatment. ***Am. J. Anat.*** 174, 455–470. doi:10.1002/aja.1001740408

Truong, M. E., Bilekova, S., Choksi, S. P., Li, W., Bugaj, L. J., Xu, K., et al. (2021). Vertebrate Cells Differentially Interpret Ciliary and Extraciliary cAMP. ***Cell*** 184, 2911–2926. e18. doi:10.1016/j.cell.2021.04.002

Tseng, T. T., Gratwick, K. S., Kollman, J., Park, D., Nies, D. H., Goffeau, A., et al. (1999). The RND Permease Superfamily: an Ancient, Ubiquitous and Diverse Family that Includes Human Disease and Development Proteins. ***J. Mol. Microbiol. Biotechnol.*** 1, 107–125.

Tukachinsky, H., Kuzmickas, R. P., Jao, C. Y., Liu, J., and Salic, A. (2012). Dispatched and Scube Mediate the Efficient Secretion of the Cholesterol-Modified Hedgehog Ligand. ***Cell Rep.*** 2, 308–320. doi:10.1016/j.celrep.2012.07.010

Tyler, K. M., Fridberg, A., Toriello, K. M., Olson, C. L., Cieslak, J. A., Hazlett, T. L., et al. (2009). Flagellar Membrane Localization via Association with Lipid Rafts. ***J. Cell Sci.*** 122, 859–866. doi:10.1242/jcs.037721

van Meer, G., Voelker, D. R., and Feigenson, G. W. (2008). Membrane Lipids: where They Are and How They Behave. ***Nat. Rev. Mol. Cell Biol.*** 9, 112–124. doi:10.1038/nrm2330

Vyas, N., Walvekar, A., Tate, D., Lakshmanan, V., Bansal, D., Cicero, A. L., et al. (2014). Vertebrate Hedgehog Is Secreted on Two Types of Extracellular Vesicles with Different Signaling Properties. ***Sci. Rep.*** 4. doi:10.1038/srep07357

Wang, Q., Asarnow, D. E., Ding, K., Mann, R. K., Hatakeyama, J., Zhang, Y., et al. (2021). Dispatched Uses Na+ Flux to Power Release of Lipid-Modified Hedgehog. ***Nature*** 599, 320–324. doi:10.1038/s41586-021-03996-0

Warner, J. F., McCarthy, A. M., Morris, R. L., and McClay, D. R. (2014). Hedgehog Signaling Requires Motile Cilia in the Sea Urchin. ***Mol. Biol. Evol.*** 31, 18–22. doi:10.1093/MOLBEV/MST176

Wassif, C. A., Maslen, C., Kachilele-Linjewile, S., Lin, D., Linck, L. M., Connor, W. E., et al. (1998). Mutations in the Human Sterol Δ7-Reductase Gene at 11q12-13 Cause Smith-Lemli-Opitz Syndrome. ***Am. J. Hum. Genet.*** 63, 55–62. doi:10.1086/301936

Wen, X., Lai, C. K., Evangelista, M., Hongo, J.-A., de Sauvage, F. J., and Scales, S. J. (2010). Kinetics of Hedgehog-dependent Full-Length Gli3 Accumulation in Primary Cilia and Subsequent Degradation. ***Mol. Cell Biol.*** 30, 1910–1922. doi:10.1128/MCB.01089-09

Wheatley, D. N. (1995). Primary Cilia in Normal and Pathological Tissues. ***Pathobiology*** 63, 222–238. doi:10.1159/000163955

Wheatley, D., Wang, A. M., and Strugnell, G. E. (1996). Expression of Primary Cilia in Mammalian Cells. ***Cell Biol. Int.*** 20, 73–81. doi:10.1006/cbir.1996.0011

Wierbowski, B. M., Petrov, K., Aravena, L., Gu, G., Xu, Y., and Salic, A. (2020). Hedgehog Pathway Activation Requires Coreceptor-Catalyzed, Lipid-dependent Relay of the Sonic Hedgehog Ligand. ***Dev. Cell*** 55, 450–467. e8. doi:10.1016/j.devcel.2020.09.017

Willert, K., Brown, J. D., Danenberg, E., Duncan, A. W., Weissman, I. L., Reya, T., et al. (2003). Wnt Proteins Are Lipid-Modified and Can Act as Stem Cell Growth Factors. ***Nature*** 423, 448–452. doi:10.1038/nature01611

Willnow, T. E., Hilpert, J., Armstrong, S. A., Rohlmann, A., Hammer, R. E., Burns, D. K., et al. (1996). Defective Forebrain Development in Mice Lacking Gp330/megalin. ***Proc. Natl. Acad. Sci. U.S.A.*** 93, 8460–8464. doi:10.1073/pnas.93.16.8460

Wills, R. C., Goulden, B. D., and Hammond, G. R. V. (2018). Genetically Encoded Lipid Biosensors. ***MBoC*** 29, 1526–1532. doi:10.1091/mbc.E17-12-0738

Wong, L. H., and Levine, T. P. (2017). Tubular Lipid Binding Proteins (TULIPs) Growing Everywhere. ***Biochimica Biophysica Acta (BBA) - Mol. Cell Res.*** 1864, 1439–1449. doi:10.1016/j.bbamcr.2017.05.019

Woods, I. G., and Talbot, W. S. (2005). The You Gene Encodes an EGF-CUB Protein Essential for Hedgehog Signaling in Zebrafish. ***PLoS Biol.*** 3, e66. doi:10.1371/journal.pbio.0030066

Xiao, X., Tang, J.-J., Peng, C., Wang, Y., Fu, L., Qiu, Z.-P., et al. (2017). Cholesterol Modification of Smoothened Is Required for Hedgehog Signaling. ***Mol. Cell*** 66, 154–162. e10. doi:10.1016/j.molcel.2017.02.015

Yao, S., Lum, L., and Beachy, P. (2006). The Ihog Cell-Surface Proteins Bind Hedgehog and Mediate Pathway Activation. ***Cell*** 125, 343–357. doi:10.1016/j.cell.2006.02.040

Yen, H.-Y., Hoi, K. K., Liko, I., Hedger, G., Horrell, M. R., Song, W., et al. (20182018). PtdIns(4,5)P2 Stabilizes Active States of GPCRs and Enhances Selectivity of G-Protein Coupling. ***Nature*** 559, 423–427. doi:10.1038/s41586-018-0325-6

Zeng, X., Goetz, J. A., Suber, L. M., Scott, W. J., Schreiner, C. M., and Robbins, D. J. (2001). A Freely Diffusible Form of Sonic Hedgehog Mediates Long-Range Signalling. ***Nature*** 411, 716–720. doi:10.1038/35079648

Zhang, W., Kang, J.-S., Cole, F., Yi, M.-J., and Krauss, R. S. (2006). Cdo Functions at Multiple Points in the Sonic Hedgehog Pathway, and Cdo-Deficient Mice Accurately Model Human Holoprosencephaly. ***Dev. Cell*** 10, 657–665. doi:10.1016/j.devcel.2006.04.005

Zhang, Y., Bulkley, D. P., Xin, Y., Roberts, K. J., Asarnow, D. E., Sharma, A., et al. (2018). Structural Basis for Cholesterol Transport-like Activity of the Hedgehog Receptor Patched. ***Cell*** 175, 1352–1364. e14. doi:10.1016/j.cell.2018.10.026

Zhu, A. J., Zheng, L., Suyama, K., and Scott, M. P. (2003). Altered Localization of Drosophila Smoothened Protein Activates Hedgehog Signal Transduction. ***Genes Dev.*** 17, 1240–1252. doi:10.1101/GAD.1080803

CHAPTER 2:

Smoothened inhibition of PKA at cilia transduces Hedgehog signals

2.1 Abstract

Hedgehog (HH) signaling in vertebrates is dependent on the primary cilium, an organelle that scaffolds signal transduction. HH signals induce Smoothened (SMO) enrichment in the cilium and indirectly triggers the conversion of GLI proteins into transcriptional activators of HH target genes. Recently, SMO has been shown to inhibit protein kinase A (PKA). To test the hypothesis that SMO specifically inhibits PKA at cilia to activate the HH signal transduction pathway, we developed a ciliary PKA biosensor. Activation of the HH signal transduction pathway by either Sonic hedgehog (SHH) or SMO agonist (SAG) inhibited ciliary PKA activity. Blocking SMO phosphorylation by GRK2/3 prevented ciliary SMO from inhibiting ciliary PKA activity. $Ga_{i/o}$ was dispensable for SMO inhibition of ciliary PKA. In contrast, mutating the SMO C-terminal tail protein kinase inhibitor (PKI) pseudosubstrate site interfered with the ability of SMO to inhibit ciliary PKA. Therefore, HH signaling is transduced via SMO direct inhibition of PKA at cilia, in a manner dependent on GRK2/3.

2.2 Introduction

The Hedgehog (HH) signaling pathway is a critical means of cell-cell communication used by metazoans to coordinate development and homeostasis of many tissues (Ingham et al., 2011; Zhang and Beachy, 2023). Indispensable to vertebrate HH signaling is the primary cilium, a microtubule-based organelle that projects itself from the body of the cell (Goetz and Anderson, 2010; Bangs and Anderson, 2017; Kong et al., 2019). Though the ciliary membrane is contiguous with the plasma membrane and the cilioplasm is not membrane bound, the composition of the primary cilium is distinct from that of the rest of the cell (Garcia-Gonzalo et al., 2011, 2015; Chávez et al., 2015; Mick et al., 2015; Breslow et al., 2018; Raleigh et al., 2018). For HH signal transduction, the primary cilium acts as a specialized microenvironment in which signaling functions distinctly from elsewhere in the cell (Delling et al., 2013; Marley et al., 2013; Truong et al., 2021).

In the absence of HH signals, the HH receptor, PTCH1, localizes to the ciliary membrane and keeps the downstream signal transduction pathway off (Rohatgi et al., 2007). In the presence of HH signals, HH binds to PTCH1, allowing the seven-pass transmembrane protein Smoothened (SMO) to accumulate in the ciliary membrane (Corbit et al., 2005). Ciliary SMO is required for activation of GLI transcription factors, the effectors of HH signaling in many tissues (Haycraft et al., 2005; Kim et al., 2009). How SMO activates GLI transcription factors remains an area of active investigation.

One possible mechanism by which SMO regulates GLI transcription factors is via protein kinase A (PKA). PKA represses HH signal transduction by phosphorylating GLI proteins to trigger the formation of their repressor forms, referred to as GLI-R (Wang et al., 2000; Haycraft et al.,

2005; Niewiadomski et al., 2014). PKA is activated by cAMP, a second messenger mediating some forms of GPCR signaling (Pierce et al., 2002).

Many G protein-coupled receptors (GPCRs) signal by acting as guanine nucleotide exchange factors for small GTPases including $G\alpha_s$, $G\alpha_i$ and $G\alpha_o$ (Gilman, 1987). These GTP-bound Gα proteins regulate the activity of adenylyl cyclases, enzymes that generate the second messenger cyclic adenosine monophosphate (cAMP) (Wettschureck and Offermanns, 2005). Adenylyl cyclases are stimulated by $G\alpha_s$ and inhibited by $G\alpha_{i/o}$ (Hurley, 1999). cAMP activates its principal effector, PKA (Taylor et al., 2012). $Ga_{i/o}$ has been investigated as an effector of SMO in HH signal transduction (Alcedo et al., 1996; Van Den Heuvel and Ingham, 1996; Riobo et al., 2006; Low et al., 2008; Ogden et al., 2008; Shen et al., 2013; Arveseth et al., 2021).

Beyond cAMP, some proteins, known as protein kinase inhibitors (PKIs), regulate PKA activity. PKIs directly bind to and inhibit the catalytic subunit of PKA (PKA-C) (Taylor et al., 2023). Recent work has demonstrated that the C-terminus of SMO can bind PKA and function as a PKI (Arveseth et al., 2021; Happ et al., 2022). We investigated whether SMO inhibits PKA at cilia to transduce HH signals, and if it does, whether PKA regulation is mediated through $Ga_{i/o}$ or through direct inhibition of the catalytic subunit.

Another regulator of HH signal transduction is GPR161, a $G\alpha_s$-coupled GPCR that localizes to the primary cilium in the absence of HH signals (Mukhopadhyay et al., 2013; Pal et al., 2016; Pusapati et al., 2018; Tschaikner et al., 2021). A model of HH signal transduction is that GPR161, signaling through $G\alpha_s$, activates adenylyl cyclases to increase levels of cAMP, activating PKA, and thus triggers the formation of GLI-R (Mukhopadhyay et al., 2013).

Previously, we found that a pool of PKA localizes to the cilium and that inhibition of ciliary PKA, but not non-ciliary PKA, is sufficient to activate HH-dependent transcription (Truong et al.,

2021). Inspired by recent discoveries that SMO inhibits PKA (Arveseth et al., 2021; Happ et al., 2022), we hypothesized that SMO activates HH signaling by specifically inhibiting PKA at cilia. To begin to test this hypothesis, we developed a sensitive measure of ciliary PKA activity.

2.3 Results

2.3.1 Development of a biosensor of ciliary PKA activity

A previously developed biosensor of cytosolic PKA activity (O'Banion et al., 2018, 2019) is based on vasodilator-stimulated phosphoprotein (VASP) Ser^{157}, which is phosphorylated specifically by PKA (Butt et al., 1994; Smolenski et al., 1998; Lambrechts et al., 2000; Priestman et al., 2011). To localize this PKA-phosphorylated peptide at cilia, we fused VASP amino acids 148 to 164 to ARL13B, a ciliary protein, and GFP (**Fig. 2.1A**). Stable expression of ARL13B-GFP-$VASP^{148-163}$ in a clonal NIH/3T3 cell line revealed that it, as predicted, localized to cilia (**Fig. 2.1B-D**).

To detect PKA-mediated phosphorylation of the VASP peptide, we employed a monoclonal antibody that specifically recognizes VASP phosphorylated at Ser^{157} (pVASP) (O'Banion et al., 2018). To test this detection mechanism, we treated ciliary VASP-expressing cells with the adenylyl cyclase agonist forskolin (FSK), which induces cAMP production (Seamon et al., 1981). Immunofluorescence imaging of ciliary VASP-expressing cells using the pVASP-specific antibody revealed that the basal level of ciliary pVASP was low and dramatically increased by FSK (**Fig. 2.1C, 2.1E, S2.1A-B, S2.1D-E**). Inhibiting PKA with H89 blocked the FSK-induced increase in ciliary pVASP (**Fig. 2.1D-E, S2.1C-D**). As this assay measures ciliary PKA-dependent phosphorylation activity, we refer to ARL13B-GFP-$VASP^{148-163}$ hereafter as the cilia PKA biosensor.

We tested the dynamic range of the cilia PKA biosensor in response to different concentrations of FSK as well as different durations of FSK treatment (**Fig. S2.1A-E**). FSK exerted dose- and time-dependent activation of the cilia PKA biosensor. Treatment of cells with 100nM of FSK, for 15 minutes, produced a half-maximal increase in cilia PKA biosensor activity.

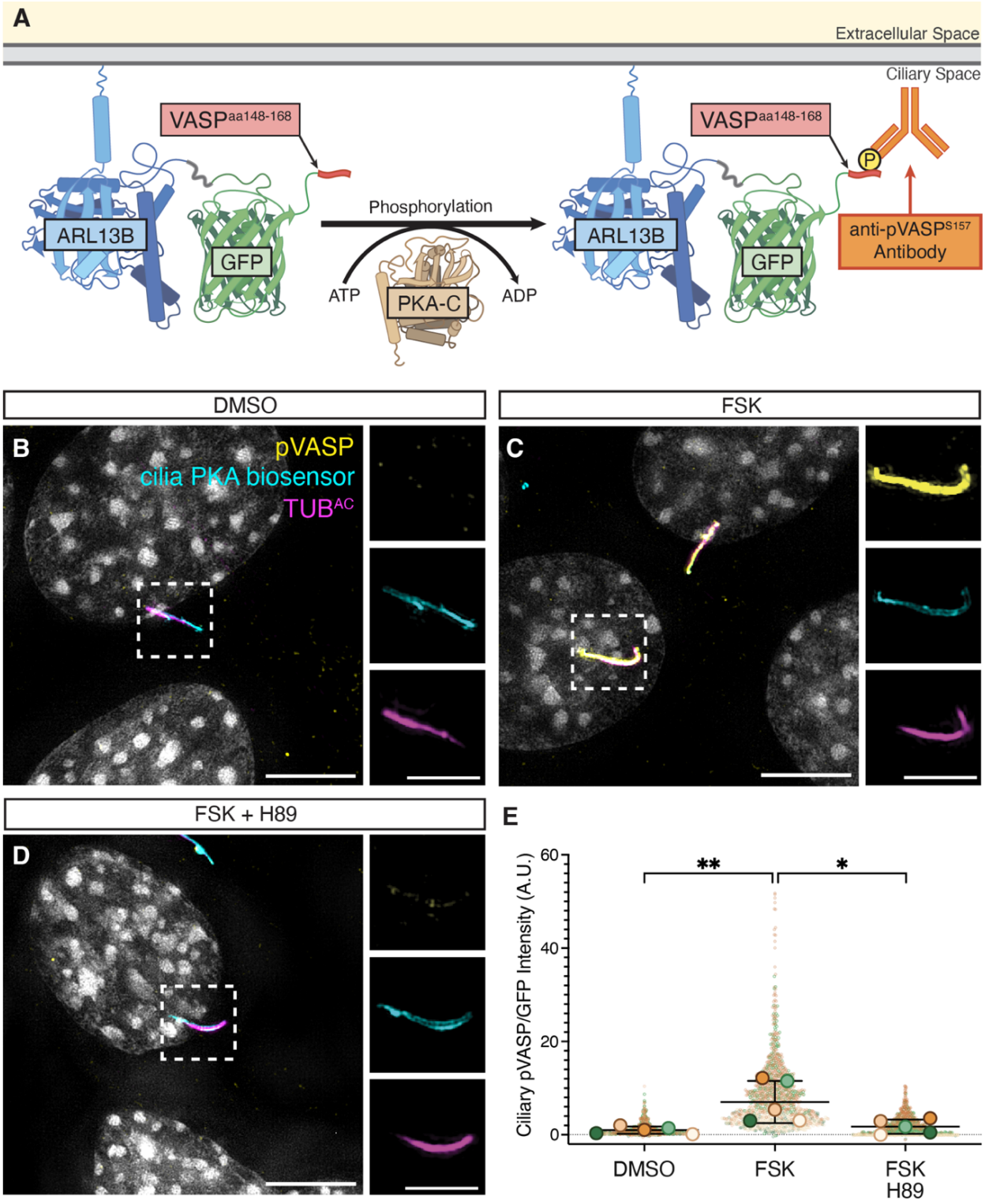

Figure 2.1: Cilia PKA biosensor detects ciliary PKA activity.

(Figure caption continued on the next page.)

(Figure caption continued from the last page.)

(A) Schematic of ARL13B-GFP-VASP$^{148\text{-}163}$, the cilia PKA biosensor.

(B-D) Immunofluorescence imaging of NIH/3T3 cells stably expressing the cilia PKA biosensor. Cells were serum-starved and then treated with either DMSO (**B**), FSK (100nM for 15 minutes) (**C**), or both FSK and H89 (100nM and 20μM, respectively, for 15 minutes) (**D**). Cells immunostained for pVASP (pVASP^{S157}, yellow), cilia PKA biosensor (GFP, cyan), cilia (acetylated tubulin, TUB^{AC}, magenta) and nuclei (Hoescht, grey). Scale bars for larger images are 5μM, and for insets are 2.5μM.

(E) Quantification of ciliary pVASP intensity normalized to ciliary GFP intensity. Representative images used for quantification are in Figure S1A-C. Each biological replicate is color coded.

Significance was determined via one-way ANOVA of the means of each biological replicate, followed by Šídák's multiple comparison test. (P values are indicated as follows: *$p < 0.04$, ** $p < 0.003$. Data are represented are means of replicates ± SD.)

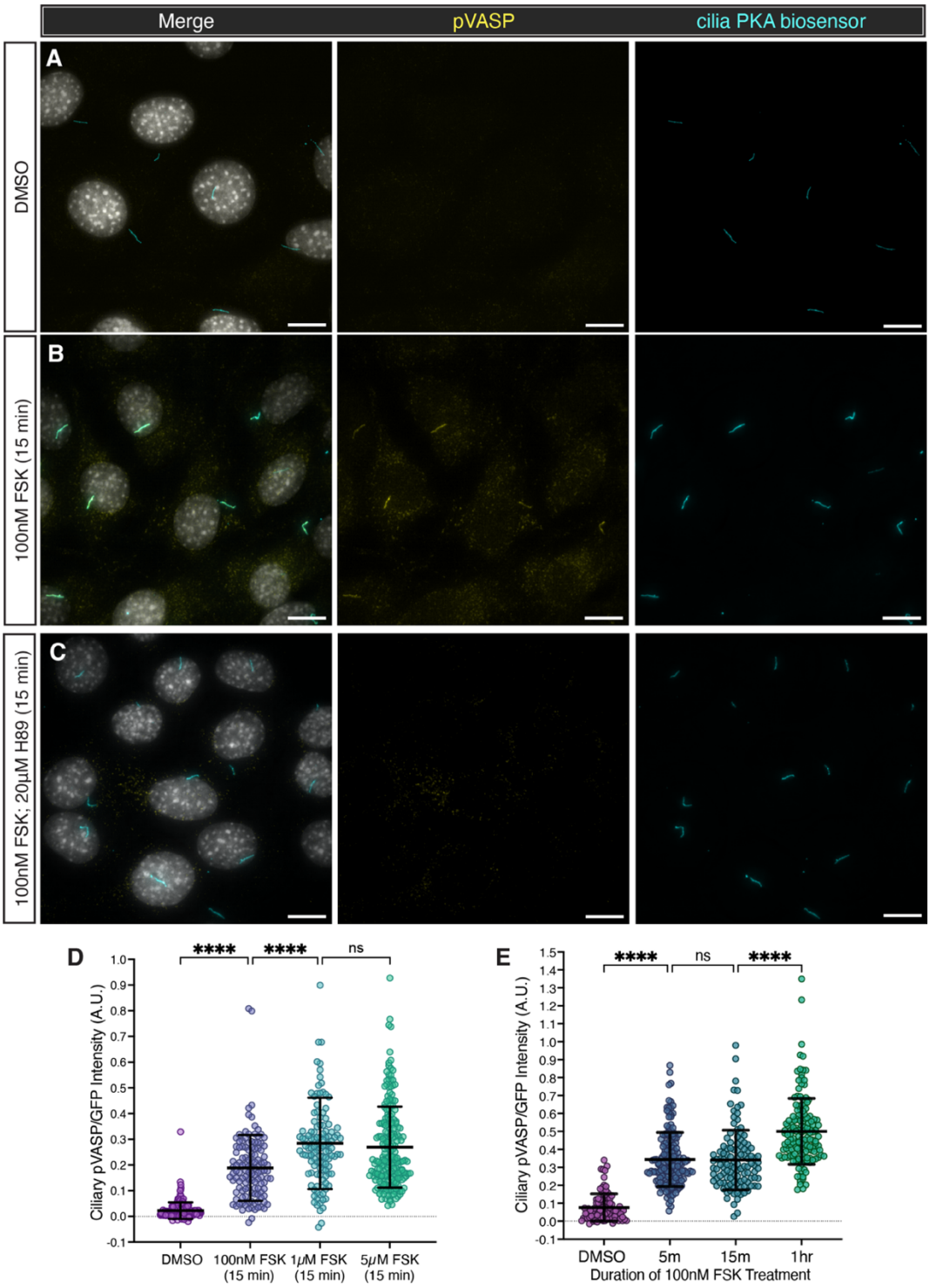

Supplemental Figure 2.1: Characterizing the dynamic range of the cilia PKA biosensor.

(Figure caption continued on the next page.)

(Figure caption continued from the last page.)

(**A-C**) Representative images of immunofluorescence staining of NIH/3T3 cells stably expressing the cilia PKA biosensor. Cells were serum-starved and then treated with either DMSO, FSK (100nM for 15 minutes), or both FSK and H89 (100nM and 20μM, respectively, for 15 minutes). Images depict cells stained for pVASP (pVASP^{S157}, yellow), cilia PKA biosensor (GFP, cyan), and nuclei (Hoescht, grey). Scale bar, 10μM.

(D) Quantification of ciliary pVASP intensity normalized to ciliary GFP intensity of cells treated with different concentrations of FSK.

(E) Quantification of ciliary pVASP intensity normalized to ciliary GFP intensity cells treated with FSK for different durations.

Significance was determined via one-way ANOVA followed by Tukey's multiple comparison test. (****$p < 0.0001$. Data are represented are means ± SD.)

2.3.2 Ciliary PKA activity is graded during zebrafish development

During zebrafish development, somites are patterned by SHH produced by the notochord, required for differentiation of muscle pioneers and slow muscle fibers (Fan and Tessier-Lavigne, 1994). Because somites are generated in an anterior to posterior manner, at any developmental timepoint, the anterior somites are more mature whereas posterior somites are still differentiating and are actively responding to SHH (Roy et al., 2001; Wolff et al., 2003).

Therefore, we hypothesized that, if ciliary PKA activity is suppressed by HH signaling, zebrafish somites would exhibit a posterior to anterior gradient of ciliary PKA activity. To test this hypothesis, we expressed the cilia PKA biosensor in zebrafish embryos and stained for pVASP and GFP (**Fig. 2.2A-D**). Cilia PKA biosensor activity was higher in anterior somites and lower in posterior somites (**Fig. 2.2E**). Thus, *in vivo*, ciliary PKA active is dynamic, and active HH signaling is associated with decreased ciliary PKA.

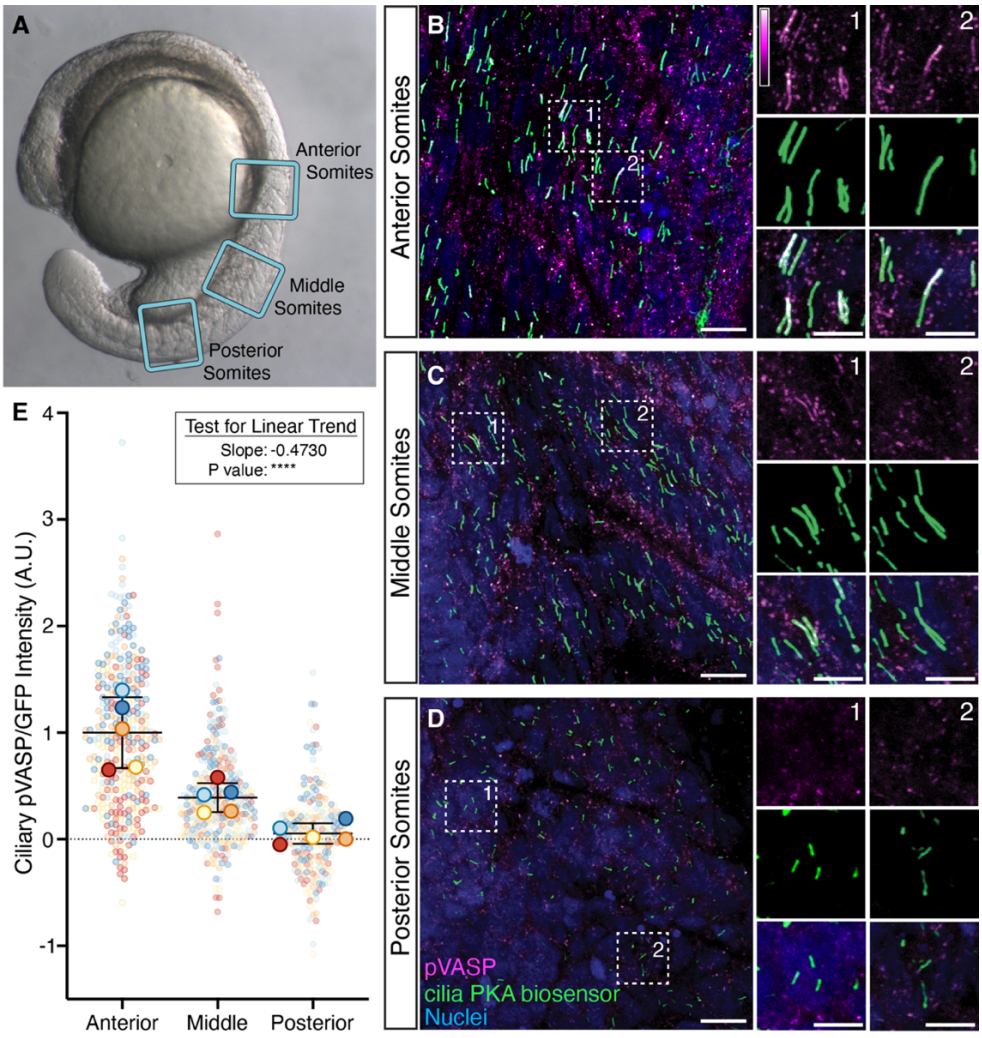

Figure 2.2: Ciliary PKA activity is graded from anterior to posterior somites in zebrafish development.

(A) 18 somite-stage zebrafish embryo, somites 2-4 of which are designated anterior, somites 7-9 of which are designated middle, and somites 12-14 of which are designated posterior.

(B) Immunofluorescence images of somites from zebrafish injected with 500pg mRNA encoding cilia PKA biosensor and stained for pVASP (pVASP^{S157}, magenta), cilia PKA biosensor (GFP, green), and nuclei (Hoescht, blue). Scale bar, 10µM.

(C) Quantification of ciliary pVASP intensity normalized to ciliary GFP within each somite region.

For all plots, each biological replicate, one fish, is color coded. Significance was determined via one-way ANOVA of the means of each biological replicate, followed by a test for linear trend. (****$p < 0.0001$. Data are represented are means of replicates ± SD.)

2.3.3 Active SMO suppresses ciliary PKA activity

As SMO can inhibit PKA (Happ et al., 2022), we hypothesized that SMO inhibits PKA at the cilium to activate HH signal transduction (**Fig. 2.3A**). Assays for PKA inhibition, such as with $Ga_{i/o}$-coupled GPCRs, are typically conducted under conditions of cAMP stimulation, often with forskolin (FSK), an agonist of adenylyl cyclase (Seamon et al., 1981; Wang et al., 2004). Therefore, to test whether SMO inhibits ciliary PKA, we treated cilia PKA biosensor-expressing NIH/3T3 cells with FSK, FSK and H89, or FSK and Smoothened Agonist (SAG) (Chen et al., 2002b; Frank-Kamenetsky et al., 2002) **(Fig. 2.3B-G)**. SAG, like H89, blocked FSK-mediated activation of the cilia PKA biosensor **(Fig. 2.3C-F)**. Treating cilia PKA biosensor-expressing cells with FSK and SHH revealed that, like SAG, SHH blocked FSK-mediated activation of the cilia PKA biosensor **(Fig. 2.3F)**. Thus, activating HH signal transduction blocks PKA activity in the primary cilium.

To test if HH pathway-mediated inhibition of ciliary PKA is mediated by SMO, we used clustered regularly interspaced short palindromic repeats (CRISPR)–mediated editing to inactivate *Smo* in NIH/3T3 cells. We treated clonal *Smo*$^{-/-}$ NIH/3T3 cells expressing the cilia PKA biosensor with FSK and SAG. In *Smo*$^{-/-}$ cells, SAG had no effect on cilia PKA biosensor activity **(Fig. 2.3E,G)**, indicating that SMO is critical for suppressing ciliary PKA activity in response to HH pathway activation.

Cyclopamine (CYA) is a small molecule inhibitor of SMO that triggers accumulation of SMO at the primary cilium but keeps SMO in an inactive conformation (Incardona et al., 1998; Chen et al., 2002b; Kim et al., 2009; Rohatgi et al., 2009; Wilson et al., 2009). Treatment of cilia PKA biosensor-expressing NIH/3T3 cells with CYA, accordingly, caused SMO to accumulate at primary cilia, at levels similar to that caused by treatment with SAG **(Fig. S2.3A-B)**. Unlike SAG, CYA did not prevent FSK-mediated activation of the cilia PKA biosensor **(Fig. 3.3D,F).** Thus,

SMO localization to the primary cilium is not sufficient to inhibit ciliary PKA; SMO must also be in an active state.

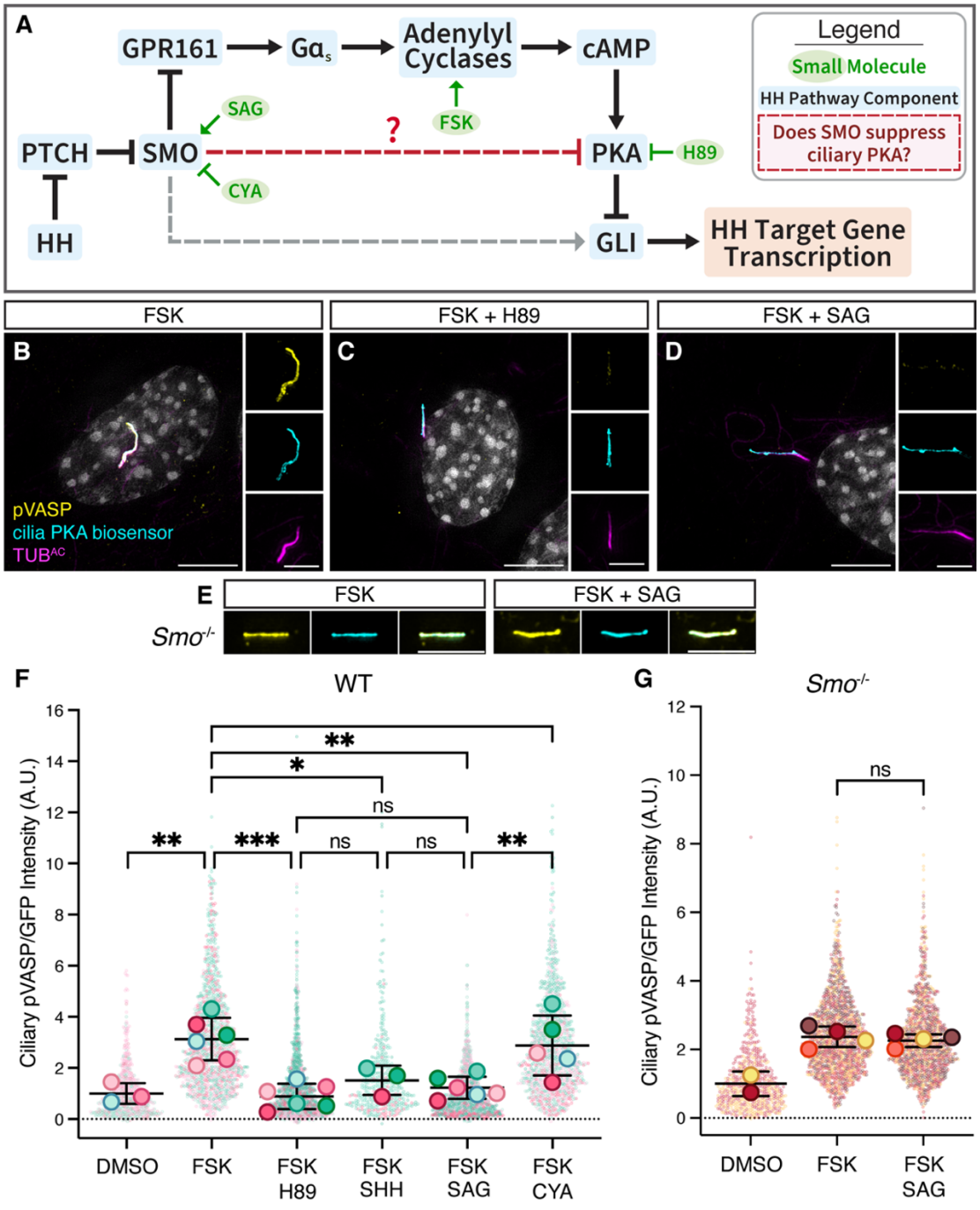

Figure 2.3: Active SMO inhibits PKA activity at cilia.

(Figure caption continued on the next page.)

(Figure caption continued from the last page.)

(A) Schematic of a working model of HH signal transduction. Red line indicates part of the system investigated in this figure.

(B-E) Immunofluorescence images of cilia PKA biosensor cells or *Smo*$^{-/-}$ cilia PKA biosensor cells serum-starved and treated with either FSK (100nM for 15 minutes) (**B**), FSK and H89 (100nM and 20μM, respectively, for 15 minutes) (**C**), or SAG and FSK (100nM for 24 h and 100nM for 15 minutes, respectively) (**D,E**). Images depict cells stained for pVASP (pVASP^{S157}, yellow), cilia PKA biosensor (GFP, cyan), cilia (TUB^{AC}, magenta), and nuclei (Hoescht, grey). Scale bars for larger images, 5 μM (**B-E**). Scale bars for insets are 2.5 μM (**B-D**).

(F) Quantification of ciliary pVASP intensity in cilia PKA biosensor cells. Cells in the FSK and SHH condition were treated with 24 hours of 4nM SHH followed by 100nM FSK for 15 minutes. Cells in the FSK and CYA condition were treated with 24 hours of 5μM cyclopamine followed by 100nM FSK for 15 minutes.

(G) As with F, but with quantification of ciliary pVASP intensity in *Smo*$^{-/-}$ cilia PKA biosensor cells. Data for this panel is also used in Fig. 6B and S6A.

For all plots, each biological replicate is color coded. Significance was determined via one-way ANOVA of the means of each biological replicate, followed by Šídák's multiple comparison test. P values are indicated as follows: *$p < 0.04$, ** $p < 0.003$ and ***$p < 0.0002$. Data are represented are means of replicates ± SD.

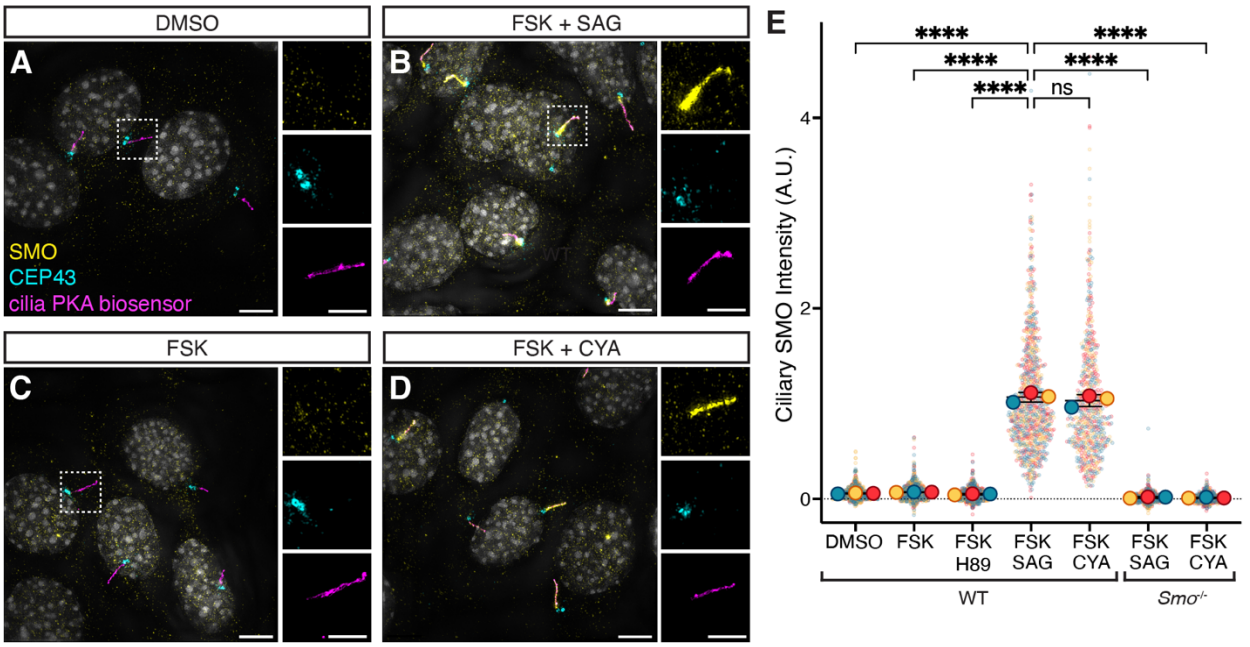

Supplemental Figure 2.3: SAG and cyclopamine induce equivalent levels of SMO accumulation at primary cilia.

(A-D) Immunofluorescence images of cilia PKA biosensor cells treated with the same regimes as in Fig. 3B-G. Images depict cells stained for SMO (pVASP^{S157}, yellow), basal bodies (CEP43, cyan), cilia PKA biosensor (GFP, magenta), and nuclei (Hoescht, grey). Scale bars for larger images, 5 µM. Scale bars for insets are 2.5 µM.

(E) Quantification of ciliary SMO localization from A-D.

For all plots, each biological replicate is color coded. Significance was determined via one-way ANOVA of the means of each biological replicate, followed by Šídák's multiple comparison test. ****$p < 0.0001$. Data are represented are means of replicates ± SD.

2.3.4 GRK2/3 phosphorylation of SMO is required to suppress PKA activity at the cilium

G protein-coupled Receptor Kinases 2 and 3 (GRK2/3) promote vertebrate HH signal transduction, and how they regulate HH signal transduction is being actively investigated (Philipp et al., 2008; Chen et al., 2011; Zhao et al., 2016; Pusapati et al., 2018; Kong et al., 2019; Arveseth et al., 2021; Happ et al., 2022). For many activated GPCRs, GRKs participate in desensitization (Moore et al., 2007). Indeed, phosphorylation of GPR161 by GRK2 triggers b-Arrestin recruitment and trafficking of GPR161 out of the cilium (Pal et al., 2016). However, GRK2/3 has GPR161-independent functions in HH signaling, as GRK2/3 is required for activation of HH target gene transcription even in the absence of GPR161 (Pusapati et al., 2018).

GRK2/3 is also able to phosphorylate the C-terminal tail of SMO (Chen et al., 2004, 2011; Arveseth et al., 2021; Walker et al., 2024), and GRK2/3-phosphorylated SMO is enriched in the primary cilium following HH activation (Walker et al., 2024). One hypothesis is that GRK2/3 mediates the interaction between SMO and PKA by phosphorylating the C-terminal tail of ciliary SMO, allowing SMO to directly bind and inhibit the catalytic subunit of PKA (PKA-C) (Arveseth et al., 2021; Happ et al., 2022; Walker et al., 2024) (**Fig. 2.4A**). We asked whether SMO-mediated inhibition of ciliary PKA depends on GRK2/3 activity.

To test whether GRK2/3 acts at the level of SMO to suppress ciliary PKA during HH signaling, we employed CMPD101, a pharmacological inhibitor of GRK2/3 (Thal et al., 2011). Consistent with previous findings (Walker et al., 2024), activating SMO with SAG increased ciliary SMO phosphorylated at a GRK2/3 consensus site and CMPD101 blocked GRK2/3-dependent phosphorylation of SMO **(Fig. 2.4B,C)**. Treatment of cilia PKA biosensor-expressing NIH/3T3 cells with FSK, SAG and CMPD101 revealed that CMPD101 blocked the ability of SMO to inhibit PKA at the cilium **(Fig. 2.4B-E)**. CYA treatment of cilia PKA biosensor cells neither

induced induce SMO inhibition of PKA, nor GRK2/3-dependent phosphorylation of SMO (**Fig. 2.4F,G**). Thus, GRK2/3 activity is required for SMO to inhibit PKA in cilia.

To assess how SMO activation affects its phosphorylation and ability to inhibit ciliary PKA, we measured the SAG dose response of cilia PKA biosensor activity and ciliary phosphorylated SMO levels. SAG increased SMO phosphorylation and decreased cilia PKA biosensor activity in a dose-dependent way **(Fig. 2.4F-G)**.

Interestingly, immunofluorescence imaging of GRK2/3 phosphorylated SMO (pSMO) and pVASP in cells treated with FSK and intermediate levels of SAG revealed that cells were heterogeneous, exhibiting ciliary pVASP or pSMO, but not high levels of both (**Fig. S2.4**). Ciliary SMO phosphorylation and ciliary PKA activity were therefore anti-correlated both at the population level and the single cell level. We conclude that GRK2/3 phosphorylation of SMO is critical for inhibition of ciliary PKA and that GRK2/3 and PKA ciliary activity are mutually exclusive.

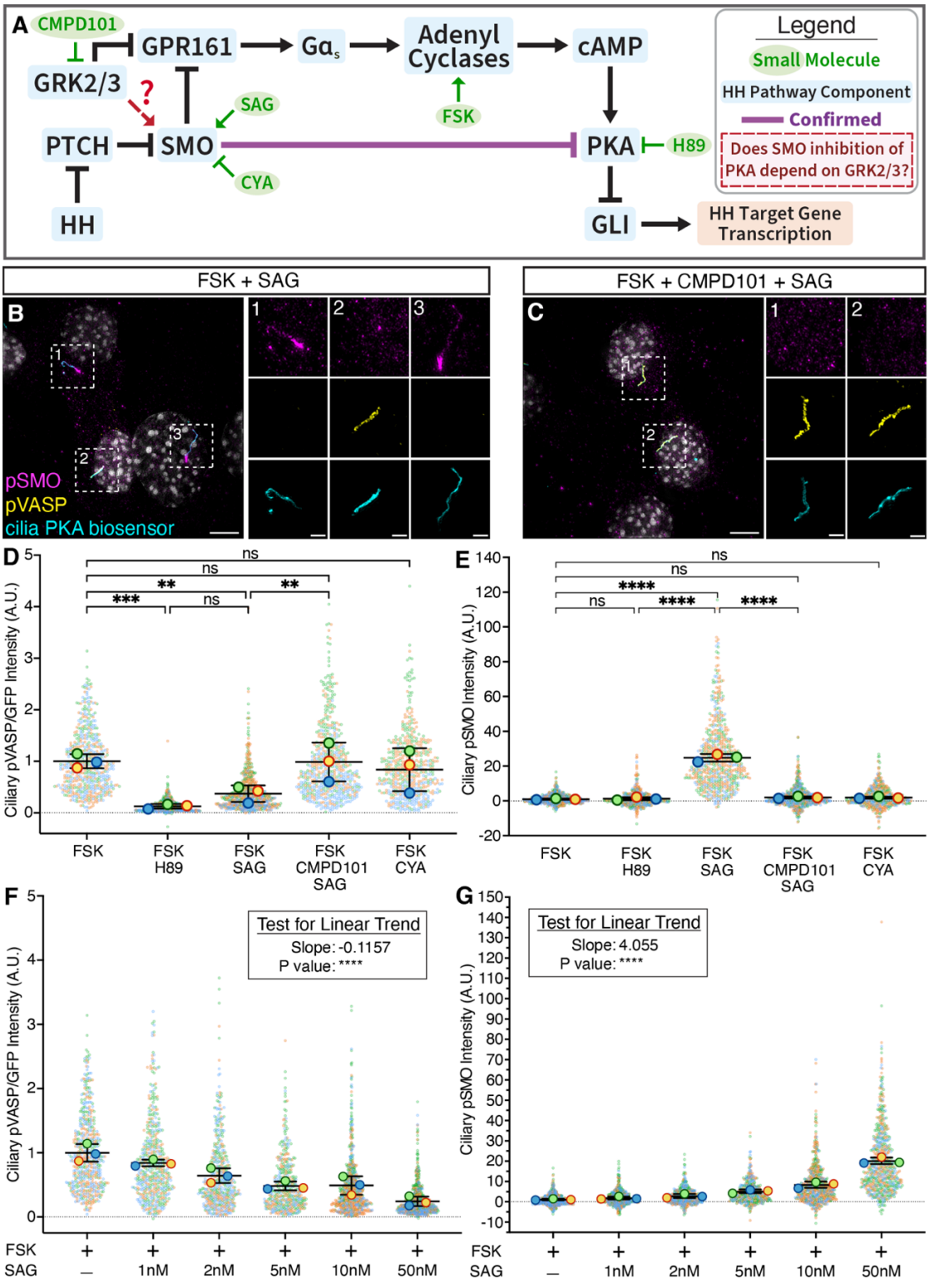

Figure 2.4: GRK2/3 activity is required for SMO to suppress ciliary PKA activity.

(Figure caption continued on the next page.)

(Figure caption continued from the last page.)

(A) Schematic of the working model of HH signaling. Red arrow indicates part of the system investigated in this figure.

(B-C) Immunofluorescence images of cilia PKA biosensor cells. Cells were treated with SAG and FSK (100nM for 24h and100nM for 15 minutes, respectively) (**B**), or SAG, CMPD101 and FSK (100nM, 30μM and 100nM for 24h, 24h and 15 minutes, respectively) (**C**). Images depict cells stained for pVASP (pVASP^{S157}, yellow), cilia PKA biosensor (GFP, cyan), pSMO (phospho-SMO S362/S363/S364, magenta) and nuclei (Hoescht, grey). Scale bars for larger images are 5μM, and for insets are 2.5μM.

(D) Quantification of ciliary pVASP intensity in cilia PKA biosensor cells stained for pVASP. Cells were treated with SAG (100nM), SAG and CMPD101 (100nM and 30μM, respectively), CYA (5μM) or H89 (20μM for 15 minutes) and FSK (100nM for 15 minutes).

(E) As with D, but for the quantification of ciliary pSMO intensity in the same cells.

(F) Quantification of ciliary pVASP intensity in cilia PKA biosensor cells. Cells were treated with increasing dosages of SAG (for 24h) and FSK (75nM for 15 minutes). Significance was determined by a one-way ANOVA followed by a post-test for linear trend.

(G) As with F, but for the quantification of ciliary pSMO intensity in the same cells.

For all plots, each biological replicate is color-coded. For D and E, significance was determined via one-way ANOVA of the means of each biological replicate, followed by Šídák's multiple comparison test (panels D and E), or by a test for linear trend (panels F and G). P values are indicated as follows: ** $p < 0.003$, ***$p < 0.0002$, and ****$p < 0.0001$. Data are represented are means of replicates ± SD.

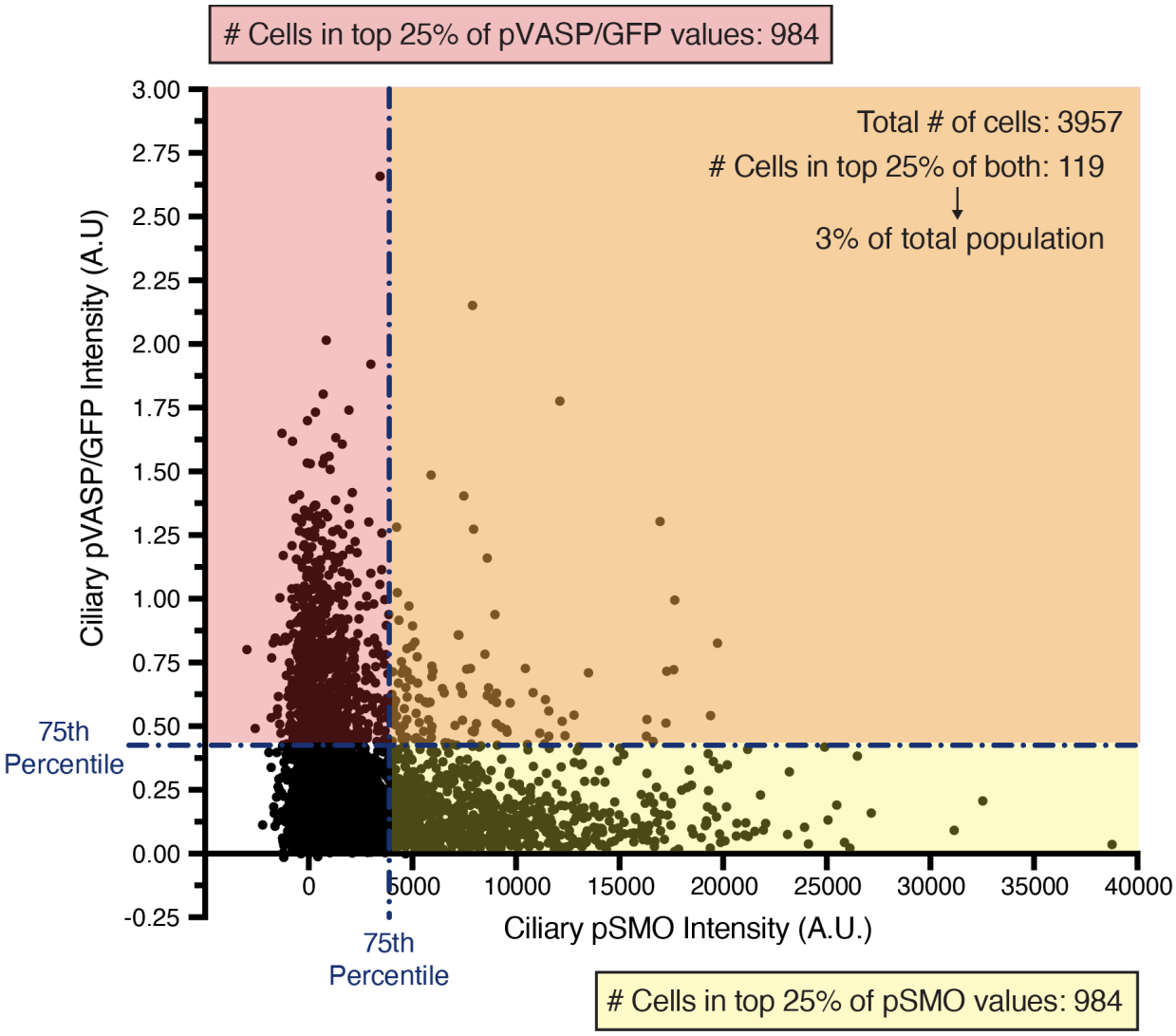

Figure S2.4: High ciliary pVASP and high ciliary pSMO intensity are mostly mutually exclusive.

Each dot represents a cilium of a cilia PKA biosensor cell treated with SAG for 24hrs followed by 15min of 75nM FSK. These data are also used in Figure 3F-G. The x-axis represents the level of ciliary pSMO in each cilium, and the y-axis represents the level of ciliary pVASP/GFP in that same cilium.

2.3.5 Gα$_i$ inhibits ciliary PKA activity downstream of a ciliary GPCR, but not downstream of SMO

In addition to GPR161, a growing number of GPCRs have been described that localize to and uniquely function at cilia (Mykytyn and Askwith, 2017). For many of these cilia-localized GPCRs, it is unclear whether they act via PKA or other effectors. To test whether a ciliary GPCR also affects ciliary PKA activity, we created cilia PKA biosensor NIH/3T3 cells stably expressing somatostatin receptor 3 (SSTR3). SSTR3 is a ciliary GPCR which couples to Gα$_{i/o}$ for its downstream signaling (Yasuda et al., 1992; Murthy et al., 1996; Green et al., 2016; Ye et al., 2018) (**Fig. 2.5A**). Stimulating FSK-treated SSTR3-expressing cells with somatostatin (SST) inhibited cilia PKA biosensor activity **(Fig. 2.5B, 2.5D)**. Thus, a ciliary GPCR also regulates ciliary PKA activity.

To assay the dependency Gα$_{i/o}$ on the ability of SSTR3 to inhibit ciliary PKA, we treated our cells with pertussis toxin (PTX), an inhibitor of Gα$_{i/o}$ proteins (Murayama and Ui, 1983; Ui et al., 1984). The ability of SST to inhibit cilia PKA biosensor activity was blocked by PTX **(Fig. 2.5B, 2.5D)**, indicating that Ga$_{i/o}$ can control ciliary PKA activity. Interestingly, we previously found that SST activation of SSTR3-expressing fibroblasts induces *Gli1* similarly to SAG, suggesting that activation of ciliary Gα$_{i/o}$ can activate the HH transcriptional response (Truong et al., 2021). We conclude that upon stimulation with SST, SSTR3 can stimulate Gα$_{i/o}$ and inhibit ciliary PKA to drive GLI-mediated HH target gene transcription.

Gα$_{i/o}$ has been investigated as an effector of SMO in HH signal transduction (Alcedo et al., 1996; Van Den Heuvel and Ingham, 1996; Riobo et al., 2006; Low et al., 2008; Ogden et al., 2008; Shen et al., 2013; Arveseth et al., 2021). To test whether Gα$_{i/o}$ is required for SMO to inhibit PKA specifically in the primary cilium, we treated cilia PKA biosensor-expressing NIH/3T3 cells with

SAG and PTX. Unlike SST activation of SSTR3, PTX did not block the ability of SAG activation of SMO to inhibit cilia PKA biosensor activity (**Fig. 2.5B-D**). Thus, despite $G\alpha_{i/o}$ being critical for ciliary GPCR-mediated control of PKA, $G\alpha_{i/o}$ activity is dispensable for SMO-mediated inhibition of PKA in the primary cilium.

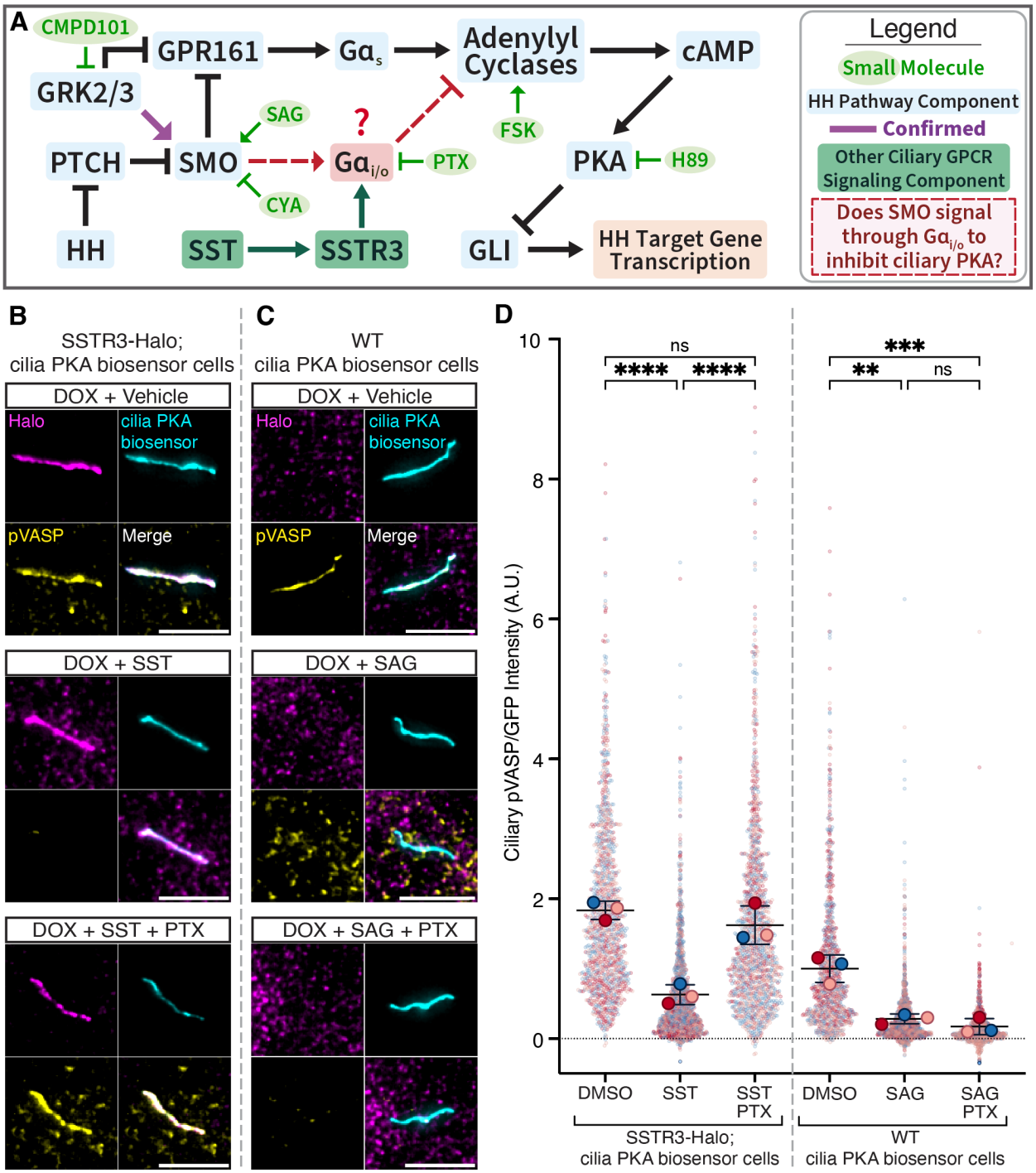

Figure 2.5: Gα$_i$ inhibits ciliary PKA, but does not mediate SMO-based control of ciliary PKA

(A) Schematic of the working model of HH signaling. Red arrows indicate areas of inquiry relevant to this figure.

(Figure caption continued on the next page.)

(Figure caption continued from the previous page.)

(B) Immunofluorescence imaging of cilia PKA biosensor cells stably expressing Halo-tagged SSTR3 in response to doxycycline (DOX). Cells were serum starved and treated with either DMSO, SST (10μM for 2h), or SST and PTX (10μM for 2h and 100ng/mL for 16h, respectively). Scale bars are 5μM.

(C) Immunofluorescence imaging of cilia PKA biosensor cells. Cells were serum starved and treated with either DMSO, SAG (100nM for 24h), or SAG and PTX (100nM for 24h and 100ng/mL for 16h, respectively).

(D) Quantification of ciliary pVASP intensity, normalized to ciliary GFP, of C and D. Each biological replicate has its own color. Significance was determined via one-way ANOVA of the means of each biological replicate, followed by Šídák's multiple comparison test. P values are indicated as follows: $**p < 0.003$, $***p < 0.0002$, and $****p < 0.0001$. Data are represented are means of replicates ± SD.

2.3.6 SMO A635 contributes to inhibition of ciliary PKA

An alternative to the hypothesis that $G\alpha_{i/o}$ mediates SMO inhibition of ciliary PKA is that SMO signals by the direct binding and inhibition of PKA-C via a PKI-like motif (Arveseth et al., 2021; Happ et al., 2022; Walker et al., 2024). A portion of the SMO proximal carboxy tail (pCT, residues 615–638) resembles PKI motifs of other PKA inhibitory proteins and these residues are necessary for SMO function in zebrafish (Happ et al., 2022).

Previous work identified that mutation of three residues in the pCT (W622A, R632A, R633A, referred to as the WRR mutation) are sufficient to prevent SMO signaling. To test the function of this SMO PKI motif, we generated *Smo*$^{-/-}$ cilia PKA biosensor NIH/3T3 cells stably expressing HALO-tagged wild-type SMO or SMO WRR **(Fig. 2.6A)**. As expected, SAG-stimulation of wild-type SMO-expressing cells showed inhibited cilia PKA biosensor activity. Surprisingly, activating cells expressing SMO with the WRR mutation also showed inhibited cilia PKA biosensor activity **(Fig. 2.6B-C).** However, consistent with previous findings (Happ et al., 2022), SMO-WRR failed to induce *Gli1* in response to SAG (**Fig. 2.6D**). Thus, the WRR mutation inhibits SMO signaling but in a way independent of inhibiting ciliary PKA.

Prior work examining the interaction of the SMO C-terminus with PKA-C in HEK293 cells revealed that there may a second PKI motif in the SMO distal carboxy tail (dCT, residues 530-545) (Happ et al., 2022). To test the involvement of this additional PKI motif, we mutated three residues within the dCT PKI motif (G538A, R539A, L540A, referred to as the GRL mutation) **(Fig. 2.6A)**. Similar to wild-type SMO and SMO WRR, *Smo*$^{-/-}$ cilia PKA biosensor NIH/3T3 cells stably expressing HALO-tagged SMO GRL also inhibited cilia PKA biosensor activity in the presence of SAG **(Fig. 2.6B-C)**. Similar to wild-type SMO, SMO-GRL was able to induce *Gli1* in response to SAG **(Fig 2.6D)**. Thus, mutation of the dCT SMO PKI motif neither abrogates the ability of SMO to inhibit ciliary PKA, nor does it interfere with downstream signal transduction.

To test whether the pCT and dCT PKI motifs may act redundantly to inhibit PKA, we generated *Smo*$^{-/-}$ cilia PKA biosensor NIH/3T3 cells stably expressing HALO-tagged SMO bearing both the WRR and GRL mutations (referred to as SMO WRRGRL). In these cells, activating SMO WRR GRL with SAG also inhibited cilia PKA biosensor activity **(Fig. 2.6B-C)**, and failed to induce Gli1 in response to SAG, to a similar extent as SMO WRR **(Fig 2.6D)**. Therefore, we did not find any evidence of overlapping function between the PKI motifs in the pCT and dCT.

Typically, PKA-C phosphorylates its substrates at a serine or threonine at a consensus (RRXS/TΦ where Φ is a hydrophobic residue) phosphorylation site (P site) (Kennelly and Krebs, 1991; Hennrich et al., 2013; Knape et al., 2015). Pseudosubstrates differ from substrates in having a non-phosphorylatable residue at the P site. Replacement of the P site residue of a PKA pseudosubstrate with serine converts them into substrates and increases dissociation from PKA-C (Scott et al., 1986; Knape et al., 2015). Happ et al. previously demonstrated that a version of SMO in which the pCT SMO PKI motif P site alanine was substituted with serine (SMO-A635S) did not activate the HH transcriptional response (Happ et al., 2022).

To assess whether converting the pCT SMO PKI motif to a PKA substrate affects the ability of SMO to inhibit ciliary PKA, we generated *Smo*$^{-/-}$ cilia PKA biosensor NIH/3T3 cells stably expressing HALO-tagged SMO-A635S and stimulated them with SAG (**Fig. 2.6A**). Compared to wild-type SMO, SMO-A635S exhibited attenuated inhibition of cilia PKA biosensor activity **(Fig. 2.6B-C)**. Unlike wild-type SMO, SMO-A635S did not induce *Gli1* in response to SAG (**Fig. 2.6D**). Thus, the PKI motif in SMO is critical for its ability to control ciliary PKA activity and activate the downstream pathway.

A constitutively active, oncogenic single amino acid substitution in SMO W5535L, better known as SMO-M2, is sufficient to cause basal cell carcinoma, medulloblastoma and

rhabdomyosarcoma (Mao et al., 2006). To assess whether oncogenic mutations affect the ability of SMO to inhibit ciliary PKA, we generated *Smo*$^{-/-}$ cilia PKA biosensor NIH/3T3 cells stably expressing HALO-tagged SMO-M2. Unlike wild-type SMO, SMO-M2 inhibited cilia PKA biosensor activity even in the absence of SAG **(Fig. 2.6B-C)**. Similarly, SMO-M2 induced *Gli1* even in the absence of SAG (**Fig. 2.6D**). Thus, an oncogenic mutation constitutively activates the ability of SMO to inhibit ciliary PKA.

To assess whether any of these mutations uncovered a cryptic dependency on $G\alpha_i$, we treated each of the mutant SMO-expressing cells with SAG and PTX. PTX did not attenuate the ability of any mutant SMO to inhibit cilia PKA biosensor activity, consistent with Ga_i being dispensable for SMO signaling **(Fig. S2.6)**. We conclude that SMO signals independently of $G\alpha_i$. Rather, the SMO pseudosubstrate site-mediated inhibition of PKA activity in the cilium activates the downstream HH signal transduction pathway (**Fig. 2.6E**).

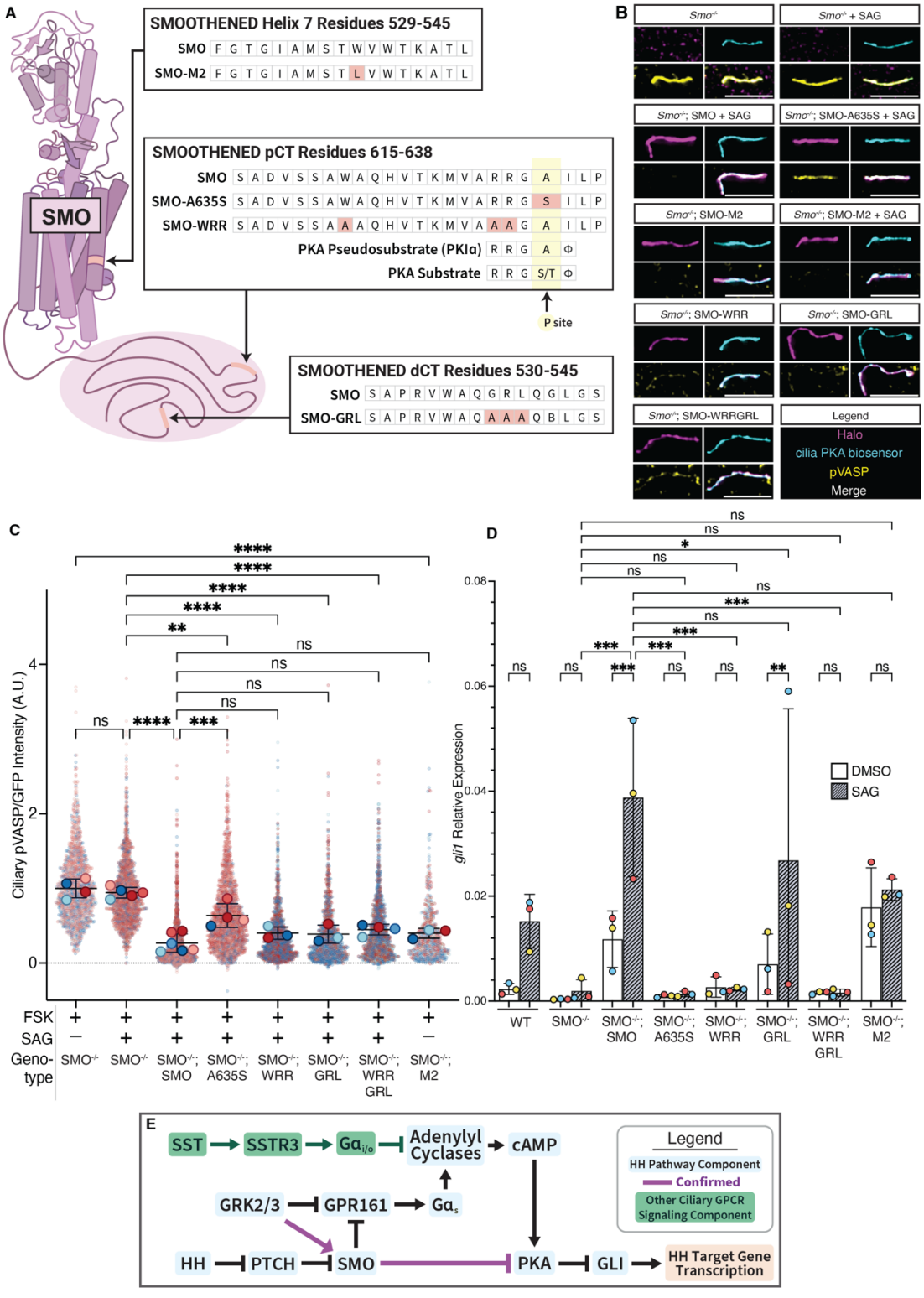

Figure 2.6: SMO PKI motif contributes to inhibiting ciliary PKA

(Figure caption continued on the nextt page.)

(Figure caption continued from the last page.)

(A) A schematic of the SMO mutations assessed in this figure.

(B) *Smo*$^{-/-}$ cilia PKA biosensor cells, stably expressing Halo-tagged wild-type SMO, SMO-A635S or SMO-M2, as indicated. Cells were treated SAG (100nM for 24h) and FSK (100nM for 15 minutes). Scale bars are 5μM.

(C) Quantification of ciliary pVASP intensity, normalized to ciliary GFP. Significance was determined via one-way ANOVA of the means of each biological replicate, followed by Šídák's multiple comparison test.

(D) qRT-PCR of *Gli1* in wild-type or *Smo*$^{-/-}$ cells expressing wild-type SMO, SMO-A635S or SMO-M2 and treated with SAG, as indicated. Significance was determined via two-way ANOVA of the means of each biological replicate, followed by Šídák's multiple comparison test.

(E) Schematic of HH signaling.

For all plots, each biological replicate is color coded. P values are indicated as follows: ** $p < 0.003$, ***$p < 0.0002$ and ****$p < 0.0001$. Data are represented are means of replicates ± SD.

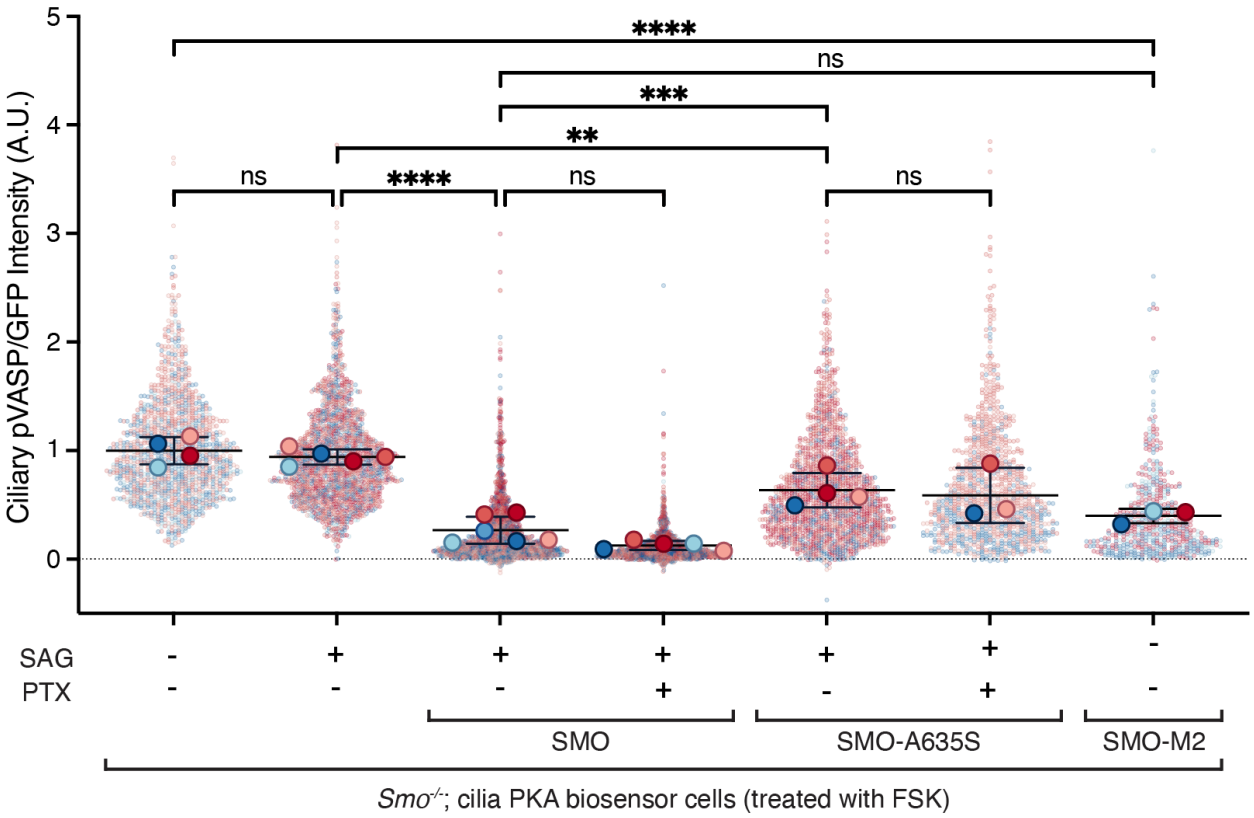

Supplemental Figure 2.6: $G\alpha_{i/o}$ does not synergize with the SMO PKI motif to inhibit ciliary PKA.

Quantification of ciliary pVASP intensity, normalized to ciliary GFP, in *Smo*$^{-/-}$ cilia PKA biosensor cells expressing wild-type SMO, SMO-A635S or SMO-M2, as indicated. As indicated, cells were treated SAG (100nM for 24h), or SAG and PTX (100nM for 24h and 100ng/mL for 16h, respectively). All conditions were treated with FSK (100nM for 15 minutes). For all plots, each biological replicate is color coded. Same data as used in Figure 6. Significance was determined via one-way ANOVA of the means of each biological replicate, followed by Šídák's multiple comparison test. P values are indicated as follows: ** $p < 0.003$, ***$p < 0.0002$ and ****$p < 0.0001$. Data are represented are means of replicates ± SD.

2.4 Discussion

Although vertebrate SMO requires the cilium to activate the downstream HH signal transduction pathway, how it does so has been elusive. Recent revelatory work has discovered that the C-terminus of vertebrate SMO can bind and inhibit PKA (*32*, *34*). PKA phosphorylates GLI to inhibit HH target gene transcription (*18–20*). Because SMO, PKA and GLI all can localize to primary cilia (*14*, *16*, *18*, *60*), we investigated whether SMO signals through inhibiting PKA at the primary cilium. To test this hypothesis, we developed a biosensor that measures ciliary PKA activity.

This biosensor revealed that SMO inhibits ciliary PKA in a state-dependent manner. SHH, (which acts through its receptor PTCH1 to activate SMO) (*74*) and SAG (which directly binds and activates SMO) (*50*, *51*) both induced SMO to accumulate at cilia and inhibit ciliary PKA. In contrast, CYA, a SMO inhibitor (*52*, *75*), induced SMO to accumulate at cilia but not inhibit ciliary PKA. Thus, the accumulation of SMO in cilia is not sufficient to inhibit ciliary PKA; SMO must also be in an active state.

Another requirement for SMO to inhibit ciliary PKA is GRK2/3: SMO is phosphorylated by GRK2/3 (*60*) and pharmacological inhibition of GRK2/3 prevented SMO from inhibiting ciliary PKA. Consistent with this conclusion, CYA prevented GRK2/3 from phosphorylating SMO and from inhibiting ciliary PKA. GRK2/3 also phosphorylates GPR161, facilitating the removal of GPR161 from the primary cilium (*36*), but GRK2/3 can still regulate HH signaling in the absence of GPR161 (*37*). Thus, another way in which GRK2/3 participates in HH signal transduction is by phosphorylating SMO to suppress ciliary PKA.

By measuring ciliary PKA activity, we assessed molecular mechanisms by which SMO could control PKA. Two models have been: 1) SMO activates $G\alpha_i$ to inhibit production of cAMP, thereby inhibiting PKA (*26–30*), and 2) SMO acts like a PKI to directly bind and inactivate PKA (*32*, *34*). We found that $G\alpha_i$ activity is dispensable for SMO to inhibit PKA. Furthermore, a mutation predicted to turn the PKI-like motif into a PKA substrate (and thus prevent PKA inhibition) blocked the ability to SMO to inhibit PKA and activate downstream transcription. As PKA substrates are generally dissociated from PKA upon phosphorylation (*71*, *72*), we propose that converting SMO from a pseudosubstrate to a substrate increases its dissociation rate from PKA-C and disrupts its ability to inhibit PKA.

Additionally, we find that an oncogenic form of SMO constitutively inhibits ciliary PKA activity. Oncogenic mutations in SMO cause a number of cancers, including medulloblastoma, basal cell carcinoma and rhabdomyosarcoma (*76*). Our findings suggest that, for SMO, constitutive ciliary localization, constitutive ciliary PKA inhibition and oncogenic activity are causally related. Although HH pathway-related medulloblastoma is responsive to small molecule inhibitors of SMO, acquisition of SMO mutations that interfere with drug binding lead to recurrence (*77*, *78*). We propose that an alternative therapeutic approach that bypasses SMO is to reactivate ciliary PKA.

Interestingly, SSTR3, a ciliary $G\alpha_i$-coupled GPCR not implicated in regulating HH signaling, could also inhibit ciliary PKA and activate HH transcription when expressed in fibroblasts. As the primary cilium is a specialized microenvironment for multiple receptors and signaling pathways, how many are mediated via ciliary PKA? A burgeoning number of other GPCRs have more recently been found to localize to primary cilia across many different tissues (*35*, *79–83*). For example, melanocortin 4 receptor (MC4R) is a neuronal cilium-localized GPCR critical for the

control of feeding behavior and long-term energy homeostasis (*83–86*). Similarly, SSTR3 endogenously localizes to the primary cilia of mammalian neurons and is implicated in learning and memory (*63*, *64*). One possibility is that there are different effectors other than PKA for other ciliary GPCRs. Another possibility is that many ciliary GPCRs act through ciliary PKA but achieve cell type-specific effects via different effectors downstream of PKA. In the case of SSTR3, it is unclear if SSTR3-expressing cells also endogenously express GLI proteins. Thus, it is possible that ciliary PKA phosphorylates a different effector in SSTR3-expressing cells.

Moreover, it is unclear if cells simultaneously communicate via multiple ciliary signaling pathways, such as the HH signal transduction pathway and ciliary GPCR signaling pathways. It is possible that the set of cells competent for HH signaling and the set of cells that are competent for other ciliary GPCR signaling are mutually exclusive, thus preventing crosstalk within their cilia. Alternatively, all $G\alpha_i$- or $G\alpha_s$-coupled ciliary GPCRs in cells competent for HH signaling may influence GLI-dependent transcription. Untangling GPCR signaling at the primary cilium will be critical to understanding, not only mechanisms of HH signaling, but how a host of signals critical to human health are transduced. Although vertebrate SMO requires the cilium to activate the downstream HH signal transduction pathway, how it does so has been elusive. Recent revelatory work has discovered that the C-terminus of vertebrate SMO can bind and inhibit PKA (Arveseth et al., 2021; Happ et al., 2022). PKA phosphorylates GLI to inhibit HH target gene transcription (Wang et al., 2000; Haycraft et al., 2005; Niewiadomski et al., 2014). Because SMO, PKA and GLI all can localize to primary cilia (Corbit et al., 2005; Haycraft et al., 2005; Truong et al., 2021; Walker et al., 2024), we investigated whether SMO signals through inhibiting PKA at the primary cilium. To test this hypothesis, we developed a biosensor that measures ciliary PKA activity.

This biosensor revealed that SMO inhibits ciliary PKA in a state-dependent manner. SHH, (which acts through its receptor PTCH1 to activate SMO) (Chen and Struhl, 1996) and SAG (which directly binds and activates SMO) (Chen et al., 2002b; Frank-Kamenetsky et al., 2002) both induced SMO to accumulate at cilia and inhibit ciliary PKA. In contrast, CYA, a SMO inhibitor (Incardona et al., 1998; Chen et al., 2002a), induced SMO to accumulate at cilia but not inhibit ciliary PKA. Thus, the accumulation of SMO in cilia is not sufficient to inhibit ciliary PKA; SMO must also be in an active state.

Another requirement for SMO to inhibit ciliary PKA is GRK2/3: SMO is phosphorylated by GRK2/3 (Walker et al., 2024) and pharmacological inhibition of GRK2/3 prevented SMO from inhibiting ciliary PKA. Consistent with this conclusion, CYA prevented GRK2/3 from phosphorylating SMO and from inhibiting ciliary PKA. GRK2/3 also phosphorylates GPR161, facilitating the removal of GPR161 from the primary cilium (Pal et al., 2016), but GRK2/3 can still regulate HH signaling in the absence of GPR161 (Pusapati et al., 2018). Thus, another way in which GRK2/3 participates in HH signal transduction is by phosphorylating SMO to suppress ciliary PKA.

By measuring ciliary PKA activity, we assessed molecular mechanisms by which SMO could control PKA. Two models have been: 1) SMO activates $G\alpha_i$ to inhibit production of cAMP, thereby inhibiting PKA (Alcedo et al., 1996; Van Den Heuvel and Ingham, 1996; Riobo et al., 2006; Ogden et al., 2008; Shen et al., 2013), and 2) SMO acts like a PKI to directly bind and inactivate PKA (Arveseth et al., 2021; Happ et al., 2022). We found that $G\alpha_i$ activity is dispensable for SMO to inhibit PKA. Furthermore, a mutation predicted to turn the PKI-like motif into a PKA substrate (and thus prevent PKA inhibition) blocked the ability to SMO to inhibit PKA and activate downstream transcription. As PKA substrates are generally dissociated from PKA upon

phosphorylation (Scott et al., 1986; Knape et al., 2015), we propose that converting SMO from a pseudosubstrate to a substrate increases its dissociation rate from PKA-C and disrupts its ability to inhibit PKA.

Additionally, we find that an oncogenic form of SMO constitutively inhibits ciliary PKA activity. Oncogenic mutations in SMO cause a number of cancers, including medulloblastoma, basal cell carcinoma and rhabdomyosarcoma (Raleigh and Reiter, 2019). Our findings suggest that, for SMO, constitutive ciliary localization, constitutive ciliary PKA inhibition and oncogenic activity are causally related. Although HH pathway-related medulloblastoma is responsive to small molecule inhibitors of SMO, acquisition of SMO mutations that interfere with drug binding lead to recurrence (Lam et al., 1999; Yauch et al., 2009). We propose that an alternative therapeutic approach that bypasses SMO is to reactivate ciliary PKA.

Interestingly, SSTR3, a ciliary $G\alpha_i$-coupled GPCR not implicated in regulating HH signaling, could also inhibit ciliary PKA and activate HH transcription when expressed in fibroblasts. As the primary cilium is a specialized microenvironment for multiple receptors and signaling pathways, how many are mediated via ciliary PKA? A burgeoning number of other GPCRs have more recently been found to localize to primary cilia across many different tissues (Händel et al., 1999; Brailov et al., 2000; Berbari et al., 2008; Mukhopadhyay et al., 2013; Siljee et al., 2018; Hilgendorf et al., 2019). For example, melanocortin 4 receptor (MC4R) is a neuronal cilium-localized GPCR critical for the control of feeding behavior and long-term energy homeostasis (Vaisse et al., 1998; Siljee et al., 2018; Wang et al., 2021; Brewer et al., 2022). Similarly, SSTR3 endogenously localizes to the primary cilia of mammalian neurons and is implicated in learning and memory (Green et al., 2016; Ye et al., 2018). One possibility is that there are different effectors other than PKA for other ciliary GPCRs. Another possibility is that

many ciliary GPCRs act through ciliary PKA but achieve cell type-specific effects via different effectors downstream of PKA. In the case of SSTR3, it is unclear if SSTR3-expressing cells also endogenously express GLI proteins. Thus, it is possible that ciliary PKA phosphorylates a different effector in SSTR3-expressing cells.

Moreover, it is unclear if cells simultaneously communicate via multiple ciliary signaling pathways, such as the HH signal transduction pathway and ciliary GPCR signaling pathways. It is possible that the set of cells competent for HH signaling and the set of cells that are competent for other ciliary GPCR signaling are mutually exclusive, thus preventing crosstalk within their cilia. Alternatively, all $G\alpha_i$- or $G\alpha_s$-coupled ciliary GPCRs in cells competent for HH signaling may influence GLI-dependent transcription. Untangling GPCR signaling at the primary cilium will be critical to understanding, not only mechanisms of HH signaling, but how a host of signals critical to human health are transduced.

2.5 Materials and Methods

2.5.1 Vector construction and generation of stable cell lines

To generate NIH/3T3 Flp-In cell lines expressing the ciliary PKA biosensor, ARL13B-GFP-VASP was cloned with the In-Fusion HD cloning kit (Takara, 639650) into a version of pGLAP5 with an attenuated EF1a promoter lacking the TATA box (Nager et al., 2017), a backbone previously generated in our lab (Truong et al., 2021). We transfected cells with this plasmid, concurrently with the pOG44 Flp-Recombinase Expression Vector (Invitrogen, V600520), with Lipofectamine LTX (Invitrogen, 15338100), according to the ThermoFisher Flp-In System protocol to generate stable Flp-In expression cell lines. Cells were selected with 70µg/mL of hygromycin B (Corning, 30-240-CR). Following selection, we selected a single clone of these cells

to characterize and build all subsequent cell lines. Plasmid encoding VASP amino acids 148-164 was a generous gift from Roshanak Irannejad.

For generating mRNA encoding ARL13B-GFP-VASP, ARL13B-GFP-VASP was cloned into the pCS107 expression vector using the In-Fusion HD cloning kit (Takara, 639650).

To generate cell lines expressing Halo-tagged SSTR3, SMO, SMO-A635S, and SMO-M2, we cloned each protein of interest into a pLVX-TetOne-Puro backbone (Takara 631849).

We used clustered regularly interspaced short palindromic repeats (CRISPR)-mediated editing to generate loss-of-function mutations in *Smo* using two different guide RNAs per gene in our cilia PKA biosensor cells. Synthetic guide RNAs for *Smo* (5'-CCCACGCACGGGGCGGCCAG-3', 5'-UCCCGCUCAAGGCCGCCCCC-3') were ordered from Synthego, complexed with TrueCut Cas9 Protein v2 (Invitrogen, A36496), and nucleofected with the Neon Transfection System (Invitrogen). Cells were clonally selected and screened via PCR for genomic deletions with primers for the genomic regions of interest for mouse *Smo* (forward primer 5'-AGGGTTCCCAGGGTTGAAGA-3', reverse primer: 5' -CACACGTTGTAGCGCAAAGG-3').

Lentivirus was generated by transfecting 7.5 μg of each plasmid of interest with 1.5 μg of pCMV-VSV-G (Addgene, 8454) and 6 μg of psPAX2 (Addgene, 12260) into a 10 cm plate of Lenti-X 293T cells (Takara, 632180) at 70–80% confluence using Fugene 6 transfection reagent (Promega, E2691). Medium containing lentiviral particles was collected 1 day after transfection and was concentrated with a Lenti-X Concentrator (Takara, 631232), incubated overnight at 4°C, and followed by centrifugation at 4000g for 45 min at 4°C. The pellet was resuspended in 120μL DPBS (Gibco, 14-90-250).

To generate SMO expression cell lines, cilia PKA biosensor *Smo*$^{-/-}$ cells were transduced with 20μL of resuspended lentivirus containing either doxycycline-inducible SMO-Halo, SMO-A635S-Halo, SMO-M2-Halo in the presence of 4 μg/mL polybrene. 24 hours after transduction, cells were selected with 1μg/mL puromycin (Gibco, A11138-03) for 5 days. Cells that survived selection where then incubated with 100ng/mL doxycycline (Sigma-Aldrich, D5207) for 48 hours and incubated in HaloTag Alexa Fluor 660 Ligand (Promega, G8472) overnight before being enriched via fluorescence-activated cell sorting (FACS) on a BD FACSAria III Cell Sorter.

To generate SSTR3 overexpression cell lines, cilia PKA biosensor cells were transduced with lentivirus containing doxycycline-inducible SSTR3-Halo-puro in the presence of 4 μg/mL polybrene. Cells were then transduced with 1μg/mL doxycycline (Sigma-Aldrich, D5207) for 48 hours, selected with 1μg/mL puromycin (Gibco, A11138-03). Cells were then incubated in HaloTag Alexa Fluor 660 Ligand (Promega, G8472) overnight before being enriched via fluorescence-activated cell sorting (FACS) on an BD FACSAria III Cell Sorter.

2.5.2 mRNA synthesis

To generate mRNA for expressing the cilia PKA biosensor in zebrafish, we grew pCS107-ARL13B-GFP-VASP in *dam*$^{-}$*/dcm*$^{-}$ competent *E. coli* (New England Biolabs, C2925H). We isolated our plasmid with the Plasmid Plus Midi Kit (QIAGEN, 12943). For zebrafish injections, we linearized the construct with *ApaI* (New England Biolabs, R0114L) and generated mRNA with the mMESSAGE mMACHINE SP6 kit (Invitrogen, AM1340).

2.5.3 Zebrafish husbandry and mRNA injection

Adult *Danio rerio* zebrafish were maintained under standard laboratory conditions. Zebrafish of Ekkwill (EKW) background were used as wild type. Embryos were maintained in egg

water containing 60 µg/mL sea salt (Instant Ocean) in distilled water. We injected 500pg of ARL13B-GFP-VASP mRNA at the one-cell stage. We incubated injected embryos in egg water, and unfertilized embryos were removed 6 hours post injection. All zebrafish protocols were approved by the Institutional Animal Care and Use Committee (IACUC) of the University of California, San Francisco.

3.5.4 Mammalian cell culture

NIH/3T3 Flp-In cells (Invitrogen, R761-07) were cultured in Dulbecco's modified Eagle's medium with high glucose (Gibco, 11965118) supplemented with 10% newborn calf serum (Gibco, 16010159) and GlutaMAX supplement (Gibco, 35050061). Cells were treated with antibiotic-antimycotic (Gibco, 152400632) following FACS for 1 week. Cells were otherwise maintained in the absence of antibiotics. To induce ciliation, cells were grown to confluence and starved overnight in Opti-MEM reduced serum medium with GlutaMAX supplement (Gibco, 51985091).

2.5.5 Immunofluorescence staining

We seeded cells on 12 mm cover glasses of 170µm thickness (Paul Marienfeld, 0117520) at a density of $8x10^4$ cells per well in a 24-well plate. After drug treatment and induction of ciliation, we fixed cells for 10 minutes in 4% PFA (VWR, 100504-782) diluted in DPBS (Gibco, 14-90-250). We diluted primary antibodies in blocking buffer (0.1% TritonX-100, 0.02% Sodium Azide, 3% BSA) and incubated them overnight at 4°C. Subsequently we incubated cells in donkey Alexa Fluor-conjugated secondary antibodies, ChromoTek GFP-Booster Alexa Fluor 488 (Proteintech, gb2AF488), and Hoechst (ThermoFisher Scientific) diluted in blocking buffer at room temperature

for 1 hour. We mounted cover glasses in ProLong Glass antifade mountant (Invitrogen, P36982) and allowed the slides to cure overnight at room temperature before imaging.

We fixed dechorionated zebrafish embryos in 4% PFA (VWR, 100504-782) diluted in DPBS (Gibco, 14-90-250) for 2 hours at room temperature. We blocked embryos in 1% BSA, 1% DMSO and 0.5% Triton X-100 in PBS (PBDT) for 1 hour. After blocking, we incubated embryos overnight at 4°C with primary antibodies diluted in PBDT. Subsequently we incubated embryos in donkey Alexa Fluor-conjugated secondary antibodies, ChromoTek GFP-Booster Alexa Fluor 488 (Proteintech, gb2AF488), and Hoechst (ThermoFisher Scientific) diluted in PBDT for 2 hours at room temperature. We incubated embryos in 70% glycerol overnight, then mounted in in ProLong Glass antifade mountant (Invitrogen, P36982) and allowed the slides to cure overnight at room temperature before imaging.

2.5.6 Image Acquisition and Ciliary Fluorescence Intensity Quantification

We imaged fixed cells on a DeltaVision-OMX-SR (GE Healthcare) equipped with a Plan ApoN 60X/1.42 Oil objective and three PCO.edge 5.5 15bit sCMOS Cameras (liquid cooled). Four-channel fluorescence imaging was captured with a Toptica 4 line laser launch light source, laser excitation wavelengths 405nm/488nm/568nm/642nm, and emission filters 435/31m, 528/48m, 609/37m, and 683/40m. Images for quantification were acquired using the widefield setting, and representative images, where indicated in the figure legend, were acquired with 3D-SIM Data. Immersion oil with refractive index of 1.518 was used for most experiments. Z stacks of 5–6 µm were collected using a 0.250µm step size for widefield imaging and 0.125 µm step size for 3D-SIM imaging. Raw images were reconstructed using SoftWorx 6.5.2 (GE Healthcare) using default parameters.

We imaged fixed zebrafish embryos with Zeiss LSM 800 laser scanning confocal microscope equipped with a 63x/1.4 oil immersion objective and captured using the Zen Imaging Software (Zeiss). While collecting images, we held constant the gain, offset and laser power for each antibody combination. We processed images identically and used ImageJ/FIJI software (Schneider et al., 2012) to generate sum and maximal projections.

We used Cell Profiler image analysis software (Stirling et al., 2021) on our sum projection images to generate fluorescence intensity quantifications. A cilia marker (ARL13B-GFP-VASP) was used to identify cilia and create a mask using the object identification module in CellProfiler using differences in signal intensity and size to segment cilia. The ciliary mask was then dilated by 10 pixels to create a dilated ciliary mask. We determined the fluorescence intensity (integrated intensity) and area (in pixels) for both the cilia mask and dilated cilia mask. We determined background-subtracted, area-normalized ciliary fluorescence intensity for all channels of interest with the following formula:

$$Background\ Ciliary\ Intensity\ (A.U.) = \frac{(Dilated\ Cilia)_{Intensity} - (Cilia)_{Intensity}}{(Dilated\ Cilia)_{Area} - (Cilia)_{Area}}$$

$$Ciliary\ Intensity\ (A.U.) = \frac{(Cilia)_{Intensity}}{(Cilia)_{Area}} - Background\ Ciliary\ Intensity\ (A.U.)$$

To represent ciliary PKA activity, we report $\frac{ciliary\ pVASP\ Intensity}{ciliary\ GFP\ Intensity}$ to account for the amount of VASP peptide able to be phosphorylated at the primary cilium in our cilia PKA biosensor cells. Ciliary intensity calculations were ultimately done through a Jupyter Notebook python script. Data were exported to .csv files and graphs were generated in GraphPad Prism 10. Statistical analyses were performed using GraphPad Prism 10. Statistical tests used for each experiment are listed in the accompanying figure legend.

2.5.7 Quantitative RT-PCR

3T3 cells were seeded in 6-well plates at a density of 300,000 cells per well. Total RNA was extracted using the RNeasy Mini Kit (QIAGEN Cat# 74106) according to the manufacturer's instructions. cDNA was reverse transcribed from 1ug of RNA using the iSCRIPT cDNA synthesis kit (Bio-Rad Cat#1708891BUN). Each qRT-PCR reaction was performed in technical quadruplicates on a 384 well plate (USA Scientific, Cat# 1438-4700) using PowerUp SYBR Green Master Mix (Applied Biosystems Cat# A25777) and run on a QuantStudio 5 real-time PCR system (Applied Biosciences) running QuantStudio Design & Analysis software (v.1.5.1). We used the following primer sequences: *Hprt* (Forward primer: 5'-CATAACCTGGTTCATCATCGC-3', Reverse primer: 5'-TCCTCCTCAGACCGCTTT T-3') and *Gli1* (Forward primer: 5'-GGTGCTGCCTATAGCCAGTGTCCTC-3', Reverse primer: 5'-GTGCCAATCCGGTGG AGTCAGACCC-3') Relative expression was calculated using the ΔΔCT method normalized to the expression of the housekeeping gene *hprt*.

2.6 References:

Alcedo, J., Ayzenzon, M., Von Ohlen, T., Noll, M., and Hooper, J. E. (1996). The Drosophila smoothened Gene Encodes a Seven-Pass Membrane Protein, a Putative Receptor for the Hedgehog Signal. *Cell* 86, 221–232. doi: 10.1016/S0092-8674(00)80094-X

Arveseth, C. D., Happ, J. T., Hedeen, D. S., Zhu, J.-F., Capener, J. L., Klatt Shaw, D., et al. (2021). Smoothened transduces Hedgehog signals via activity-dependent sequestration of PKA catalytic subunits. *PLoS Biol* 19, e3001191. doi: 10.1371/journal.pbio.3001191

Bangs, F., and Anderson, K. V. (2017). Primary Cilia and Mammalian Hedgehog Signaling. *Cold Spring Harb Perspect Biol* 9, a028175. doi: 10.1101/cshperspect.a028175

Berbari, N. F., Johnson, A. D., Lewis, J. S., Askwith, C. C., and Mykytyn, K. (2008). Identification of Ciliary Localization Sequences within the Third Intracellular Loop of G Protein-coupled Receptors. *MBoC* 19, 1540–1547. doi: 10.1091/mbc.e07-09-0942

Brailov, I., Bancila, M., Brisorgueil, M.-J., Miquel, M.-C., Hamon, M., and Vergé, D. (2000). Localization of 5-HT6 receptors at the plasma membrane of neuronal cilia in the rat brain. *Brain Research* 872, 271–275. doi: 10.1016/S0006-8993(00)02519-1

Breslow, D. K., Hoogendoorn, S., Kopp, A. R., Morgens, D. W., Vu, B. K., Kennedy, M. C., et al. (2018). A CRISPR-based screen for Hedgehog signaling provides insights into ciliary function and ciliopathies. *Nat Genet* 50, 460–471. doi: 10.1038/s41588-018-0054-7

Brewer, K. M., Brewer, K. K., Richardson, N. C., and Berbari, N. F. (2022). Neuronal cilia in energy homeostasis. *Front. Cell Dev. Biol.* 10, 1082141. doi: 10.3389/fcell.2022.1082141

Butt, E., Abel, K., Krieger, M., Palm, D., Hoppe, V., Hoppe, J., et al. (1994). cAMP- and cGMP-dependent protein kinase phosphorylation sites of the focal adhesion vasodilator-stimulated phosphoprotein (VASP) in vitro and in intact human platelets. *Journal of Biological Chemistry* 269, 14509–14517. doi: 10.1016/S0021-9258(17)36652-8

Chávez, M., Ena, S., Van Sande, J., de Kerchove d'Exaerde, A., Schurmans, S., and Schiffmann, S. N. (2015). Modulation of Ciliary Phosphoinositide Content Regulates Trafficking and Sonic Hedgehog Signaling Output. *Developmental Cell* 34, 338–350. doi: 10.1016/j.devcel.2015.06.016

Chen, J. K., Taipale, J., Cooper, M. K., and Beachy, P. A. (2002a). Inhibition of Hedgehog signaling by direct binding of cyclopamine to Smoothened. *Genes Dev.* 16, 2743–2748. doi: 10.1101/gad.1025302

Chen, J. K., Taipale, J., Young, K. E., Maiti, T., and Beachy, P. A. (2002b). Small molecule modulation of Smoothened activity. *Proc. Natl. Acad. Sci. U.S.A.* 99, 14071–14076. doi: 10.1073/pnas.182542899

Chen, W., Ren, X.-R., Nelson, C. D., Barak, L. S., Chen, J. K., Beachy, P. A., et al. (2004). Activity-Dependent Internalization of Smoothened Mediated by ß-Arrestin 2 and GRK2. *Science* 306, 2257–2260. doi: 10.1126/science.1104135

Chen, Y., Sasai, N., Ma, G., Yue, T., Jia, J., Briscoe, J., et al. (2011). Sonic Hedgehog Dependent Phosphorylation by CK1α and GRK2 Is Required for Ciliary Accumulation and Activation of Smoothened. *PLoS Biol* 9, e1001083. doi: 10.1371/journal.pbio.1001083

Chen, Y., and Struhl, G. (1996). Dual Roles for Patched in Sequestering and Transducing Hedgehog. *Cell* 87, 553–563. doi: 10.1016/S0092-8674(00)81374-4

Corbit, K. C., Aanstad, P., Singla, V., Norman, A. R., Stainier, D. Y. R., and Reiter, J. F. (2005). Vertebrate Smoothened functions at the primary cilium. *Nature* 437, 1018–1021. doi: 10.1038/nature04117

Delling, M., DeCaen, P. G., Doerner, J. F., Febvay, S., and Clapham, D. E. (2013). Primary cilia are specialized calcium signalling organelles. *Nature* 504, 311–314. doi: 10.1038/nature12833

Fan, C.-M., and Tessier-Lavigne, M. (1994). Patterning of mammalian somites by surface ectoderm and notochord: Evidence for sclerotome induction by a hedgehog homolog. *Cell* 79, 1175–1186. doi: 10.1016/0092-8674(94)90009-4

Frank-Kamenetsky, M., Zhang, X. M., Bottega, S., Guicherit, O., Wichterle, H., Dudek, H., et al. (2002). Small-molecule modulators of Hedgehog signaling: identification and characterization of Smoothened agonists and antagonists. *J Biol* 1, 10. doi: 10.1186/1475-4924-1-10

Garcia-Gonzalo, F. R., Corbit, K. C., Sirerol-Piquer, M. S., Ramaswami, G., Otto, E. A., Noriega, T. R., et al. (2011). A transition zone complex regulates mammalian ciliogenesis and ciliary membrane composition. *Nat Genet* 43, 776–784. doi: 10.1038/ng.891

Garcia-Gonzalo, F. R., Phua, S. C., Roberson, E. C., Garcia, G., Abedin, M., Schurmans, S., et al. (2015). Phosphoinositides Regulate Ciliary Protein Trafficking to Modulate Hedgehog Signaling. *Developmental Cell* 34, 400–409. doi: 10.1016/j.devcel.2015.08.001

Gilman, A. G. (1987). G PROTEINS: TRANSDUCERS OF RECEPTOR-GENERATED SIGNALS. *Annu. Rev. Biochem.* 56, 615–649. doi: 10.1146/annurev.bi.56.070187.003151

Goetz, S. C., and Anderson, K. V. (2010). The primary cilium: a signalling centre during vertebrate development. *Nat Rev Genet* 11, 331–344. doi: 10.1038/nrg2774

Green, J. A., Schmid, C. L., Bley, E., Monsma, P. C., Brown, A., Bohn, L. M., et al. (2016). Recruitment of β-Arrestin into Neuronal Cilia Modulates Somatostatin Receptor Subtype 3 Ciliary Localization. *Molecular and Cellular Biology* 36, 223–235. doi: 10.1128/MCB.00765-15

Händel, M., Schulz, S., Stanarius, A., Schreff, M., Erdtmann-Vourliotis, M., Schmidt, H., et al. (1999). Selective targeting of somatostatin receptor 3 to neuronal cilia. *Neuroscience* 89, 909–926. doi: 10.1016/S0306-4522(98)00354-6

Happ, J. T., Arveseth, C. D., Bruystens, J., Bertinetti, D., Nelson, I. B., Olivieri, C., et al. (2022). A PKA inhibitor motif within SMOOTHENED controls Hedgehog signal transduction. *Nat Struct Mol Biol* 29, 990–999. doi: 10.1038/s41594-022-00838-z

Haycraft, C. J., Banizs, B., Aydin-Son, Y., Zhang, Q., Michaud, E. J., and Yoder, B. K. (2005). Gli2 and Gli3 Localize to Cilia and Require the Intraflagellar Transport Protein Polaris for Processing and Function. *PLoS Genet* 1, e53. doi: 10.1371/journal.pgen.0010053

Hennrich, M. L., Marino, F., Groenewold, V., Kops, G. J. P. L., Mohammed, S., and Heck, A. J. R. (2013). Universal Quantitative Kinase Assay Based on Diagonal SCX Chromatography and Stable Isotope Dimethyl Labeling Provides High-definition Kinase Consensus Motifs for PKA and Human Mps1. *J. Proteome Res.* 12, 2214–2224. doi: 10.1021/pr400074f

Hilgendorf, K. I., Johnson, C. T., Mezger, A., Rice, S. L., Norris, A. M., Demeter, J., et al. (2019). Omega-3 Fatty Acids Activate Ciliary FFAR4 to Control Adipogenesis. *Cell* 179, 1289-1305.e21. doi: 10.1016/j.cell.2019.11.005

Hurley, J. H. (1999). Structure, Mechanism, and Regulation of Mammalian Adenylyl Cyclase. *Journal of Biological Chemistry* 274, 7599–7602. doi: 10.1074/jbc.274.12.7599

Incardona, J. P., Gaffield, W., Kapur, R. P., and Roelink, H. (1998). The teratogenic *Veratrum* alkaloid cyclopamine inhibits Sonic hedgehog signal transduction. *Development* 125, 3553–3562. doi: 10.1242/dev.125.18.3553

Ingham, P. W., Nakano, Y., and Seger, C. (2011). Mechanisms and functions of Hedgehog signalling across the metazoa. *Nat Rev Genet* 12, 393–406. doi: 10.1038/nrg2984

Kennelly, P. J., and Krebs, E. G. (1991). Consensus sequences as substrate specificity determinants for protein kinases and protein phosphatases. *Journal of Biological Chemistry* 266, 15555–15558. doi: 10.1016/S0021-9258(18)98436-X

Kim, J., Kato, M., and Beachy, P. A. (2009). Gli2 trafficking links Hedgehog-dependent activation of Smoothened in the primary cilium to transcriptional activation in the nucleus. *Proc. Natl. Acad. Sci. U.S.A.* 106, 21666–21671. doi: 10.1073/pnas.0912180106

Knape, M. J., Ahuja, L. G., Bertinetti, D., Burghardt, N. C. G., Zimmermann, B., Taylor, S. S., et al. (2015). Divalent Metal Ions Mg^{2+} and Ca^{2+} Have Distinct Effects on Protein Kinase A Activity and Regulation. *ACS Chem. Biol.* 10, 2303–2315. doi: 10.1021/acschembio.5b00271

Kong, J. H., Siebold, C., and Rohatgi, R. (2019). Biochemical mechanisms of vertebrate hedgehog signaling. *Development* 146, dev166892. doi: 10.1242/dev.166892

Lam, C.-W., Xie, J., To, K.-F., Ng, H.-K., Lee, K.-C., Yuen, N. W.-F., et al. (1999). A frequent activated smoothened mutation in sporadic basal cell carcinomas. *Oncogene* 18, 833–836. doi: 10.1038/sj.onc.1202360

Lambrechts, A., Kwiatkowski, A. V., Lanier, L. M., Bear, J. E., Vandekerckhove, J., Ampe, C., et al. (2000). cAMP-dependent Protein Kinase Phosphorylation of EVL, a Mena/VASP Relative, Regulates Its Interaction with Actin and SH3 Domains. *Journal of Biological Chemistry* 275, 36143–36151. doi: 10.1074/jbc.M006274200

Low, W.-C., Wang, C., Pan, Y., Huang, X.-Y., Chen, J. K., and Wang, B. (2008). The decoupling of Smoothened from Gαi proteins has little effect on Gli3 protein processing and Hedgehog-regulated chick neural tube patterning. *Developmental Biology* 321, 188–196. doi: 10.1016/j.ydbio.2008.06.014

Mao, J., Ligon, K. L., Rakhlin, E. Y., Thayer, S. P., Bronson, R. T., Rowitch, D., et al. (2006). A Novel Somatic Mouse Model to Survey Tumorigenic Potential Applied to the Hedgehog Pathway. *Cancer Research* 66, 10171–10178. doi: 10.1158/0008-5472.CAN-06-0657

Marley, A., Choy, R. W.-Y., and Von Zastrow, M. (2013). GPR88 Reveals a Discrete Function of Primary Cilia as Selective Insulators of GPCR Cross-Talk. *PLoS ONE* 8, e70857. doi: 10.1371/journal.pone.0070857

Mick, D. U., Rodrigues, R. B., Leib, R. D., Adams, C. M., Chien, A. S., Gygi, S. P., et al. (2015). Proteomics of Primary Cilia by Proximity Labeling. *Developmental Cell* 35, 497–512. doi: 10.1016/j.devcel.2015.10.015

Moore, C. A. C., Milano, S. K., and Benovic, J. L. (2007). Regulation of Receptor Trafficking by GRKs and Arrestins. *Annu. Rev. Physiol.* 69, 451–482. doi: 10.1146/annurev.physiol.69.022405.154712

Mukhopadhyay, S., Wen, X., Ratti, N., Loktev, A., Rangell, L., Scales, S. J., et al. (2013). The Ciliary G-Protein-Coupled Receptor Gpr161 Negatively Regulates the Sonic Hedgehog Pathway via cAMP Signaling. *Cell* 152, 210–223. doi: 10.1016/j.cell.2012.12.026

Murayama, T., and Ui, M. (1983). Loss of the inhibitory function of the guanine nucleotide regulatory component of adenylate cyclase due to its ADP ribosylation by islet-activating protein, pertussis toxin, in adipocyte membranes. *Journal of Biological Chemistry* 258, 3319–3326. doi: 10.1016/S0021-9258(18)32863-1

Murthy, K. S., Coy, D. H., and Makhlouf, G. M. (1996). Somatostatin Receptor-mediated Signaling in Smooth Muscle. *Journal of Biological Chemistry* 271, 23458–23463. doi: 10.1074/jbc.271.38.23458

Mykytyn, K., and Askwith, C. (2017). G-Protein-Coupled Receptor Signaling in Cilia. *Cold Spring Harb Perspect Biol* 9, a028183. doi: 10.1101/cshperspect.a028183

Nager, A. R., Goldstein, J. S., Herranz-Pérez, V., Portran, D., Ye, F., Garcia-Verdugo, J. M., et al. (2017). An Actin Network Dispatches Ciliary GPCRs into Extracellular Vesicles to Modulate Signaling. *Cell* 168, 252-263.e14. doi: 10.1016/j.cell.2016.11.036

Niewiadomski, P., Kong, J. H., Ahrends, R., Ma, Y., Humke, E. W., Khan, S., et al. (2014). Gli Protein Activity Is Controlled by Multisite Phosphorylation in Vertebrate Hedgehog Signaling. *Cell Reports* 6, 168–181. doi: 10.1016/j.celrep.2013.12.003

O'Banion, C. P., Priestman, M. A., Hughes, R. M., Herring, L. E., Capuzzi, S. J., and Lawrence, D. S. (2018). Design and Profiling of a Subcellular Targeted Optogenetic cAMP-Dependent Protein Kinase. *Cell Chemical Biology* 25, 100-109.e8. doi: 10.1016/j.chembiol.2017.09.011

O'Banion, C. P., Vickerman, B. M., Haar, L., and Lawrence, D. S. (2019). Compartmentalized cAMP Generation by Engineered Photoactivated Adenylyl Cyclases. *Cell Chemical Biology* 26, 1393-1406.e7. doi: 10.1016/j.chembiol.2019.07.004

Ogden, S. K., Fei, D. L., Schilling, N. S., Ahmed, Y. F., Hwa, J., and Robbins, D. J. (2008). G protein Gαi functions immediately downstream of Smoothened in Hedgehog signalling. *Nature* 456, 967–970. doi: 10.1038/nature07459

Pal, K., Hwang, S., Somatilaka, B., Badgandi, H., Jackson, P. K., DeFea, K., et al. (2016). Smoothened determines β-arrestin–mediated removal of the G protein–coupled receptor Gpr161 from the primary cilium. *Journal of Cell Biology* 212, 861–875. doi: 10.1083/jcb.201506132

Philipp, M., Fralish, G. B., Meloni, A. R., Chen, W., MacInnes, A. W., Barak, L. S., et al. (2008). Smoothened Signaling in Vertebrates Is Facilitated by a G Protein-coupled Receptor Kinase. *MBoC* 19, 5478–5489. doi: 10.1091/mbc.e08-05-0448

Pierce, K. L., Premont, R. T., and Lefkowitz, R. J. (2002). Seven-transmembrane receptors. *Nat Rev Mol Cell Biol* 3, 639–650. doi: 10.1038/nrm908

Priestman, M. A., Sun, L., and Lawrence, D. S. (2011). Dual Wavelength Photoactivation of cAMP- and cGMP-Dependent Protein Kinase Signaling Pathways. *ACS Chem. Biol.* 6, 377–384. doi: 10.1021/cb100398e

Pusapati, G. V., Kong, J. H., Patel, B. B., Gouti, M., Sagner, A., Sircar, R., et al. (2018). G protein–coupled receptors control the sensitivity of cells to the morphogen Sonic Hedgehog. *Sci. Signal.* 11, eaao5749. doi: 10.1126/scisignal.aao5749

Raleigh, D. R., and Reiter, J. F. (2019). Misactivation of Hedgehog signaling causes inherited and sporadic cancers. *Journal of Clinical Investigation* 129, 465–475. doi: 10.1172/JCI120850

Raleigh, D. R., Sever, N., Choksi, P. K., Sigg, M. A., Hines, K. M., Thompson, B. M., et al. (2018). Cilia-Associated Oxysterols Activate Smoothened. *Molecular Cell* 72, 316-327.e5. doi: 10.1016/j.molcel.2018.08.034

Riobo, N. A., Saucy, B., Dilizio, C., and Manning, D. R. (2006). Activation of heterotrimeric G proteins by Smoothened. *Proc Natl Acad Sci U S A* 103, 12607–12612. doi: 10.1073/pnas.0600880103

Rohatgi, R., Milenkovic, L., Corcoran, R. B., and Scott, M. P. (2009). Hedgehog signal transduction by Smoothened: Pharmacologic evidence for a 2-step activation process. *Proc. Natl. Acad. Sci. U.S.A.* 106, 3196–3201. doi: 10.1073/pnas.0813373106

Rohatgi, R., Milenkovic, L., and Scott, M. P. (2007). Patched1 Regulates Hedgehog Signaling at the Primary Cilium. *Science* 317, 372–376. doi: 10.1126/science.1139740

Roy, S., Wolff, C., and Ingham, P. W. (2001). The *u-boot* mutation identifies a Hedgehog-regulated myogenic switch for fiber-type diversification in the zebrafish embryo. *Genes Dev.* 15, 1563–1576. doi: 10.1101/gad.195801

Schneider, C. A., Rasband, W. S., and Eliceiri, K. W. (2012). NIH Image to ImageJ: 25 years of image analysis. *Nat Methods* 9, 671–675. doi: 10.1038/nmeth.2089

Scott, J. D., Glaccum, M. B., Fischer, E. H., and Krebs, E. G. (1986). Primary-structure requirements for inhibition by the heat-stable inhibitor of the cAMP-dependent protein kinase. *Proc. Natl. Acad. Sci. U.S.A.* 83, 1613–1616. doi: 10.1073/pnas.83.6.1613

Seamon, K. B., Padgett, W., and Daly, J. W. (1981). Forskolin: unique diterpene activator of adenylate cyclase in membranes and in intact cells. *Proc. Natl. Acad. Sci. U.S.A.* 78, 3363–3367. doi: 10.1073/pnas.78.6.3363

Shen, F., Cheng, L., Douglas, A. E., Riobo, N. A., and Manning, D. R. (2013). Smoothened is a fully competent activator of the heterotrimeric G protein G(i). *Mol Pharmacol* 83, 691–697. doi: 10.1124/mol.112.082511

Siljee, J. E., Wang, Y., Bernard, A. A., Ersoy, B. A., Zhang, S., Marley, A., et al. (2018). Subcellular localization of MC4R with ADCY3 at neuronal primary cilia underlies a common pathway for genetic predisposition to obesity. *Nat Genet* 50, 180–185. doi: 10.1038/s41588-017-0020-9

Smolenski, A., Bachmann, C., Reinhard, K., Hönig-Liedl, P., Jarchau, T., Hoschuetzky, H., et al. (1998). Analysis and Regulation of Vasodilator-stimulated Phosphoprotein Serine 239

Phosphorylation in Vitro and in Intact Cells Using a Phosphospecific Monoclonal Antibody. *Journal of Biological Chemistry* 273, 20029–20035. doi: 10.1074/jbc.273.32.20029

Stirling, D. R., Swain-Bowden, M. J., Lucas, A. M., Carpenter, A. E., Cimini, B. A., and Goodman, A. (2021). CellProfiler 4: improvements in speed, utility and usability. *BMC Bioinformatics* 22, 433. doi: 10.1186/s12859-021-04344-9

Taylor, S. S., Herberg, F. W., Veglia, G., and Wu, J. (2023). Edmond Fischer's kinase legacy: History of the protein kinase inhibitor and protein kinase A. *IUBMB Life* 75, 311–323. doi: 10.1002/iub.2714

Taylor, S. S., Ilouz, R., Zhang, P., and Kornev, A. P. (2012). Assembly of allosteric macromolecular switches: lessons from PKA. *Nat Rev Mol Cell Biol* 13, 646–658. doi: 10.1038/nrm3432

Thal, D. M., Yeow, R. Y., Schoenau, C., Huber, J., and Tesmer, J. J. G. (2011). Molecular Mechanism of Selectivity among G Protein-Coupled Receptor Kinase 2 Inhibitors. *Mol Pharmacol* 80, 294–303. doi: 10.1124/mol.111.071522

Truong, M. E., Bilekova, S., Choksi, S. P., Li, W., Bugaj, L. J., Xu, K., et al. (2021). Vertebrate cells differentially interpret ciliary and extraciliary cAMP. *Cell* 184, 2911-2926.e18. doi: 10.1016/j.cell.2021.04.002

Tschaikner, P. M., Regele, D., Röck, R., Salvenmoser, W., Meyer, D., Bouvier, M., et al. (2021). Feedback control of the Gpr161-Gαs-PKA axis contributes to basal Hedgehog repression in zebrafish. *Development* 148, dev192443. doi: 10.1242/dev.192443

Ui, M., Katada, T., Murayama, T., Kurose, H., Yajima, M., Tamura, M., et al. (1984). Islet-activating protein, pertussis toxin: a specific uncoupler of receptor-mediated inhibition of adenylate cyclase. *Adv Cyclic Nucleotide Protein Phosphorylation Res* 17, 145–151.

Vaisse, C., Clement, K., Guy-Grand, B., and Froguel, P. (1998). A frameshift mutation in human MC4R is associated with a dominant form of obesity. *Nat Genet* 20, 113–114. doi: 10.1038/2407

Van Den Heuvel, M., and Ingham, P. W. (1996). smoothened encodes a receptor-like serpentine protein required for hedgehog signalling. *Nature* 382, 547–551. doi: 10.1038/382547a0

Walker, M. F., Zhang, J., Steiner, W., Ku, P.-I., Zhu, J.-F., Michaelson, Z., et al. (2024). GRK2 kinases in the primary cilium initiate SMOOTHENED-PKA signaling in the Hedgehog cascade. *PLoS Biol* 22, e3002685. doi: 10.1371/journal.pbio.3002685

Wang, B., Fallon, J. F., and Beachy, P. A. (2000). Hedgehog-Regulated Processing of Gli3 Produces an Anterior/Posterior Repressor Gradient in the Developing Vertebrate Limb. *Cell* 100, 423–434. doi: 10.1016/S0092-8674(00)80678-9

Wang, T., Li, Z., Cvijic, M. E., Zhang, L., and Sum, C. S. (2004). “Measurement of cAMP for Gαs- and Gαi Protein-Coupled Receptors (GPCRs),” in *Assay Guidance Manual*, eds. S. Markossian, A. Grossman, M. Arkin, D. Auld, C. Austin, J. Baell, et al. (Bethesda (MD): Eli Lilly & Company and the National Center for Advancing Translational Sciences). Available at: http://www.ncbi.nlm.nih.gov/books/NBK464633/ (Accessed November 14, 2024).

Wang, Y., Bernard, A., Comblain, F., Yue, X., Paillart, C., Zhang, S., et al. (2021). Melanocortin 4 receptor signals at the neuronal primary cilium to control food intake and body weight. *Journal of Clinical Investigation* 131, e142064. doi: 10.1172/JCI142064

Wettschureck, N., and Offermanns, S. (2005). Mammalian G Proteins and Their Cell Type Specific Functions. *Physiological Reviews* 85, 1159–1204. doi: 10.1152/physrev.00003.2005

Wilson, C. W., Chen, M.-H., and Chuang, P.-T. (2009). Smoothened Adopts Multiple Active and Inactive Conformations Capable of Trafficking to the Primary Cilium. *PLoS ONE* 4, e5182. doi: 10.1371/journal.pone.0005182

Wolff, C., Roy, S., and Ingham, P. W. (2003). Multiple Muscle Cell Identities Induced by Distinct Levels and Timing of Hedgehog Activity in the Zebrafish Embryo. *Current Biology* 13, 1169–1181. doi: 10.1016/S0960-9822(03)00461-5

Yasuda, K., Rens-Domiano, S., Breder, C. D., Law, S. F., Saper, C. B., Reisine, T., et al. (1992). Cloning of a novel somatostatin receptor, SSTR3, coupled to adenylylcyclase. *Journal of Biological Chemistry* 267, 20422–20428. doi: 10.1016/S0021-9258(19)88719-7

Yauch, R. L., Dijkgraaf, G. J. P., Alicke, B., Januario, T., Ahn, C. P., Holcomb, T., et al. (2009). *Smoothened* Mutation Confers Resistance to a Hedgehog Pathway Inhibitor in Medulloblastoma. *Science* 326, 572–574. doi: 10.1126/science.1179386

Ye, F., Nager, A. R., and Nachury, M. V. (2018). BBSome trains remove activated GPCRs from cilia by enabling passage through the transition zone. *Journal of Cell Biology* 217, 1847–1868. doi: 10.1083/jcb.201709041

Zhang, Y., and Beachy, P. A. (2023). Cellular and molecular mechanisms of Hedgehog signalling. *Nat Rev Mol Cell Biol* 24, 668–687. doi: 10.1038/s41580-023-00591-1

Zhao, Z., Lee, R. T. H., Pusapati, G. V., Iyu, A., Rohatgi, R., and Ingham, P. W. (2016). An essential role for Grk2 in Hedgehog signalling downstream of Smoothened. *EMBO Reports* 17, 739–752. doi: 10.15252/embr.201541532

CHAPTER 3:

Future directions and considerations

3.1 Open questions

The work in this thesis has largely been focused on Hedgehog signaling, but I believe that some of the most powerful use cases for the ciliary PKA biosensor will be to assess ciliary GPCR signaling in contexts other than Hedgehog signaling.

As previously mentioned, an abundance of GPCRs specifically localize to neuronal cilia (Mykytyn and Askwith, 2017). As one example, dopamine receptor 1 (D1DR) has been shown to be enriched on the cilia of neurons in the central nervous system (Domire *et al.*, 2011). D1DR is able to signal at various subcellular compartments, namely the Golgi and plasma membrane (Puri *et al.*, 2022). Does D1DR also signal at the primary cilium? Is there a different signaling output of D1DR at the cilium than at the plasma membrane? Are they both read through PKA?

If multiple G-alpha-coupled ciliary GPCRs can affect ciliary adenylyl cyclases, and thus cAMP concentrations and ciliary PKA signaling, how do these different GPCRs avoid crosstalk? Ciliary PKA toggles the activity of the Gli transcription factors by phosphorylating GLI, affecting the overall stability of the transcription factor (Wang, Wang and Jiang, 1999; Haycraft *et al.*, 2005; Niewiadomski *et al.*, 2014). Are the signaling outputs of different ciliary GPCRs also read through Gli?

For GPCRs that signal through ciliary PKA to affect pathways other than Gli signaling implies that PKA must phosphorylate proteins outside of the Hedgehog pathway. What are the other targets of PKA in the primary cilium? One possible way to assess this is by isolating cilia from cells (treated with forskolin) expressing ciliary or extraciliary dominant-negative versions PKA (dnPKA) for phosphoproteomics to screen for potential targets of ciliary PKA. Here, phosphorylated proteins that are present in the FSK + extraciliary dnPKA but not in the FSK +

ciliary dnPKA condition would the potential candidates to follow up on. There is some potential for dnPKA to be toxic to cells when stably expressed, so an inducible version of this construct may be warrented. LLC-PK1 cells are renal epithelial cells that have long cilia suitable for this ciliary isolation (Raleigh *et al.*, 2018), and may be a tractable system for this particular experiment. LLC-PK1 cells are epithelial cells isolated from an adult pig kidney, which are likely quite different from the mesenchymal fibroblasts of embryonic origin usually used to assay Hedgehog signaling (i.e., mouse embryonic fibroblasts, and NIH/3T3s). LLC-PK1 cells are not known to be Hedgehog-responsive under normal conditions, thus any potential hits from this screen are more likely to result in identification of novel ciliary substrates for PKA outside of Hedgehog signaling.

3.2 References

Domire, J. S., Green, J. A., Lee, K. G., Johnson, A. D., Askwith, C. C., and Mykytyn, K. (2011). Dopamine receptor 1 localizes to neuronal cilia in a dynamic process that requires the Bardet-Biedl syndrome proteins. *Cell. Mol. Life Sci.* 68, 2951–2960. doi: 10.1007/s00018-010-0603-4

Haycraft, C. J., Banizs, B., Aydin-Son, Y., Zhang, Q., Michaud, E. J., and Yoder, B. K. (2005). Gli2 and Gli3 Localize to Cilia and Require the Intraflagellar Transport Protein Polaris for Processing and Function. *PLoS Genet* 1, e53. doi: 10.1371/journal.pgen.0010053

Mykytyn, K., and Askwith, C. (2017). G-Protein-Coupled Receptor Signaling in Cilia. *Cold Spring Harb Perspect Biol* 9, a028183. doi: 10.1101/cshperspect.a028183

Niewiadomski, P., Kong, J. H., Ahrends, R., Ma, Y., Humke, E. W., Khan, S., et al. (2014). Gli Protein Activity Is Controlled by Multisite Phosphorylation in Vertebrate Hedgehog Signaling. *Cell Reports* 6, 168–181. doi: 10.1016/j.celrep.2013.12.003

Puri, N. M., Romano, G. R., Lin, T.-Y., Mai, Q. N., and Irannejad, R. (2022). The organic cation transporter 2 regulates dopamine D1 receptor signaling at the Golgi apparatus. *eLife* 11, e75468. doi: 10.7554/eLife.75468

Raleigh, D. R., Sever, N., Choksi, P. K., Sigg, M. A., Hines, K. M., Thompson, B. M., et al. (2018). Cilia-Associated Oxysterols Activate Smoothened. *Molecular Cell* 72, 316-327.e5. doi: 10.1016/j.molcel.2018.08.034

Wang, G., Wang, B., and Jiang, J. (1999). Protein kinase A antagonizes Hedgehog signaling by regulating both the activator and repressor forms of Cubitus interruptus. *Genes & Development* 13, 2828–2837. doi: 10.1101/gad.13.21.2828

Publishing Agreement

It is the policy of the University to encourage open access and broad distribution of all theses, dissertations, and manuscripts. The Graduate Division will facilitate the distribution of UCSF theses, dissertations, and manuscripts to the UCSF Library for open access and distribution. UCSF will make such theses, dissertations, and manuscripts accessible to the public and will take reasonable steps to preserve these works in perpetuity.

I hereby grant the non-exclusive, perpetual right to The Regents of the University of California to reproduce, publicly display, distribute, preserve, and publish copies of my thesis, dissertation, or manuscript in any form or media, now existing or later derived, including access online for teaching, research, and public service purposes.

DocuSigned by:
Thi Nguyen
FFC031FBDF46490...
Author Signature

8/23/2025
Date